geodiversitas

2023 • 45 • 9

Early Eocene hippomorph perissodactyls (Mammalia) from the Paris Basin

Constance BRONNERT & Grégoire MÉTAIS

art. 45 (9) — Published on 8 June 2023
www.geodiversitas.com

PUBLICATIONS SCIENTIFIQUES

MUSÉUM NAL HIST NATURELLE

Directeur de la publication / *Publication director* : Bruno David,
Président du Muséum national d'Histoire naturelle

Rédacteur en chef / *Editor-in-chief*: Didier Merle

Assistant de rédaction / *Assistant editor*: Emmanuel Côtez (geodiv@mnhn.fr)

Mise en page / *Page layout*: Emmanuel Côtez

Comité scientifique / *Scientific board*:
Christine Argot (Muséum national d'Histoire naturelle, Paris)
Beatrix Azanza (Museo Nacional de Ciencias Naturales, Madrid)
Raymond L. Bernor (Howard University, Washington DC)
Henning Blom (Uppsala University)
Jean Broutin (Sorbonne Université, Paris, retraité)
Gaël Clément (Muséum national d'Histoire naturelle, Paris)
Ted Daeschler (Academy of Natural Sciences, Philadelphie)
Bruno David (Muséum national d'Histoire naturelle, Paris)
Gregory D. Edgecombe (The Natural History Museum, Londres)
Ursula Göhlich (Natural History Museum Vienna)
Jin Meng (American Museum of Natural History, New York)
Brigitte Meyer-Berthaud (CIRAD, Montpellier)
Zhu Min (Chinese Academy of Sciences, Pékin)
Isabelle Rouget (Muséum national d'Histoire naturelle, Paris)
Sevket Sen (Muséum national d'Histoire naturelle, Paris, retraité)
Stanislav Štamberg (Museum of Eastern Bohemia, Hradec Králové)
Paul Taylor (The Natural History Museum, Londres, retraité)

Couverture / *Cover*:
Réalisée à partir des Figures de l'article/*Made from the Figures of the article*.

Geodiversitas est indexé dans / Geodiversitas *is indexed in:*
– Science Citation Index Expanded (SciSearch®)
– ISI Alerting Services®
– Current Contents® / Physical, Chemical, and Earth Sciences®
– Scopus®

Geodiversitas est distribué en version électronique par / Geodiversitas *is distributed electronically by:*
– BioOne® (http://www.bioone.org)

Les articles ainsi que les nouveautés nomenclaturales publiés dans *Geodiversitas* sont référencés par / *Articles and nomenclatural novelties published in* Geodiversitas *are referenced by:*
– ZooBank® (http://zoobank.org)

Geodiversitas est une revue en flux continu publiée par les Publications scientifiques du Muséum, Paris
Geodiversitas *is a fast track journal published by the Museum Science Press, Paris*

Les Publications scientifiques du Muséum publient aussi / *The Museum Science Press also publish:* ***Adansonia***, ***Zoosystema***, ***Anthropozoologica***, ***European Journal of Taxonomy***, ***Naturae***, ***Cryptogamie*** **sous-sections** ***Algologie***, ***Bryologie***, ***Mycologie, Comptes Rendus Palevol***

Diffusion – Publications scientifiques Muséum national d'Histoire naturelle
CP 41 – 57 rue Cuvier F-75231 Paris cedex 05 (France)
Tél. : 33 (0)1 40 79 48 05 / Fax : 33 (0)1 40 79 38 40
diff.pub@mnhn.fr / http://sciencepress.mnhn.fr

© Publications scientifiques du Muséum national d'Histoire naturelle, Paris, 2023
ISSN (imprimé / *print*) : 1280-9659/ ISSN (électronique / *electronic*) : 1638-9395

Early Eocene hippomorph perissodactyls (Mammalia) from the Paris Basin

Constance BRONNERT
Grégoire MÉTAIS
Muséum national d'Histoire naturelle,
Centre de Recherche en Paléontologie – Paris (CR2P, UMR 7207),
CNRS/MNHN/Sorbonne Université,
case postale 38, 57 rue Cuvier, F-75231 Paris cedex 05 (France)
constance.bronnert@mnhn.fr (corresponding author)
gregoire.metais@mnhn.fr

Submitted on 22 January 2020 | accepted on 14 October 2022 | published on 8 June 2023

urn:lsid:zoobank.org:pub:1C430978-5EE6-49AE-AF7C-23C710161CB7

Bronnert C. & Métais G. 2023. — Early Eocene hippomorph perissodactyls (Mammalia) from the Paris Basin. *Geodiversitas* 45 (9): 277-326. https://doi.org/10.5252/geodiversitas2023v45a9. http://geodiversitas.com/45/9

ABSTRACT
Perissodactyls (nowadays including horses, rhinos and tapirs) appear early in the Eocene and quickly spread throughout the Northern Hemisphere. Their geographical origin, probably Asian, as well as their phylogenetic relationships are currently debated. Early perissodactyl fossils from Europe have been poorly studied since the 1960s, and many specimens have been deposited since then in the European institutions, today allowing us to have a better vision of the evolution of the early Eocene hippomorph perissodactyls. This work presents a study and a revision of the early Eocene hippomorphs (MP7-MP10) of the Paris Basin. The majority of the material is unpublished and allowed to identify nine species of hippomorphs: *Pliolophus vulpiceps* Owen, 1858, *Pliolophus barnesi* Hooker, 2010, *Pliolophus quesnoyensis* Bronnert, Gheerbrant, Godinot & Métais, 2018, *Cymbalophus cuniculus* (Owen, 1842), *Hyracotherium leporinum* Owen, 1841, *Propalaeotherium gaudryi* (Lemoine, 1878), *Orolophus maldani* (Lemoine, 1878), *Hallensia louisi* Hooker, 1994 and *Hallensia parisiensis* Franzen, 1990. In these European early hippomorphs, we observe a trend toward increase of the lophodonty, as well as the increase of the centrocrista flexure on upper molars. Likewise, sexual dimorphism is reflected in the robustness of the mandibles. The faunas close to MP7 show differences between Northern and Southern Europe, confirming the hypothesis of a climatic barrier between them. A perissodactyl turnover at the generic level takes place between the sites close to MP7 and those close to MP8-9, as well as a homogenization of species between Northern and Southern Europe. The MP8-9 sites and those close to MP10 have similar perissodactyl faunas.

KEY WORDS
Perissodactyla,
Hippomorpha,
Equoidea,
Europe,
Early Eocene.

RÉSUMÉ
Les périssodactyles hippomorphes (Mammalia) de l'Éocène inférieur du bassin de Paris.
Les périssodactyles (comprenant aujourd'hui les chevaux, les rhinocéros et les tapirs) apparaissent au début de l'Éocène et se dispersent rapidement dans tout l'hémisphère Nord. Leur origine géographique, probablement asiatique, ainsi que leur origine phylogénétique, est actuellement débattue. Les fossiles provenant d'Europe ont été peu étudiés depuis les années 1960, et les nombreux spécimens déposés depuis dans les institutions européennes permettent aujourd'hui d'avoir une meilleure vision de l'évolution des périssodactyles hippomorphes de l'Éocène inférieur. Ce travail présente une étude et une révision des hippomorphes de l'Éocène inférieur (MP7-MP10) du bassin de Paris. La majorité du matériel est inédite et a permis d'identifier neuf espèces d'hippomorphes : *Pliolophus vulpiceps* Owen, 1858, *Pliolophus barnesi* Hooker, 2010, *Pliolophus quesnoyensis* Bronnert, Gheerbrant, Godinot & Métais, 2018, *Cymbalophus cuniculus* (Owen, 1842), *Hyracotherium leporinum* Owen, 1841, *Propalaeotherium gaudryi* (Lemoine, 1878), *Orolophus maldani* (Lemoine, 1878), *Hallensia louisi* Hooker, 1994 et *Hallensia parisiensis* Franzen, 1990. Une tendance à l'augmentation de la lophodontie, ainsi que l'augmentation de la flexure de la centrocrista des molaires supérieures est observée. Un dimorphisme sexuel au niveau de la robustesse des mandibules est observé. Les faunes rapprochées du MP7 présentent des différences entre le nord et le sud de l'Europe, confirmant l'hypothèse d'une barrière climatique. Un renouvellement des périssodactyles au niveau générique s'effectue entre les sites rapprochés du MP7 et ceux rapproché du MP8-9, ainsi qu'une homogénéisation des espèces entre le nord et le sud de l'Europe. Les sites MP8-9 et ceux proches du MP10 possèdent des faunes de périssodactyles similaires.

MOTS CLÉS
Perissodactyla,
Hippomorpha,
Equoidea,
Europe,
Éocène inférieur.

INTRODUCTION

The perissodactyls appeared at the beginning of the Eocene in the Northern Hemisphere. They probably originated in Asia, and they seem to have quickly spread across the whole Northern Hemisphere (Beard 1998; Bai *et al.* 2018). Because it is difficult to make precise correlation between continents, the Equoidea superfamily seems to appear at the same time in North America and Europe (e.g., Gingerich 2006). The fossil record of this group is well known, especially in North America where it documents the appearance of the equoids and their subsequent diversification. The equoids are well documented in North America, mainly due to the work of Cope (1872), and the syntheses of Granger (1908), Kitts (1956), Gingerich (1991), MacFadden (1992) and Froehlich (2002). In Europe, the fossil record is scarcer, and mainly composed of dental remains. The three oldest species (*Hyracotherium leporinum* Owen, 1841, *Pliolophus vulpiceps* Owen, 1858 and '*Hyracotherium*' *cuniculus* Owen, 1842) were described by Owen (1841, 1842, 1858) from England. Two species, *Propachynolophus gaudryi* Lemoine, 1878 and *Propachynolophus maldani* (Lemoine, 1878), were then described in the French Paris Basin by Lemoine (1878, 1891). *Hyracotherium* and *Pliolophus* have often been synonymized (Depéret 1901; Forster-Cooper 1932b; Simpson 1952; McKenna & Bell 1997). Savage *et al.* (1965) provided a synthesis of the previous works and classified the three oldest species from the early Eocene within the genus *Hyracotherium*, as well as another unidentified species of small equoid from France found in localities correlated to MP7 and MP8-9 reference levels (Biochrom' 1997). Generally, the equoids from MP7 to MP8-9 belong to the genus *Hyracotherium*, and the French species from MP10 are classically lumped into the genus *Propachynolophus*. Hooker (1994) revised the English material from the early Eocene London Clays, and resurected the genus *Pliolophus* Owen, 1858 for the species *P. vulpiceps* previously refered to *Hyracotherium* (Savage *et al.* 1965; Hooker 1980). Hooker (1984) also erected the genus *Cymbalophus* for the *Hyracotherium cuniculus* Owen 1842 from Abbey Wood. This genus has also been recognized from Palette (MP7, southern France) under a new species *C. hookeri* Godinot, Crochet, Hartenberger, Lange-Badré, Russell & Sigé 1987 (Godinot *et al.* 1987). Franzen & Haubold (1986) created the genus and species *Hallensia matthesi* based on bunodont dental material from MP11 levels of the Geiseltal, and additional material (almost complete skeleton) was subsequently recovered in the MP11 locality of Messel (Franzen, 1990). The two early Eocene species of *Hallensia*, *H. louisi* and *H. parisiensis* are only known by a scarce material but are characterized by an unusual bunodont morphology. Hooker (1994) created the species *Hallensia louisi* Hooker, 1994 and *Propachynolophus levei* Hooker, 1994, both based on fossils from the Paris Basin. More recently, two species of *Pliolophus* have been described, *P. barnesi* Hooker, 2010 and *P. quesnoyensis* Bronnert, Gheerbrant, Godinot & Métais, 2018. The species of *Propachynolophus* were recently splitted in *Propalaeotherium gaudryi*, *Orolophus maldani*, and the two other species in "*Hyracotherium*" *levei* and "*Hyracotherium*" *remyi* (Remy, 2017).

The Muséum national d'Histoire naturelle of Paris (France) acquired a large collection of early Eocene equoids, especially with the donation of the Louis collection and the contribution of many amateurs, which has so far never been thoroughly studied. We propose here a description of this new material, and the revision of the early Eocene material from the Paris Basin *s.l.* (Paris Basin, London Basin, Belgium Basin).

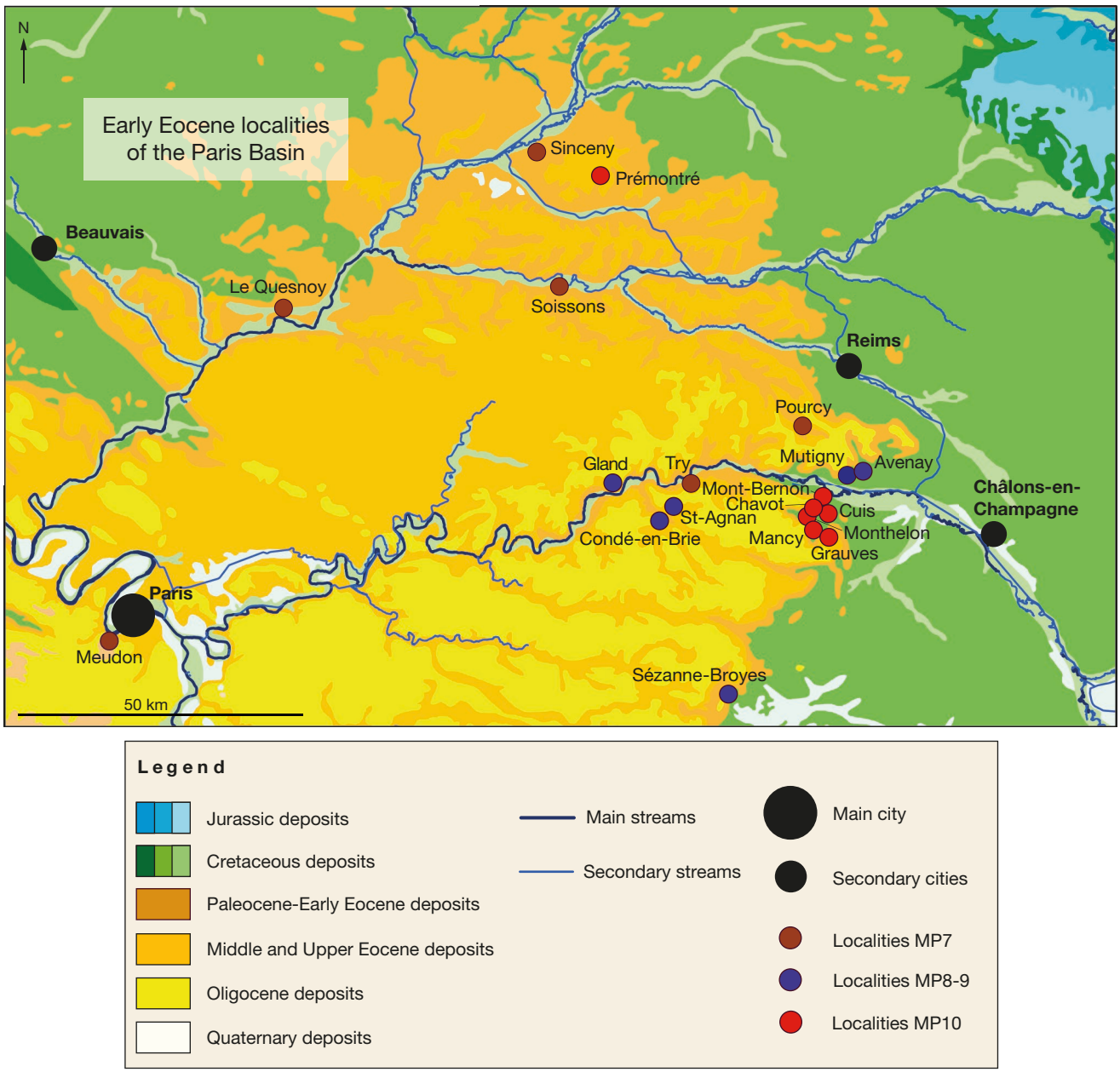

FIG. 1. — Location of the early Eocene perissodactyls yielding sites in the Paris Basin.

LOCALITIES AND GEOLOGICAL SETTING

The European localities are classified using a biochronologic scale based on reference-levels (Biochrom' 1997). A locality is supposed to be close to a reference-level if its fauna matches taxonomically the fauna of the reference-level. Three reference-levels are defined for the early Eocene, running from MP7 to MP10. The MP8-9 reference-levels are not separated because of the lack of well-preserved faunas allowing a good description of the two levels.

About twenty localities have yielded early Eocene perissodactyl fossils in the French Paris Basin (Fig. 1). The localities closely related to the MP7 reference fauna (Dormaal, Belgium) only yield scarce material composed of isolated teeth, with the exception of the Le Quesnoy locality which has yielded a large quantity of dental and postcranial elements (Nel *et al.* 1999; Bronnert *et al.* 2018, 2019). The localities correlative to MP8-9 have dominantly yielded dental material. The sites correlative to MP10 have yielded the largest number of specimens, including dental and postcranial remains.

The fossil locality Dormaal (Belgium), which is in the Carbone Isotopic Excursion of the PETM (Steurbaut *et al.* 2003) and the MP7 reference-level, has yielded a DP3 attributed to *Hallensia louisi* Hooker, 1994. Smith & Smith (2004) claim that given the unusual patina of the tooth, the tooth may come from a contamination, as do other specimens in the collection. Given its doubtful provenance, this material is not included in this study and Dormaal is considered as not having yielded perissodactyls. Few localities are known from Belgium (Oosterzele, Hoe-

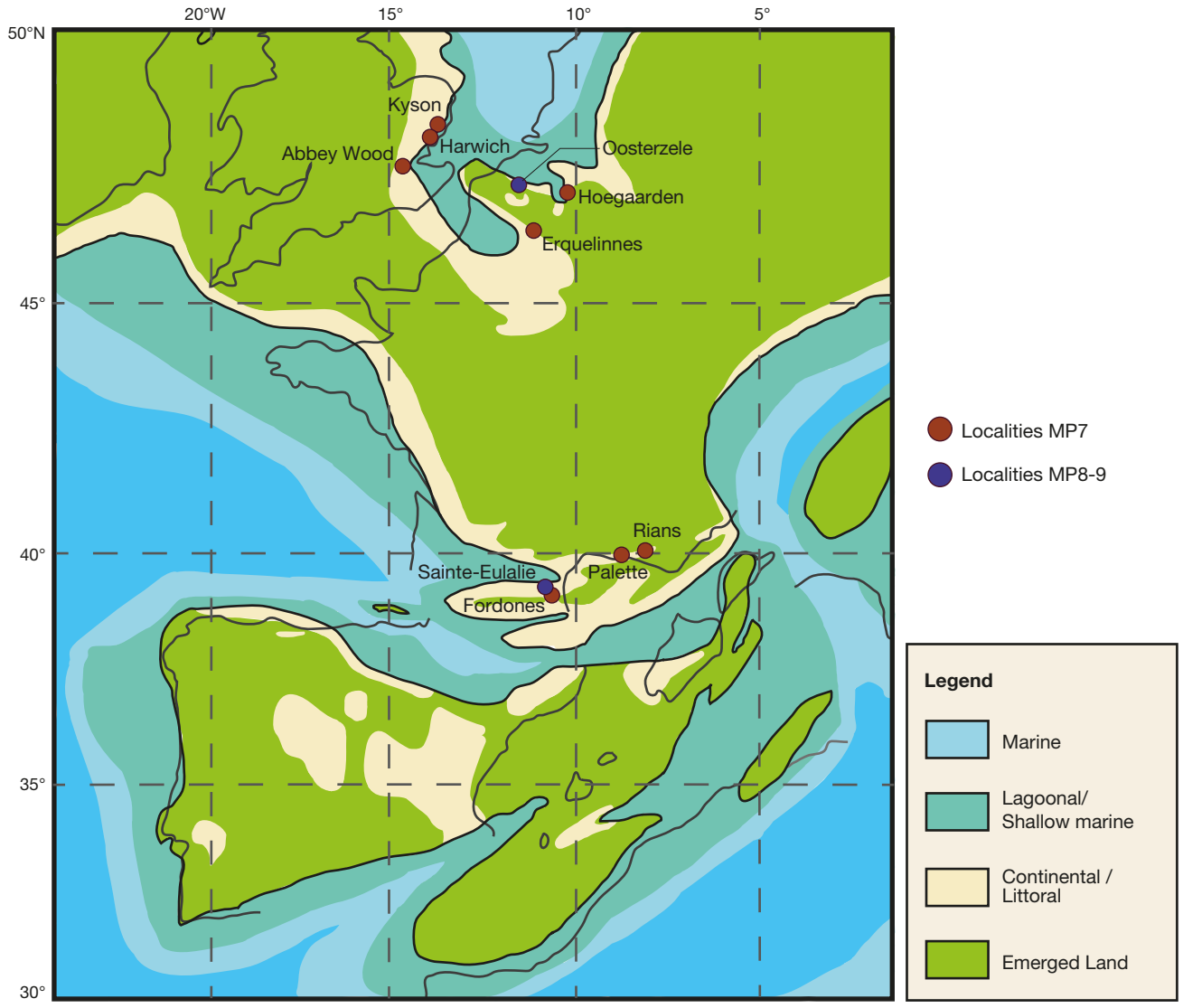

Fig. 2. — Paleogeographic map of the main European localities outside the Paris Basin at the beginning of the Eocene (modified from Marandat *et al.* 2012).

gaarden, Erquelinnes) (Fig. 2), and they have only yielded few dental remains. Likewise, the localities from England have yielded little material, with the exception of Abbey Wood where a large number of dental and postcranial remains have been discovered (Hooker 2010). Even if the English fossil record is poor, some of these fossils are well preserved, such as the holotype complete skull and mandible of *Pliolophus vulpiceps* from Harwich (England), and the holotype partial skull of *Hyracotherium leporinum* from Kyson (England). In France (Fig. 1), six fossil localities are correlated with the MP7: Meudon, Sinceny, Soissons, Try, Le Quesnoy and Pourcy; six are correlative to the MP8-9: Mutigny, Avenay, Gland, Condé-en-Brie, Sézanne-Broyes and Saint-Agnan; and the MP10 localities are distributed in three main areas: Prémontré, Fossoy and the localities of the Sables à Unios et Térédines near Epernay, including Grauves (the type locality of MP10), Cuis, Mancy, Monthelon, Mont-Bernon and Chavot. The localities from the Sables à Unios et Térédines are sometimes designated as Grauves *s.l.* Lemoine (1891) created the term "Ageian" for these localities, and mixed the fossils from these sites. The holotypes of *Propalaeotherium gaudryi* and *Orolophus maldani* come from "environs d'Epernay" (Savage *et al.* 1965), which correspond to one of these localities.

MATERIAL AND METHODS

Terminology

The dental terminology follows Hooker (1989, 1994) for the molars (Fig. 3) and Holbrook (2015) and Butler (1952b) for the premolars. The terminology of Butler (1952a) is used for the deciduous teeth.

Measurements

The measurements follow Bronnert *et al.* (2018). They include the greatest length and the largest width of the teeth. The measurements follow the protocone-paracone

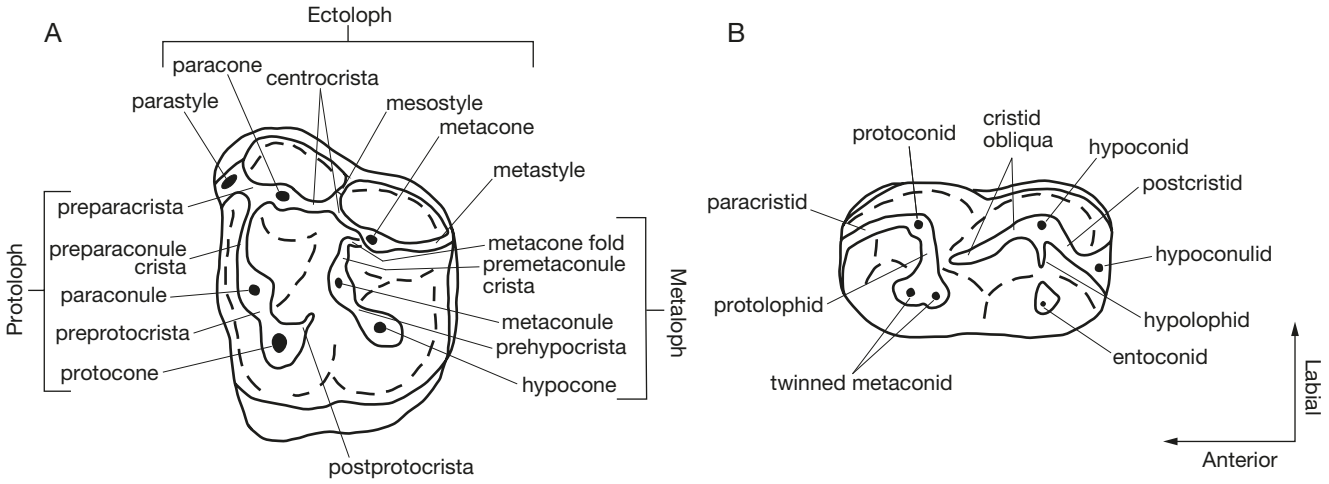

FIG. 3. — Dental terminology of early perissodactyls (modified from Bronnert *et al.* 2018): **A**, upper tooth; **B**, lower tooth.

alignment for the upper molars, and the protoconid-hypoconid alignment for the lower molars. The measurements are shown in Appendix 1.

ABBREVIATIONS

Institutional abbreviations

AMNH	American Museum of Natural History, New York;
BMNH	British Museum of Natural History, London;
FSL	Faculté des Sciences de Lyon, Université Claude Bernard Lyon 1, Lyon;
IRSNB	Institut royal des Sciences naturelles de Belgique, Brussel;
MNHN	Muséum national d'Histoire naturelle, Paris;
NHM	Natural History Museum, London;
TS	Naturhistorisches Museum, Basel.

Locality abbreviations

AL	Lemoine's Ageian;
AV	Avenay;
CB, CEB	Condé-en-Brie;
CH, CHO	Chavot;
CUI	Cuis;
GL, GLD	Gland;
GR	Grauves;
MA	Mancy;
MU	Mutigny;
PE, PMT, PR, PRE	Prémontré;
PY	Pourcy;
SEZ, SZ	Sézanne-Broyes;
STA	Saint-Agnan;
TRY	Try.

Collection abbreviations

BN	Braillon collection (MNHN);
CN	Cazeneuve collection;
L	collection Louis (MNHN);
Ph	Phélizon collection;
SLP-29-PR	Hautefeuille collection, Société laonnoise de Paléontologie.

Anatomical abbreviations

L	left;
R	right.

SYSTEMATICS

Order PERISSODACTYLA Owen,1848
Suborder HIPPOMORPHA Wood, 1937
Superfamily EQUOIDEA Gray, 1821
Family *incertae sedis*

Genus *Pliolophus* Owen, 1858

Pliolophus Owen, 1858: 54-70.

TYPE SPECIES. — *Pliolophus vulpiceps* Owen, 1858 by original designation.

INCLUDED SPECIES. — *Pliolophus barnesi* Hooker, 2010; *P. quesnoyensis* Bronnert, Gheerbrant, Godinot & Métais, 2018.

EMENDED DIAGNOSIS (based on Hooker 2010). — Upper molar paraconule more mesial than protocone. No mesostyle. Twinned lower molar metaconid. Notched protolophid. Cristid obliqua joining the protolophid in the middle. Lower molar hypoconulid generally linked to the hypoconid. Post-p1 diastema absent or reduced.

DIFFERENTIAL DIAGNOSIS. — Differs from *Cymbalophus*, which displays a small hypoconulid closely appressed to the hypolophid by a lower molar hypoconid-hypoconulid junction on m1-2. Differs from *Hyracotherium* by the absence of mesostyle. Differs from *Orolophus* and *Propalaeotherium gaudryi* by a straight centrocrista and a less developed lophodonty.

NOTES

The genus *Pliolophus* was established by Owen (1858), who considered that *P. vulpiceps* differs from *Hyracotherium* by more developed conules, more developed cingulae on upper teeth, and a P1-P2 diastema longer. *P. vulpiceps* displays a well-developed entoconid on p4. Cope (1884) includes the American species with the same character within the genus *Pliolophus*. Wortman (1896) judged this character variable, and classified *Pliolophus* as a sub-genus of *Hyracotherium*. Type specimens of *Pliolophus* and *Hyracotherium* possess several common features, and Forster-Cooper (1932b) and Simpson (1952) synonymized the two genera. Hooker (1994)

resurrected the genus based on a phylogenetic analysis. The phylogenetic analysis of Froehlich (2002) supported this result, and indicated that *Pliolophus* might be the only European species belonging to the Equidae.

Pliolophus vulpiceps Owen, 1858

Pliolophus vulpiceps Owen, 1858: 54-70, pls 2-4.

Hyracotherium leporinum – Owen 1865: 340 (*partim*), pl.10, fig. 2. — Lydekker 1886: 11. — Depéret 1901: 200, 201 (*partim*), pl. 4, fig. 1.

Hyracotherium vulpiceps – Forster-Cooper 1932b: 432-436, figs 2D, 3A, pl. 50, figs 1-3. — Simpson 1952: 195-206, pl. 37, figs a-d. — Hooker 1980: 104, 106, 108, fig. 3.

Hyracotherium sp. – Simpson 1952: pl. 40, fig. a.

Hyracotherium [sic] – Savage *et al.* 1965: 8-10, figs 3c, e, f. v.

Hyracotherium aff. *vulpiceps* – Hooker 1980: 106-108, fig. 2; 1989: 83-84, figs 6.3L, 6.4I-K.

Holotype. — BMHN-44115, BMNH-44115a, BMNH-M.10567-61, skull and partial skeleton.

Material. — See Hooker (1980).

Type locality. — Harwich (United-Kingdom), MP8-9.

Distribution. — Harwich (United-Kingdom), MP8-9.

Diagnosis (modified from Hooker 1980). — "*Medium-sized species of* Pliolophus*, length of P^2-M^3 41 mm in holotype. Upper molars with very sligthly buccally flexed centrocrista and a very faint rib in the mesostylar position, separated from the buccal cingulum. Lower molar cristid obliqua tend to join trigonids equidistant between protoconids and metaconids. M_3 hypoconulid lobe relatively large and with a median main cusp. P^3 with large paraconule; distolingually placed protocone; slightly convex mesiolingual margin and little or no postprotocrista.*"

Differential diagnosis. — Largest species of *Pliolophus*. Upper molar centrocrista more flexed than *P. barnesi* and *P. quesnoyensis*, and metaconule larger. Differs from *P. barnesi* and *P. vulpiceps* by longer mandibular diastemas.

Description

A part of the description is based on the drawings of Owen (1858). The type-specimen was a complete skull with the articulated mandible. This specimen has been splited in several parts, the mandible and the left maxillary were removed, which considerably damaged the teeth. Some other parts of the skull have been lost, such as the basicranium. The complete history of the specimen is reported by Simpson (1952).

Teeth

Three incisors are present on each premaxillary. A 1 cm diastema is present between the third incisor and the canine.

The P1 is two-rooted and possesses a main cusp labially. There is no P1-P2 diastema. The P2 is narrower anteriorly. A cingular bulge is present at the level of the protocone. There is no parastyle. The P3 is nonmolariform and triangular in occlusal view. The paraconule is large and located in the middle of the protoloph. The cingulum is developed and almost continuous, blured close to the protocone. The P4 is nonmolariform and triangular in occlusal view. The parastyle is small and low. The paraconule is large, slightly smaller than the paracone and located in the middle of the protoloph. The preparaconule crista links the preparacrista in the middle. The upper molar parastyle is developed and high. The centrocrista is flexed. The paraconule is large and included within the protoloph. The metaconule is smaller than the metacone. The protoloph links the preparacrista. The metaloph is interrupted at the base of the metacone. The mandibular symphysis is long and narrow (see Owen, 1858). Three incisors are present on each hemimandible. A diastema as long as the canine mesio-distal length is present between the incisors and the canine. A 1 cm post-canine diastema is present. The p1 is simple and large, unicuspid. A short p1-p2 diastema (2 mm) is present. The p2 displays one single cusp, located anteriorly. The p3 possesses a small metaconid closely appressed to the protoconid. The paraconid is absent. The hypoconulid seems developed. The p4 has a low protolophid. The protoconid and the metaconid are about the same height. The cristid obliqua is oriented toward the middle of the protolophid. The entoconid is very small. The lower m1-2 have a twinned metaconid. The cristid obliqua joins the middle of the protolophid at half height. The hypolophid is low, the protolophid is slightly higher. The m3 has a developed hypoconulid, but the lobe is quite short. The hypoconulid is linked to the hypoconid by a postcristid. The cristid obliqua is oriented toward the middle of the protolophid.

Skull

The nasal incisure is interrupted at the level of the canine. It is formed by the premaxillary and the nasal. The anterior border of the orbit is above the M1. The infra-orbital foramen is located at the level of the P2. The sagittal crest is poorly developed. The basicranium and the rostrum have the same length. The horizontal ramus of the mandible is low.

Postcrania

The humeral head is rounded and situated at the end of a short neck. The distal trochlea is shallow. The epicondyles are poorly developed. The supracondylar foramen is large and located in the radial fossa. The greater trochanter of the femur is high. The lesser trochanter is slightly less projected than the third trochanter. The third trochanter is located distally to the distal part of the lesser trochanter. The femoral head possesses a notched *fovea capitis*. Distally, the lateral condyle is broken.

Comparisons

The mandible and the teeth are larger than those of *P. quesnoyensis*. The hypoconulid-hypoconid junction on m1-2 is the same than the one observed in *P. quesnoyensis* and some specimens of *P. barnesi*. It differs from the small hypoconulid closely appressed to the hypolophid in *Cymbalophus*. The upper molar centrocrista is slightly more flexed than the one of *P. barnesi* and *P. quesnoyensis*. The upper molar metaconule is more developed than in the other species of *Pliolophus*. The paraconule is more developed than in *P. quesnoyensis*. The p1 is more developed than in *P. quesnoyensis*.

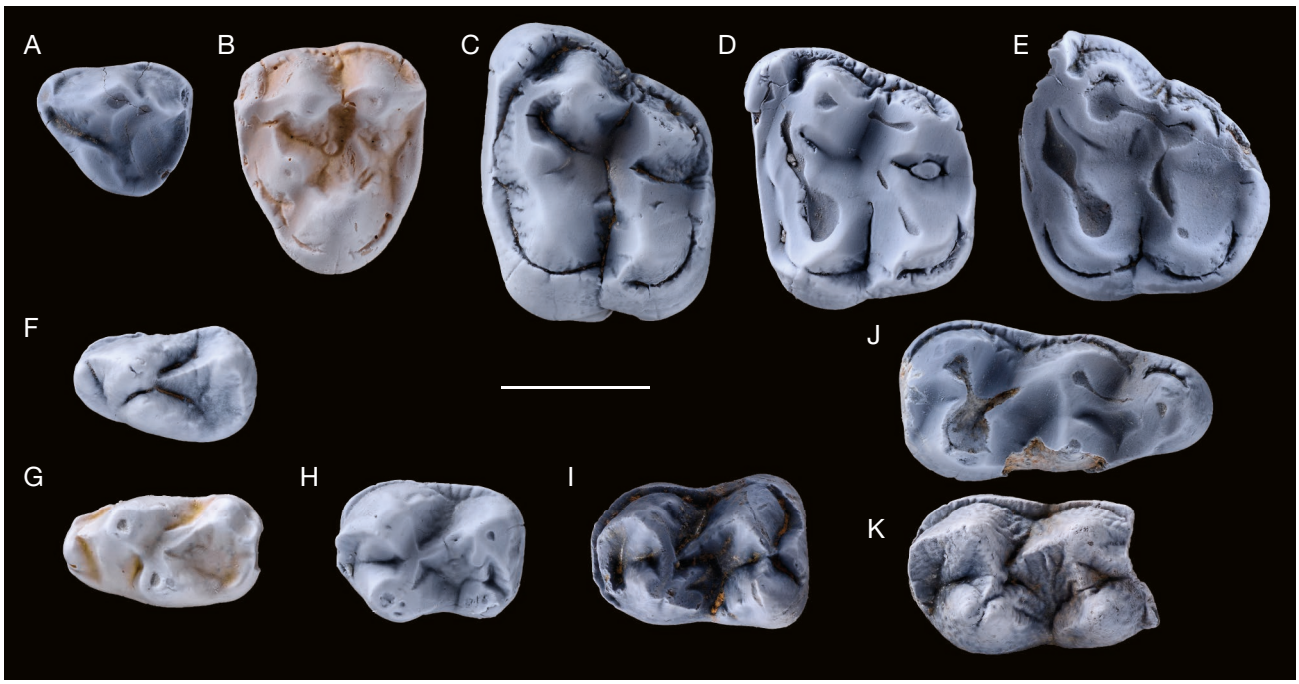

FIG. 4. — Teeth of *Pliolophus barnesi* from Pourcy and Soissons in occlusal view: **A**, left P2 (MNHN-PY75715); **B**, left P4, cast, unnumbered; **C**, left M3 (MNHN-PY41-L); **D**, left M3 (MNHN-PY39-L); **E**, right M3 (MNHN-PY40-L [reversed]); **F**, left p3 (MNHN-PY45-L [reversed]); **G**, left p3 (MNHN-PY34-Cn [reversed]); **H**, left p4 (MNHN-PY20-Ph [reversed]); **I**, right m1/2 (MNHN-SN34-BN); **J**, left m3 (MNHN-PY43-L [reversed]); **K**, left m3 (unnumbered [reversed]). Coated with magnesium. Scale bar: 5 mm.

COMMENT

The few known specimens hinder the study of intraspecific variability in *P. vulpiceps*. *P. vulpiceps* displays several more derived features than *P. barnesi* and *P. quesnoyensis*, such as a more flexed centrocrista and longer mandibular diastemata.

Pliolophus barnesi Hooker, 2010
(Fig. 4)

Pliolophus barnesi Hooker, 2010: 117, 119, figs 52, 53.

Hyracotherium sp. – White 1931: 18, 25. — Simpson 1952: pl. 40, figs b-d. — Kühne 1969: 199.

Hyracotherium [sic] – Forster-Cooper 1932a: 458. — Savage *et al.* 1965: 8-10, figs 3c, e, f.

Hyracotherium (*Pliolophus*) *vulpiceps* – Forster-Cooper 1932b: 437-438, pl 51, figs 4-5.

Hyracotherium aff. *vulpiceps* – Hooker 1980: 106-107, fig. 2; 1984: 234-235, figs 6, 13, 17, 20; 1989: 83-84, figs 6.3L, 6.4I-K, Q.

Pliolophus aff. *vulpiceps* – Hooker 1994: 54, fig 16.

Pliolophus vulpiceps – Hooker 1994: 52-54. — Hooker & Dashzeveg 2003: 493-494; 2004, fig. 6G, H. — Hooker *et al.* 2005: 85.

HOLOTYPE. — BMHN M44910, right mandible with p3-m3.

PARATYPES. — See Hooker (2010).

MATERIAL. — **Abbey Wood**: see Hooker (2010).
Soissons: m2 (R: MNHN-SN34-BN); m3 (L: MNHN unnumbered).
Pourcy: P2 (L: MNHN-PY15715), P4 (L: PY cast), M1 (L: MNHN-PY133-L), M1/2 (R: PY unnumbered, MNHN-PY42-L [broken], PY72-L [broken]), PY146-Lx (cast); L: PY-2-Cn (cast), PY-16-Cn (broken, cast); M3 (R: MNHN-PY40-L; L: MNHN-PY39-L, PY41-L); p3 (L: MNHN-PY45-L, PY34-CN); p4 (L: MNHN-PY20-Ph); m1/2 (R: MNHN-PY9-L [broken], PY143-L [broken]; L: MNHN-PY10-L [broken], PY11-L [broken]); m3 (L: MNHN-PY43-L).

TYPE LOCALITY. — Abbey Wood (London, United-Kingdom), MP8-9.

DISTRIBUTION. — Abbey Wood (London, United-Kingdom); Soissons, Pourcy (Marne, France), MP8-9.

EMENDED DIAGNOSIS. — Large upper molar metaconule. Labially flexed centrocrista. Large P3 paraconule. Lower molar hypoconulid joining the hypoconid (mostly) or to the hypolophid.

DIFFERENTIAL DIAGNOSIS. — Upper molar centrocrista slightly more flexed than *P. quesnoyensis* and less flexed than *P. vulpiceps*. Upper molar and premolar conules less developed than *P. vulpiceps*.

DESCRIPTION

Teeth

The P2 (Fig. 4A) is triangular in occlusal view, and the posterior part is transversally wider than the anterior part. The paracone is developed. The metacone is very reduced and closely appressed to the paracone. The protocone is absent but a cingular bulge is present lingually. Elsewhere, the cingulum is poorly developed or absent. The parastyle is absent. The P4 parastyle is very small and low (Fig. 4B). The paraconule is large, slightly smaller than the paracone. The preparaconule crista is interrupted by a notch close to the center of the preparacrista. The metaconule is small, and slightly elongated. The cingulum is continuous, slightly reduced close to the protocone. The M3 parastyle is devel-

oped but low (Fig. 4C-E). The cingula are well-developed. The centrocrista is slightly flexed. The paraconule is high and merged with the loph. The metaconule varies in size but is generally small, sometimes indistinguishable. The protoloph joins the preparacrista. The metaloph is interrupted at the base of the metacone. The p3 protoconid is larger than the metaconid (Fig. 4F, G). The metaconid and protoconid are close on MNHN-PY45 and more separated on MNHN-PY34-Cn. A small paraconid is present. A crest runs from the protoconid and joins a low but well-developed hypoconid. The metaconid of p4 is twinned (Fig. 4H). The protoconid and metaconid are about the same height. The protolophid is low. The cristid obliqua is directed toward the center of the protolophid. The entoconid is developed but smaller than the hypoconid. A crest joins the hypoconid and the entoconid. A more developed crest runs disto-lingually to the hypoconulid. The lower molar cristid obliqua joins the protolophid in the middle (Fig. 4I-K). The hypolophid is low. The metaconid is twinned. The hypoconulid is linked to the hypoconid by a postcristid. The hypoconulid is small on m1-2. The hypoconulid is large on m3 but the hypoconulid lobe is narrower than the rest of the tooth.

Comparisons

The upper molar centrocrista in *P. barnesi* is slightly more flexed than that in *P. quesnoyensis*, but less flexed than that in *P. vulpiceps*. The m3 display more intraspecific variability on the hypoconulid junction (with hypoconid or hypolophid) than *P. quesnoyensis*. The p4 entoconid is more developed than in *P. quesnoyensis*. Compared with *P. vulpiceps*, the upper molar and premolar conules and p1 are less developed in *P. barnesi*.

Comment

Hooker (1994) described *P. vulpiceps* in Pourcy. However, our revision of the material indicates that the specimens discovered in Pourcy belong to *P. barnesi* rather than *P. vulpiceps*. These fossils, as for *P. barnesi*, notably display less developed conules on upper molars than *P. vulpiceps*.

Pliolophus quesnoyensis
Bronnert, Gheerbrant, Godinot & Métais, 2018
(Fig. 5)

Pliolophus quesnoyensis Bronnert, Gheerbrant, Godinot & Métais, 2018: 239, figs 3-7.

Hyracotherium sp. – Russell *et al.* 1988: 432.

Pliolophus aff. *vulpiceps* – Hooker 1994: 53-54, fig. 17.

"*Propachynolophus*" sp. 1 – Hooker 1994: 60, fig. 26.

Pliolophus sp. 1 – Hooker 1994: 60 (*partim*), fig. 26; 2010: 117 (*partim*).

Holotype. — MNHN-QNY2-2696, right mandible with m1-m3.

Paratypes. — MNHN-QNY2-3022, right mandible, P1 missing; MNHN-QNY2-2700, right maxillary with P4-M3; MNHN-QNY2-2705, right M1/2.

Material. — **Le Quesnoy**: see Bronnert *et al.* 2018; p2 (R: MNHN-QNY2-3076).
Meudon: mandible with p4-m3 (L: coll. Phélizon); P3 (R: unnumbered [Marseille]); M1/2 (R: MNHN-ME-16325, unnumbered [Marseille]); m1/2 (L: MNHN-ME-16322); m3 (R: unnumbered [Marseille]).
Sinceny: P2 (R: MNHN-SY3-CN); P3 (R: MNHN-SY1-CN; L: unnumbered MNHN coll. Cahuzac); P4 (L: MNHN-SY5-DE); M1/2 (L: MNHN-SY4-DE); M3 (R: unnumbered MNHN coll. Berton).
Try: DP3 (R: MNHN-M-TRY10); DP4 (R: MNHN-M-TRY3); M1/2 (R: MNHN-M-TRY23, TRY17-L; L: MNHN-M-TRY9, M-TRY11); M3 (L: MNHN-M-TRY8); p3 (R: MNHN-M-TRY16); p4 (R: MNHN-TRY22-L); m1 (L: MNHN-M-TRY5).

Type locality. — Le Quesnoy (Oise, France), MP7.

Distribution. — Le Quesnoy (Oise, France), Try (Marne), Meudon (Hauts-de-Seine, France), Sinceny (Aisne, France), MP7.

Diagnosis (Bronnert *et al.* 2018). — Small brachyodont perissodactyl; post-p1 diastema extremely short, almost absent; complete cheek tooth formula; sub-lophodont molars; paraconule close to protocone on P3; protocone on P2; straight centrocrista; enlarged crenulated cingulum on M3; hypoconulid lobe on m3 developed.

Differential diagnosis (Bronnert *et al.* 2018). — Species smaller than *P. vulpiceps* and *P. barnesi*. Differs from the latters by a straighter centrocrista and a smaller metaconule on upper molars. Further differs from *P. vulpiceps* by a shorter postcanine diastema.

Description

See Bronnert *et al.* (2018) for a complete description of the species. Here is only described new material.

Teeth

The P3 is nonmolariform (Fig. 5I). The paracone and the metacone are close, and linked by a short centrocrista. A small paraconule is present. The postprotocrista is absent. The P4 is nonmolariform and more symmetrical than the P3.The cingulum is interrupted close to the protocone. The parastyle is small and crescentiform. The paraconule is developed and anterior to the paracone. The postprotocrista extends posteriolabially to the metacone. An endoprotocrista is present posterior to the postprotocrista. There is no mesostyle on upper molars (Fig. 5D, E, K-L). The centrocrista is straight. The paraconule is smaller than the protocone. The protoloph is slightly notched between the protocone and the paraconule. The metaconule is weak or absent. The metaloph ends by a metacone fold. The preparaconule crista joins the preparacrista. The ectocingulum is continuous. An accessory cusp is sometimes present on the cingulum between the metacone and the hypocone. The mandible is very worn and broken. The teeth are so worn that no enamel is present in occlusal view. The p2 has a single large cusp (Fig. 5A). On some unworn upper molars, denticules are present on the metaloph (Fig. 5E), and we interpreted that as intraspecific variation. A small paraconid is present. Three crest extends posterior to the main cusp. A small hypoconid is present. The p3 display a protoconid larger than the metaconid. They are closely appressed. A cristid obliqua links the protolophid to the hypoconid. The paraconid is absent. The p4 is submolariform. The protoconid is larger than the metaconid, and

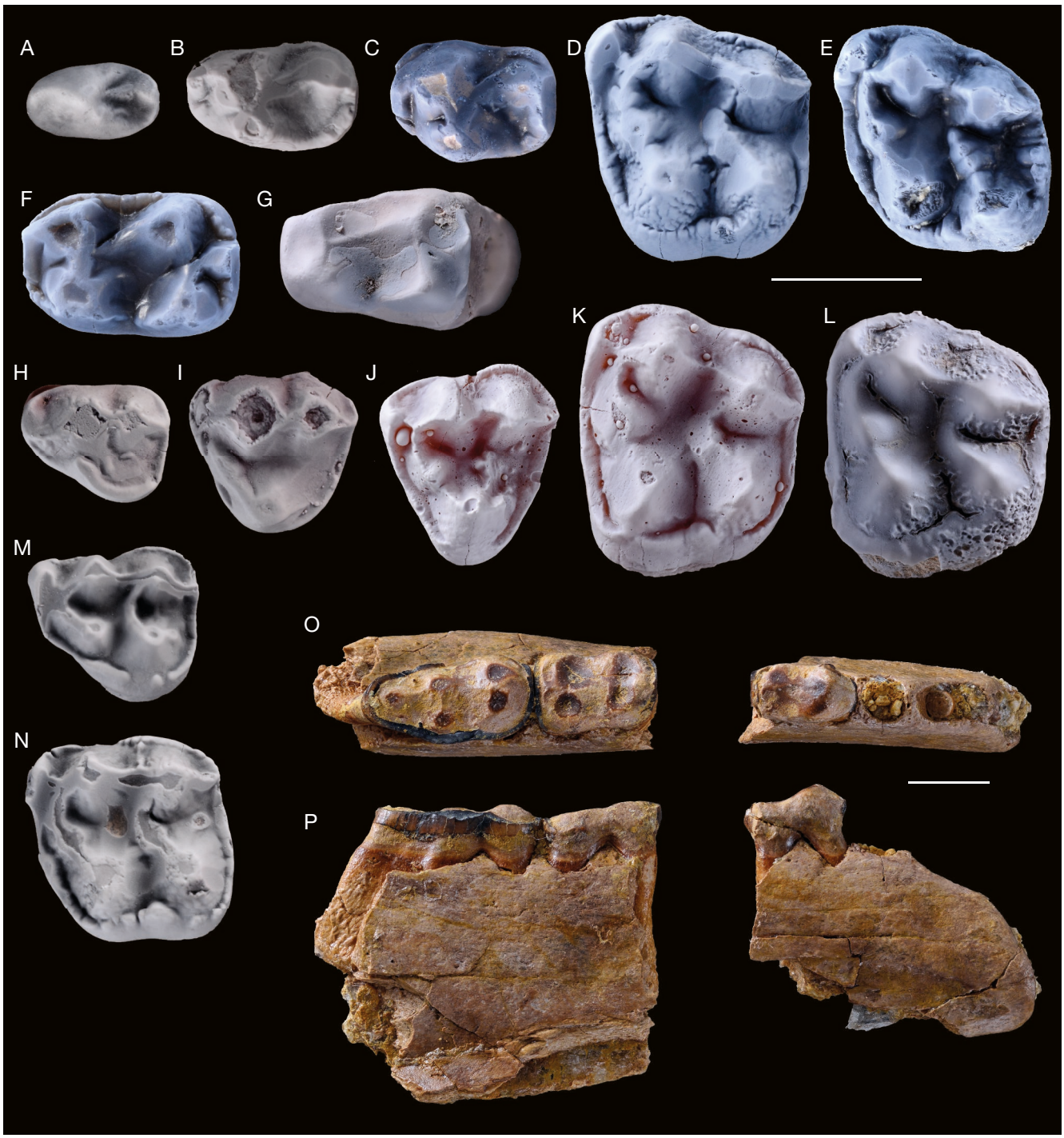

Fig. 5. — Teeth of *Pliolophus quesnoyensis* Bronnert, Gheerbrant, Godinot & Métais, 2018 from Le Quesnoy, Try, Meudon and Sinceny: **A**, left p2 (MNHN-QNY2-3076); **B**, left p3 (MNHN-TRY16); **C**, left p4 (MNHN-TRY22-L); **D**, right M1/2 (MNHN-M-TRY23 [reversed]); **E**, left M3 (MNHN-M-TRY8); **F**, left m1 (MNHN-M-TRY5 [reversed]); **G**, left m1/2 (MNHN-ME16322 [reversed]); **H**, right DP2 (MNHN-SY3-Cn [reversed]); **I**, right P3 (MNHN-SY1-Cn [reversed]); **J**, left P4 (MNHN-SY5-DE); **K**, left M1/2 (MNHN-SY4-DE); **L**, right M1/2 (MNHN-ME16325 [reversed]); **M**, right DP3 (MNHN-M.TRY10 [reversed]); **N**, right DP4 (MNHN-M.TRY3 [reversed]); **O**-**P**, left mandible with p4, m2-m3 (coll. Phélizon); **A**-**O**, occlusal views; **P**, mesial view; **A**-**N**, coated with magnesium; **H**-**K**, casts. Scale bars: 5 mm.

they are closely appressed. The hypoconid is large and linked to the protolophid by the cristid obliqua. The m1 displays a cristid obliqua oriented slightly labially. The hypolophid is formed by two crests. A transversal crest linked to the entoconid extends toward the hypoconid and this crest suddenly becomes directed toward the hypoconulid, thus forminga right angle (Fig. 5F). A very faint crest extends from the hypoconid toward the transversal crest starting from the entoconid and reaches the point where the latter forms a right angle. This configuration of the hypolophid is unusual in *P. quesnoyensis* in which the hypolophid is generally formed by a transversal crest joining the hypoconid

Deciduous teeth
The DP2 possesses a large paracone, much larger than the metacone (Fig. 5H). The parastyle is small. There is neither protocone nor hypocone, but a developed cingulum is present on the anteriolingual margin. The DP3 displays a larger parastyle (Fig. 5M). There is no metaconule nor paraconule. The hypocone is larger than the protocone. The cingulum is interrupted close to the hypocone. The DP4 has a protocone larger than the hypocone (Fig. 5N). A small paraconule and metaconule are present. The centrocrista is straight. The cingulum is continuous.

Family *incertae sedis*

Genus *Cymbalophus* Hooker, 1984

Cymbalophus Hooker, 1984: 230.

TYPE SPECIES. — *Hyracotherium cuniculus* (Owen, 1842) by original designation.

INCLUDED SPECIES. — *Cymbalophus hookeri*.

EMENDED DIAGNOSIS (based on Hooker 1994). — Moderate lophodonty. Hypoconulid of m1-2 small and closely appressed to the hypolophid. Hypoconulid of m3 linked to the hypoconid. Medium sized upper molar paraconule, metaconule smaller. Centrocrista of upper molar straight.

DIFFERENTIAL DIAGNOSIS. — Smaller than *Pliolophus* and *Hyracotherium*. Hypoconulid of m1-2 small and closely appressed to the hypolophid, whereas it is linked to the hypoconid in *Pliolophus*. More developed lophodonty than *Pliolophus* and *Hallensia*. Differs from *Hyracotherium* by the absence of mesostyle.

NOTES
The genus *Cymbalophus* was created by Hooker (1984) for the species *C. cuniculus*, previously classified within *Hyracotherium* (Owen 1842). Hooker (1984) considered *Cymbalophus* as a ceratomorph, not a hippomorph. Hooker (1994) subsequently considered this species to be a hippomorph, but its phylogenetic position is still debated, probably because the type species is poorly known.

Cymbalophus cuniculus (Owen, 1842)
(Fig. 6)

Hyracotherium cuniculus Owen, 1842: 1-2, figs 2, 5. — Forster-Cooper 1932b: 438-441, figs 1A, C, 2B, E, F, 6, 9, pl. 51. — Simpson 1952: 196-204, fig. 4B. — Hooker 1980: 104-108, fig. 1.

Macacus [sic] – Wood 1839: 444-445, fig. 57.

Macacidae [sic] – Owen 1839: 446-448, fig. 58.

Macacus eocaenus Owen, 1846: 1-10, figs 1, 3.

Hyracotherium sp. – Teilhard de Chardin 1927: 27, 28, figs 28c, 22, pl. 5.

Hyracotherium [sic] – Quinet & Verlinden 1970: 1-10, pls 2-3.

Cymbalophus cuniculus – Hooker 1984: 230-237, figs 1-12.

LECTOTYPE. — BMNH-36569, M3.

MATERIEL. — see Hooker 1980, 1984.

TYPE LOCALITY. — Kyson, United-Kingdom.

DISTRIBUTION. — Kyson (United-Kingdom); Erquelinnes, (Belgium), MP7.

EMENDED DIAGNOSIS. — Lower molar cristid obliqua joining the protolophid, slightly labially. Straight upper molar centrocrista. Short p1-p2 diastema.

DIFFERENTIAL DIAGNOSIS. — Larger than *C. hookeri*. More labially oriented cristid obliqua, less developed and straighter centrocrista than *C. hookeri*. Reduced m1-2 hypoconulid that is closely appressed to the hypolophid, whereas it is linked to the hypoconid in *Pliolophus*.

DESCRIPTION
Erquelinnes mandible
The alveoli indicate that three incisors are present on each hemimandible. The alveoli indicate that the canines are large and anteriorly oriented (Fig. 6A). The left hemimandible shows a reduced alveolus of p1 (less than 1 mm). The right hemimandible is broken at the level of the p1 alveolus, but this alveolus seems larger than that of the left hemi-mandible. The symphysis is long and narrow. The post-canine diastema is long (9 mm), and the post-p1 diastema is shorter (4 mm on the right hemi-mandible). The p3 displays a small paraconid (Fig. 6F). The protoconid is larger than the metaconid. The hypoconid is developed. The cingulum extends lingually toward the hypoconid. The protoconid and metaconid of p4 are well-separated. Two crests extend lingually from the hypoconid. One is transversal (possibly the posthypocristid), and the second is oriented posteriorly toward a small cingular bulge, located at the position of the hypoconulid. A small entoconid is present. The cristid obliqua ends on the lingual side of the protoconid. The m1-2 have a twinned metaconid (Fig. 6F). The metaconid and the entoconid are higher than the protoconid and the hypoconid. The cristid obliqua ends on the lingual side of the protoconid. The paralophid is short. The protolophid is slightly notched. The hypolophid is more deeply notched than the protolophid. The hypoconulid is closely appressed to the hypolophid, but slightly more lingually placed. The labial part of the hypolophid joins the lingual part anterior to the hypoconulid. The cingulum is continuous.

Fossils from Kyson
The P3 is nonmolariform (Fig. 6D). The paraconule is small but well defined. A very small metaconule is present and linked to the metacone by a small crest. The postprotocrista runs from the protocone to the lingual side of the metaconule. The cingulum is continuous and posteriorly elongated. The parastyle of upper molars is small (Fig. 6E). The centrocrista is straight and low. The paraconule is small and the metaconule is absent or very weak. The cingulum is well developed and continuous. The metaloph is interrupted close to the metacone. A small crest is present between the metaloph and the metacone. The m3 lophids are well developed (Fig. 6C, G).

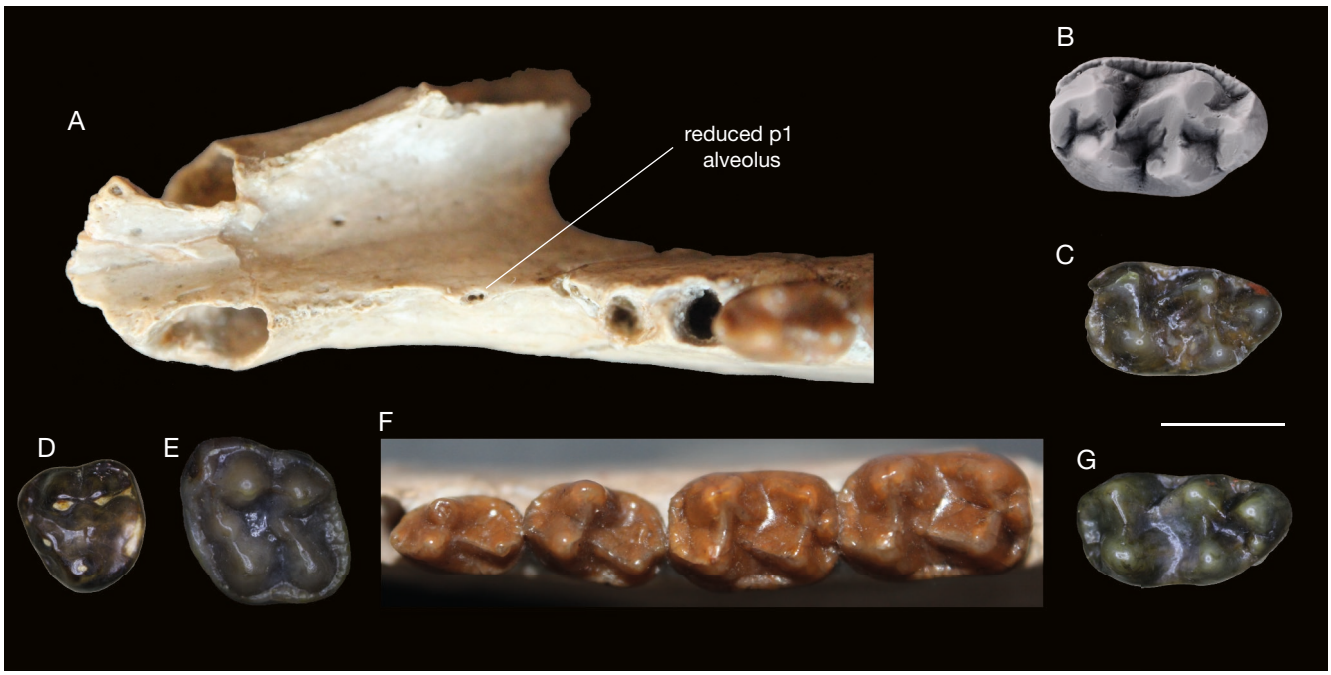

Fig. 6. — Teeth of *Cymbalophus cuniculus* (Owen, 1842) from Erquelinnes and Kyson, and *C.* aff. *cuniculus* from Condé-en-Brie in occlusal view; **A**, mandibular symphysis (IRSNB-M-167); **B**, right m3 (MNHN-CB1597); **C**, right m3 (BMNH-14113); **D**, left P3 (BMNH-36572); **E**, left M3 (lectotype, BMNH-36569); **F**, left p3-m2 (IRSNB-M-167); **G**, right m3 (BMNH-29710). **B**, coated with magnesium. Scale bar: 5 mm. Photo credits A, C-G, C. Bronnert.

The cristid obliqua is oriented labially. The metaconid can be twinned or not. A small pre-entocristid is present. The hypoconulid lobe is small and narrow. The hypoconulid is linked to the hypoconid by a postcristid.

Comparisons

The lower canine of *C. cuniculus* is anteriorly oriented, whereas it is more lateral in *Pliolophus quesnoyensis* and *P. barnesi*. The symphysis is long and narrower than in *Pliolophus*. The m3 cusps are more obliquely aligned in *C. cuniculus* than in *P. quesnoyensis*, and a pre-entocristid is present. The upper molar cingulum is continuous, whereas it is interrupted close to the hypocone in *Pliolophus*, but the intraspecific variability of *Cymbalophus* is unknown. The lower molar hypoconulid-hypolophid junction (hypoconulid closely appressed to the hypolophid) in *C. cuniculus* is similar to that of *Sifrhippus sandrae* (Gingerich, 1989), but differs from the hypoconulid-hypoconid junction observed in *Pliolophus* (hypoconulid linked to the hypoconid by a postcristid). The cusps of p3 are spaced and transversally aligned, whereas they are closely appressed and obliquely aligned in *Cymbalophus* aff. *cuniculus* from Rians (Godinot 1981). The p4 trigonid is larger than in *C.* aff. *cuniculus* from Rians.

Comment

The mandible from Erquelinnes possesses a reduced p1 alveolus on the left ramus. The right ramus is broken at the level of the p1 alveolus, which seems much larger in posterior view than on the left ramus. We hypothesize that the p1 was about as large as in *Pliolophus*. Thus, the left p1 was probably broken during the animal's life, and the corresponding alveolus was probably reabsorbed (Thierry Smith pers. com.).

On the mandible from Erquelinnes, m1-2 display a twinned metaconid, but the m3 is missing. The same character is observed on a m3 (1951.28.25) housed in the collection of the Ipswich museum and referred to *C. cuniculus* by Hooker (1984). The rest of the m3 referred to this species display predominantly a unicuspid metaconid according to Hooker (1984). Whether a twinned metaconid is present on the m1-2 is not clear on the few specimens collected in Kyson because those molars are generally heavily worn.

Cymbalophus aff. *cuniculus*
(Fig. 6B)

Material. — m3 (R: MNHN-MU12263 [broken]; L: MNHN-CB1597).

Distribution. — Mutigny, Condé-en-Brie (MP8+9).

Description

m3 from Mutigny

The tooth is worn and broken, only the talonid is preserved. The hypoconulid lobe is very short.

m3 from Condé-en-Brie (Fig. 6B)

The metaconid is not twinned. The lophs are high and well developed. The protolophid is more notched than the hypolophid. The hypoconulid is small, the hypoconulid lobe is very short. A postcristid links the hypoconid to the hypoconulid. The cristid obliqua is oriented toward the middle of the protolophid.

Comparisons
The teeth have the same proportion as those of *C. cuniculus*. The protolophid is less developed than in *C. cuniculus*, and the cristid obliqua is slightly more lingual. The cristid obliqua ends higher on the protolophid than in *C.* aff. *cuniculus* from Rians (Godinot 1981). The paralophid is much shorter than in *C.* aff. *cuniculus* from Rians.

Comment
The dental morphology is very similar to that of *C. cuniculus*, except for the more lingually directed cristid obliqua which is a derived feature. However, such a character could be intraspecific variation (*C. cuniculus* is not well known), or temporal and/or geographic variation within a population. The fossil record of *Cymbalophus* is very scarce as this genus has been recorded only from localities close to the MP7. The discovery of specimens in Condé-en-Brie and Mutigny (MP8-9) extends its range, and this allows to assume some morphological variation of the species through time. Nevertheless, considering the few fossils discovered for this species in these MP8-9 localities, and particularly in Prémontré (MP10) which has yielded a large number of specimens, we do not exclude that this is an extreme and poorly represented variation of *Orolophus maldani*, which is widespread in these deposits.

Genus *Hyracotherium* Owen, 1841

Hyracotherium Owen, 1841: 203-206.

Type species. — *Hyracotherium leporinum* Owen, 1841 by original designation.

Diagnosis. — Same as the type species.

Hyracotherium leporinum Owen, 1841
(Fig. 7)

Hyracotherium leporinum Owen, 1841: 203-206; 1865: 340 (*partim*), pl. 10, fig. 2. — Depéret 1901: 200-201 (*partim*), pl. 4, fig. 1. — Savage *et al.* 1965: 6-8, fig. 2h. — Lydekker 1886: 11.

Hyracotherium aff. *leporinum* – Hooker 1994: 53-57, fig. 20.

Holotype. — BMNH M16336, skull with right P2-M3 and left P4-M2.

Material. — **Herne Bay** (see Hooker 1980, 1994).

Mutigny: P4 (R: MNHN-MU5919); M1/2 (R: MNHN-MU220-L, MU12329 [broken]; L: MNHN-MU222-L, MU17167, MU12375 [worn]); M3? (L: MNHN-MU192-L); dp3 (L: MNHN-MU200-L); p3 (R: MNHN-MU5640), dp4 (R : MNHN-MU12300, MU12385 [broken]); p4 (L: MNHN-MU6574) ; m1/2 (R: MNHN-MU12292 [broken]); m3 (R: MNHN-MU12378; L: MNHN-MU1210 [broken], MU6567 [broken]).

Avenay: dP3 (L: MNHN-AV4664, AV14684); P4 (R: MNHN-AV42-Ph; L: MNHN-AV4789); M1 (L: MNHN-AV65514); M1/2 (L: MNHN-AV1012-L); dp4 (R: MNHN-AV15815); p3 (R: MNHN-AV4634); m3 (L: MNHN-AV14685).

Prémontré: m3 (R: MNHN-SLP-29-PR1906).

Type locality. — Herne Bay (Kent, United-Kingdom), MP8-9.

Distribution. — Mutigny, Avenay (MP8-9), Prémontré (MP10) (France).

Emended diagnosis. — Lower molar hypoconulid linked to the hypoconid. High cristid obliqua oriented toward the center of the protolophid. P2 without labial cusp. Mesostyle or mesostylar crest on upper molars. Developed paraconule.

Differential diagnosis. — Differs from *Pliolophus* and *Cymbalophus* by the presence of a mesostyle on upper molars, and by a more flexed centrocrista.

Description
Teeth
The parastyle of P4 is low (Fig. 7B, G). The paraconule is developed, it is half the size of the protocone. The metaconule is large but smaller than the paraconule. The protoloph is interrupted before joining the preparacrista. A small postprotocrista is present, as well as a small endoprotocrista. The cingulum is continuous. The upper molars parastyle is developed (Fig. 7C-E, H-I). The paraconule and the metaconule are well developed. The centrocrista is labially flexed. A small mesostyle is usually present, often as a ridge starting from the centrocrista but it can be absent (Fig. 7E). The cingulum is continuous, but sometimes interrupted around the hypocone. The protoloph joins the preparacrista, and is sometimes interrupted just before the connection. The metaloph is interrupted at the base of the metacone. The slightly more labially situated hypocone on Fig. 7I could indicate that the tooth is a M3.

The protoconid and metaconid of p3 are quite apart (Fig. 7J, K). A small paraconid is present. The hypoconid is developed and low. The entoconid is absent. The cristid obliqua connects the center of the protolophid to the hypoconid. The p4 metaconid is twinned (Fig. 7M). The entoconid is absent. The hypoconid is low and well developed. The protolophid is notched. The cristid obliqua connects the hypoconid to the protolophid towards its center, slightly labially. The m3 metaconid is twinned (Fig. 7P). The cristid obliqua is oriented towards the center of the protolophid (Fig. 7O, P). The hypoconulid lobe is well developed. A postcristid links the hypoconid to the hypoconulid. The protolophid is notched. The hypolophid is poorly developed.

Deciduous teeth
The parastyle of DP3 is large and anteriorly projected. The centrocrista is almost straight. The hypocone is larger than the protocone. The paraconule and the metaconule are small. The protoloph joins the paracone. The cingulum is almost continuous, slightly interrupted at the level of the hypocone.

The dp3 is very worn. The paraconid is well developed. The heavy wear seems to indicate that the hypoconulid is linked to hypoconid and entoconid. The dp4 is molariform and the talonid is wider than the trigonid. The metaconid is twinned. The cristid obliqua is oriented toward the center of the protolophid. The hypoconulid is low. It is linked to the hypoconid by a postcristid. The protolophid is notched. The hypolophid is low.

Comparisons
The morphology of the P2, with no protocone, is not found in other European hippomorph species but can be observed on

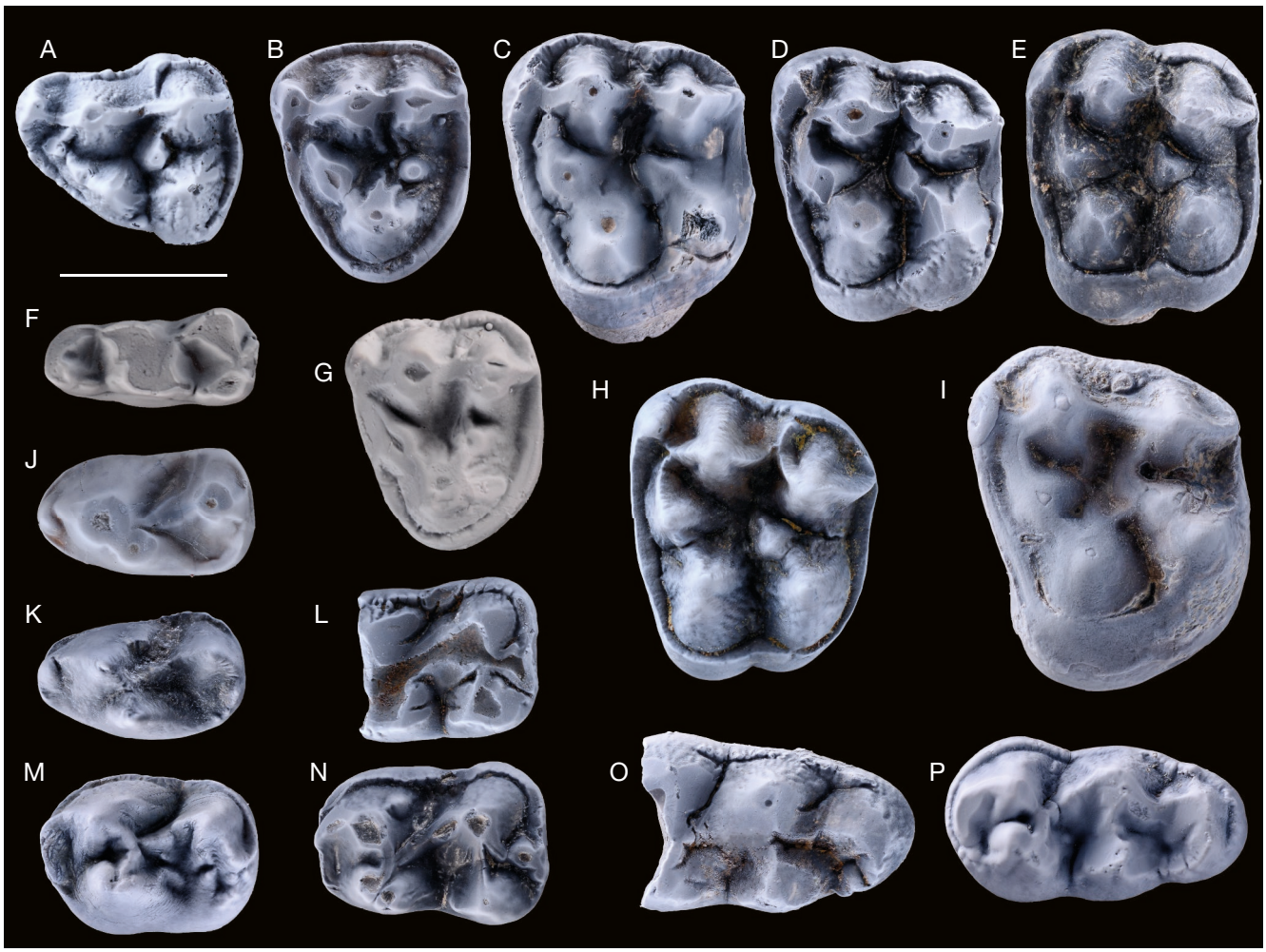

Fig. 7. — Teeth of *Hyracotherium leporinum* Owen, 1841 from Mutigny and Avenay in occlusal view: **A**, left DP3 (MNHN-AV14684); **B**, right P4 (MNHN-MU5919 [reversed]); **C**, left M1/2 (MNHN-MU17167); **D**, right M1/2 (MNHN-MU220-L [reversed]); **E**, left M1/2 (MNHN-MU222-L); **F**, right dp3 (MNHN-MU200-L); **G**, right P4 (AV-42-Ph [reversed]); **H**, left M1/2 (MNHN-AV1012-L); **I**, left M1/2 (MNHN-MU192-L); **J**, right p3 (MNHN-AV4634); **K**, right p3 (MNHN-MU5640); **L**, right dp4 (MNHN-AV15815); **M**, left p4 (MNHN-MU6574 [reversed]); **N**, right dp4 (MNHN-MU12300); **O**, left m3 (MNHN-MU1210 [reversed]); **P**, right m3 (MNHN-SLP-29-PR1906). Coated with magnesium. Scale bar: 5 mm.

some American equids, such as *Orohippus* and '*Hyracotherium*' *craspedotum*. The upper molar centrocrista is more flexed than in *Pliolophus* and *Cymbalophus*. A mesostyle is present while it is absent in *Pliolophus* and *Cymbalophus*. The m3 postcristid links the hypoconid in a more lingual position than in *Pliolophus* and *Cymbalophus*, but more labially than in *Orolophus* and *Propalaeotherium gaudryi* in which the hypoconulid is connected to the hypolophid. *Hyracotherium* is larger than *Sifrhippus sandrae*. The upper molar centrocrista is more flexed than in *S. sandrae*, and the mesostyle is always absent in *S. sandrae*. The upper premolar metaconule is larger in *Hyracotherium* than in *S. sandrae*.

Comment

The upper molars of the Mutigny specimens resemble those of the type-specimen and specimens found in the London Clay in England. In contrast, the lower molars show some differences with the Sheppey mandible (Hooker 1994). The metaconid is twinned and the hypoconulid lobe of m3 is wider in the Paris Basin, but this may result from intra-specific variation.

Family Equidae Gray, 1821

Genus *Sifrhippus* Froehlich, 2002

Sifrhippus Froehlich, 2002: 159-161.

Type species. — *Hyracotherium sandrae* Gingerich, 1989, by original designation.

cf. *Sifrhippus sandrae* Gingerich, 1989

cf. *Sifrhippus sandrae* – Missiaen *et al.* 2013: 271, fig. 7E-G.

Material. — m3 (R: IRSNB-M-130) (Missiaen *et al.* 2013).

Locality. — Erquelinnes, Belgium.

Description

The paralophid is short. The cristid obliqua is oriented toward the lingual side of the protoconid. The hypolophid is absent. The hypoconulid is small, the lobe is very short. A post-cristid

links the hypoconid to the hypoconulid. A small cusp is present lingually to the hypoconulid. The labial cingulum is dimmed close to the hypoconid.

Comparisons

The cristid obliqua is oriented toward the protolophid, close to the lingual side of the protoconid, as in *Pliolophus quesnoyensis* and *Sifrhippus sandrae* (Gingerich, 1989). It is more central in *Pliolophus barnesi*. The hypolophid is absent, as in some *S. sandrae*, or the extreme morphotypes of *P. quesnoyensis* (MNHN-QNY2-2801). The lobe of the hypoconulid is very short, as in *S. sandrae* and *Cymbalophus*.

Comment

This tooth, the only perissodactyl remains of the lower level from Erquelinnes, is probably the oldest known perissodactyl fossil from Europe. Its morphology is very similar to that of *Sifrhippus sandrae* (Gingerich, 1989), an American hippomorph. However, the dental variability of *Cymbalophus cuniculus* is poorly known, and we cannot rule out that this tooth belong to this species.

Family Palaeotheriidae Bonaparte, 1850
Subfamily Pachynolophinae Pavlow, 1888

Genus *Propalaeotherium* Gervais, 1849

Propalaeotherium Gervais, 1849: 383.

Type species. — *Propalaeotherium isselanum* Gervais, 1849 by original designation.

Included species. — *P. argentonicum* Gervais, 1849; *P. hassiacum* Haupt, 1925; *P. helveticum* Savage, Russell & Louis, 1965; *P. voigti* Matthes, 1977; *P. gaudryi* Lemoine, 1878.

Diagnosis of genus (modified from Remy *et al.* 2016). — Small to large Eocene equoids with estimated skull length from 120 to over 250 millimeters; dental formula: 3.1.4.3/3.1.4.3; brachylophodont dentition; upper molars with more or less pronounced mesostyle; upper premolars non-molariform, lacking hypocone; mesostyle on P3-4/ and entoconid on P/3-4 appearing in youngest species; lower cheek teeth without paraconid; lower molars with rounded crescentic lobes and prominent metaconid that is twinned; lingual cingula on upper molars, usually weak or absent; lower cheek teeth with more or less developed labial cingula, but with weak or absent lingual cingula; rather short postcanine diastema. *Propalaeotherium* differs from *Eurohippus* by a wider skull and narrower ascending ramus with regard to its height.

Propalaeotherium gaudryi (Lemoine, 1878)
(Figs 8; 9)

Pachynolophus gaudryi Lemoine, 1878: 19.

Pachynolophus (*Propachynolophus*) *gaudryi* – Lemoine 1891: 285-286, figs 109-115.

Hyracotheryus [sic] – Lemoine 1891: 266, pl. XI, fig. 121.

Propachynolophus gaudryi – Teilhard de Chardin 1921: 71-73, fig. 35. — Savage *et al.* 1965: 15-27, figs 7-8, 10-11.

Propalaeotherium gaudryi – Remy 2017: figs 1A-C, 2A-D, 10A, B, 12A-C.

Lectotype (Savage *et al.* 1965). — MNHN-AL5210, fragmentary left mandible with m1-m3.

Material. — **Ageian**: Maxillary (composite) with P2-M3 (L: MNHN-AL6540); dP3 (R: MNHN-AL5219, AL6560); P3 (R: MNHN-AL6539); M2 (R: MNHN-AL6549; L: MNHN-AL6533, AL6553); M1/2 (R: MNHN-AL6534, AL6536; L: MNHN-AL6565); M3 (R: MNHN-AL6532, AL6547; L: MNHN-AL6566); symphysis (MNHN-AL5214); mandible p1-p4 (L: MNHN-AL5212); mandible p3-m3 (MNHN-AL5211); mandible m2-m3 (L: MNHN-AL5213); p1 (L: MNHN-AL5218); p3 (R: MNHN-AL6542; L: MNHN-AL6541); p4 (R: MNHN-AL6544); astragalus (R: MNHN.unumbered), calcaneus (L: MNHN.unumbered).
Chavot: M1/2 (R: MNHN-CHO15569; L: MNHN-CHO15519, CHO15521); mandible dp1-m3 (L: MNHN-CHO14953 [cast]); mandible dp3-m2 (L: MNHN-CHO14801); mandible p2-m3 (L: MNHN-CHO14884); mandible p4-m3 (L: MNHN-CHO14911); mandible m2-m3 (L: MNHN-CHO14789); symphysis (MNHN-CHO14787).
Cuis: maxillary P2-M3 (L: FSL-2096); maxillary P3-P4 (R: MNHN-CUI15540); P3 (R: MNHN-CUI15548); M1/2 (R: MNHN-CUI15537, CUI15538, CUI15546, CUI-5-L; L: MNHN-2003-2-78, MNHN-CUI15506, CUI15513); dp4 (R: MNHN.2003-2-20); p4 (L: MNHN-CUI15510); m1 (R: MNHN-CUI15511; L: MNHN-CUI15504); m2 (L: MNHN-CUI15505); m1/2 (R: MNHN-CUI15545); m3 (R: MNHN-CUI192, MNHN-2003-2-18); humerus (L: MNHN.2003-2).
Grauves: Maxillary M2-M3 (R: MNHN-GR61-L; L: MNHN-GR62-L); M1 (R: MNHN-GR60-L; L: MNHN-GR42-L, MNHN-GR46-L); M1/2 (R: MNHN-GR29-L); mandible m1-m3 (L: MNHN.unnumbered); upper canine (MNHN-GR280-L); dP3 (R: MNHN-GR7888, GR187); dP4 (L: MNHN-GR8-L); P2 (R: MNHN-GR7400, GR7401, GR276-L); upper premolar (R: MNHN-GR14-L); P3 (R: MNHN-GR7380, GR24-L, GR28-L, GR32-L; L: MNHN-GR7576, GR13-L, GR39-L); P4 (R: MNHN-GR10850, GR10-L, GR36-L, GR268-L; L: MNHN-GR7573, GR31-L, GR40-L); M1/2 (R: MNHN-GR7409, GR10847, GR10841, GR10786, GR10787, GR271-L, GR193-L; L: MNHN-GR7408, GR10839, GR10849, GR15-L); M3 (L: MNHN-GR59-L); mandible m1-m3 (R: MNHN-GR10788); dp3 (R: MNHN-GR7890; L: MNHN-GR10784); dp4 (R: MNHN-GR180); p1 (MNHN-GR7546); p2 (MNHN-GR7-L); p3 (R: MNHN-GR4-L; L: MNHN-GR48-L); p4 (R: MNHN-GR7572, GR266-L; L: MNHN-GR2-L, GR18-L); m1 (L: MNHN-GR7381); m1/2 (R: MNHN-GR20-L, GR57-L; L: MNHN-GR7571, GR26-L, GR27-L, GR55-L, GR272-L); m3 (R: MNHN-GR10776, GR34-L, GR50-L, GR52-L, GR56-L; L: MNHN-GR17-L, GR45-L, GR47-L, GR270-L); metacarpal II (R: MNHN.F.GR18004); astragalus (R: MNHN-GR10911); metatarsal III (L: MNHN.F.GR18002, MNHN.F.GR18003); metatarsal IV (R: MNHN.F.GR18001; L: MNHN.F.GR18000).
Mancy: Maxillary P1-M3 (L: MNHN-MA14948); maxillary M1-M2 (L: MNHN-MA14795); maxillary M1-M3 (R: MNHN-MA14948); maxillary M2-M3 (L: MNHN-MA14788, MA14802); P2 (L: MNHN-MA61-L); M1/2 (R: MNHN-MA14988, MA14995; L: MNHN-MA14989, MA14990, MA14993, MA14994, MA14996, MA39-L, MA50-L, MA54-L, MA56-L); M2 (R: MNHN-MA15571); M3 (L: MNHN-MA14985); mandible dp4-m1 (R: MNHN-MA3-L); mandible p1-m3 (L: MNHN-MA9-L); mandible p3-m3 (R: MNHN-MA14902; L: MNHN-MA14907); mandible p4 (R: MNHN-MA14977); mandible p4-m3 (R: MNHN-MA14886; L: MNHN-MA10-L); mandible m1 (L: MNHN-MA14796); mandible m1-m3 (R: MNHN-MA14883 [cast]); mandible m2 (L: MNHN-MA14803);

FIG. 8. — Lower teeth and mandibles of *Propalaeotherium gaudryi* (Lemoine, 1878) from the Paris Basin: **A**, **B**, p1 (MNHN.F.GR7546) in lateral (**A**) and occlusal (**B**) views; **C**, left dp3 (MNHN.F.GR10784 [reversed]) in occlusal view; **D**, right mandible with dp4-m1 (MNHN.F.MA3-L) in occlusal view; **E**, right p4 (MNHN.F.GR7572) in occlusal view; **F**, right mandible with dp3-m2 (MNHN-CHO14801) in occlusal view; **G**, left mandible with p1-p4 (MNHN.F.AL5212 [reversed]) in occlusal view; **H**, **O**, left mandible with m1-m3 (holotype MNHN.F.AL5210 [**H**, reversed]) in occlusal (**H**) and lateral (**O**) views; **I**, **K**, right mandible with p3-m3 (MNHN.F.MA14902) in occlusal (**I**) and lateral (**K**) views; **J**, **L**, right mandible with m1-m3 (MNHN.F.GR10788) in occlusal (**J**) and lateral (**L**) views; **M**, **N**, symphysis (MNHN-CHO14787) in anterior (**M**) and occlusal (**N**) views. **A**-**F**, **H**, coated with magnesium. Scale bars: 5 mm.

mandible m2-m3 (R: MNHN-MA14791; L: MNHN-MA14790); mandible m3 (R: MNHN-MA14797, MA14793, MA70-L; L: MNHN-MA14978); symphysis (MNHN-MA14908, MA14786); P1 (R: MNHN-MA78-L); P2 (L: MNHN-MA14842); M3 (R: MNHN-MA75-L); dp4 (R: MNHN-MA14755); p1 (L: MNHN-MA29-L); p2 (L: MNHN-MA15501); p3 (R: MNHN-MA23-L; L: MNHN-MA14739, MA15502); p4 (R: MNHN-MA27-L; L: MNHN-MA15573, MA25-L); m1 (L: MNHN-MA14986, MA14999); m1/2 (R: MNHN-MA14754, MA17-L, MA18-L, GR30-L); m3 (L: MNHN-MA21-L, MA22-L), metacarpal II (R: MNHN.F.MA18001); metatarsal III (R: MNHN.F.MA18000); metatarsal IV (R: MNHN.F.MA18002).
Mont Bernon: p3 (R: MNHN-B5-L); p4 (R: MNHN-B10-L); m3 (L: MNHN-B4-L); metatarsal III (L: MNHN.F.MTB18000).
Monthelon: Maxillary DP3-DP4 (L: MNHN-MTH53-L); maxillary M1-M3 (L: MNHN-MTH48-L); incisor (MNHN-MT23-L); upper canine (R: MNHN-MTH45-L; L: MNHN-MTH57-L); P4 (R: MNHN-MTH24-L); M1/2 (L: MNHN-MTH14-L, MTH44-L, MTH56-L, MTH57-L); mandible dp3-m3 (R: MNHN-MTH5-L); mandible p3-m3 (R: MNHN-MTH2-L); p4 (L: MNHN-MTH22-L), m1/2 (R: MNHN-MTH54-L); m3 (R: MNHN-MTH27-L), metatarsal II (L: MNHN.F.MTH18000).
Saint-Agnan: Fragmentary m3 (R: MNHN-STA605-L).

TYPE LOCALITY. — Environs d'Epernay, Cuisien (Ageian), MP10.

DISTRIBUTION. — Grauves, Cuis, Mancy, Monthelon, Mont Bernon, Chavot, St Agnan.

EMENDED DIAGNOSIS (modified from Savage *et al.* 1965). — Medium sized hippomorph (estimated skull length: 170-200 mm); well-developed lophodonty; hypoconulid linked to the middle of the hypolophid; cristid obliqua oriented lingually; lower molar lophs slightly notched.

DIFFERENTIAL DIAGNOSIS. — Much larger than all the other hippomorph species from the MP10 or earlier related localities of the Paris Basin. More lingual cristid obliqua than *O. maldani*, cingula generally more developed than *O. maldani*. More developed lophodonty than *O. maldani*.

DESCRIPTION

Teeth

The symphysis of the mandible is long (3.5 cm on MNHN-MA14902) and narrow (1.3 cm on MNHN-MA14902). The lower post-canine diastema is long (2.2 cm on MNHN-MA14902; 3 cm for MNHN-MA14908), but there is no post-p1 diastema (Fig. 8I). The p1 is simple and unicuspid. It can be uniradiculate (MNHN-MA14902, female morphotype, Fig. 8I) or biradiculate (MNHN-CHO14801, MNHN-MA9-L, male morphotype, and Fig. 8F, juvenile). The protoconid and metaconid of p2 are close one each other and obliquely aligned. A crest extends between the hypoconid and the labial side of the metaconid. The p3 is larger than the p2 but displays the same morphology. The protoconid and metaconid of p4 are close and almost aligned transversally. The entoconid is absent or well developed (MNHN-GR7572). A crest extends from the hypoconid to the labial side of the metaconid. The metaconid is twinned on MNHN-GR7572, and barely visible on most teeth due to the wear. The paralophid of m1-m2 is very short (Fig. 8I, J, H). The metaconid is twinned and the two cusps are aligned obliquely. The cristid obliqua joins the labial side of the metaconid. The hypoconulid is reduced and almost lingual. The postcristid is connected to the hypoconulid and to the hypolophid, at the level of the notch which lies closer to the entoconid. The cingulum is very reduced between protoconid and hypoconid, or absent. The paralophid of m3 is short, and the metaconid is twinned. The cristid obliqua joins the metaconid. The lobe of the hypoconulid is developed, it has the same length than the anterior part of the talonid, but stays narrower. The postcristid is linked to the center of the hypolophid, at mid-height. It forms an obliquely oriented horseshoe with the lingual part of the hypoconulid. The protolophid and the hypolophid are slightly notched.

The upper post-canine diastema is long (1.8 cm in MNHN-MA14948). There is no post-P1 diastema. The P1 is simple, elongated and posteriorly enlarged. One or two cusps are present labially. The P2 has three roots and the paracone and metacone are developed. Two morphologies of P2 are observable. In the first one, the P2 is triangular in occlusal view (MNHN-MA14948, Fig. 9J), the protocone is shifted anteriorly and aligned transversely with the paracone, the paraconule and metaconule are absent, the protoloph is interrupted before joining the preparacrista, the parastyle is absent. The second morphology of P2 (MNHN-GR7400, Fig. 9A; MNHN-MA14842, Fig. 9B) displays a posteriorly enlarged premolar in occlusal view, with a posteriorly displaced protocone, which is aligned transversely with the metacone. The metacone is reduced sometimes missing (Fig. 9A). The protoloph is short and interrupted before joining the preparacrista. A cingular ridge extends posteriorly to the protocone. The parastyle is absent, but a small metastyle is present. The paraconule of P3 is small compared to the protocone and paracone, and the metaloph is located in the center of the tooth and interrupted labially at the base of the metacone. The parastyle of P4 is poorly developed (Fig. 9D). The metaconule is absent and the paraconule is wide. The metaloph (possibly the postprotocrista) is directed toward the middle of the two labial cusps, but preferably towards the metacone, and stops at the base of these cusps. The protoloph is interrupted before joining the preparacrista. The mesostyle of upper molars is generally absent (Fig. 9I, J), but it can be sometimes present as a small or developed crest running upward from the cingulum (Fig. 9F, G). The centrocrista is more or less labially flexed and high. The paraconule is larger than the metaconule, and both are well merged in the lophs. The cingulums are well developed but sometimes interrupted on the lingual side of the teeth. Generally, the M3 has a large enlargement of the posterior cingulum. A fusion of the posterior roots is observable on MNHN-CUI15513.

Deciduous teeth

The metaconule of DP3 is much larger than the paraconule (Fig. 9E, H). The lophs do not reach the labial cusps. The metaloph can form a crescent or is interrupted labially. The protoloph forms a crescent at its labial extremity. The parastyle is developed. The labial cingulum is interrupted

close to the paracone. The DP4 is molariform, but the lingual side is narrower than the labial side (Fig. 9H). The centrocrista is flexed. The parastyle is slightly smaller than the paracone. It projects anteriorly and labially relative to the paracone. The metaconule is very small, and the paraconule is larger, but smaller than the protocone and paracone. The protoloph and the metaloph are well developed. The protoloph joins the preparacrista. The metaloph is interrupted at the base of the centrocrista, between the paracone and the metacone.

The dp2 metaconid is reduced and closely appressed to the protoconid (Fig. 8F). A crest extends anteriorly to the protoconid. A second crest runs from the protoconid to the posterior part of the tooth. The dp3 is molariforme (Fig. 8C, F). A small paraconid is present. The metaconid is twinned. The cristid obliqua joins the protolophid in the middle, slightly lingually. The hypoconulid is closely appressed to the base of the hypolophid, slightly lingually. The dp4 is molariform, and the morphology is similar to that of the molars (Fig. 8D, F). The tooth is slightly narrower at the trigonid, and longer than molars.

Postcranial elements

Humerus. Only the distal part is known. The supracondylar foramen (6 mm large and 5 mm high) perforates the radial fossa (Fig. 9Q, R). The ulnar fossa is triangular and perforated by the supracondylar foramen. The epicondyles are small, but the medial epicondyle projects farther than the lateral epicondyle. A small fovea is present below the medial epicondyle. A larger fovea is present on the lateral epicondyle.

Metacarpals. The metacarpal II is more robust than the metatarsals (Fig. 9Y, Z). The distal articular surface is asymmetrical and keeled. The distal articulation is asymmetric, with a medial part larger than the lateral part. The proximal facet is slightly concave. The trapezoid facet is oval and narrow.

Astragalus. The trochlea is deep and broad, slightly oblique with respect to the vertical axis of the astragalus (Fig. 9K, L). The trochlea does not join the navicular facet. The articular facets are well defined. The navicular facet is saddle-shaped. The ectal and sustentacular facets are well separated (Fig. 9M, N). The sustentacular facet joins the navicular facet. The distal calcaneal facet is laterally elongated.

Calcaneus. It is elongated and medio-laterally flattened (Fig. 9O, P). The calcaneal tuber is laterally compressed. The astragalar facet is small and slightly concave. The sustentacular facet is rounded, slightly triangular. The ectal facet is too worn to be described.

Metatarsals. The second metatarsal is slightly flattened mediolaterally on its proximal part (Fig. 9S). The distal facet was broken away. In dorsal view, the mesocuneiform facet has a concave crescent shape. The triangular entocuneiform facet is present posteriorly. The distal end curves medially away from metatarsal III. The metatarsal III is elongated and straight (Fig. 9T). The proximal cross section is triangular. The metatarsal III is flattened anteroposteriorly, and the distal cross section is elliptical. The proximal facet of articulation with the ectocuneiform is flat. The distal articular surface is symmetrical and keeled. The metatarsal IV is elongated and mediolaterally compressed proximally (Fig. 9U). This compression is less marked at the distal part. The distal articulation is asymmetric, with a medial part larger than the lateral part.

Comparisons

P. gaudryi is larger in size than *Cymbalophus*, *Pliolophus*, *Hyracotherium*, *Orolophus* and *Hallensia*. The teeth of *P. gaudryi* are more lophodont than those of *O. maldani* which is smaller in size (Fig. 10). Their dental morphology is globally similar. The cristid obliqua of *P. gaudryi* is more lingual than that of *O. maldani*. Its cingulums are generally more developed than those of *O. maldani*. There is a wider range of size than other lower Eocene taxa. The upper molar mesostyle is variable, whereas it is always present in *Propalaeotherium sudrei* Remy, Krasovec & Marandat, 2016 and *Propalaeotherium helveticum* Savage, Russell & Louis, 1965. The upper premolar mesostyle is absent in *P. gaudryi* but present in *P. sudrei* and *Propalaeotherium helveticum*. The parastyle is more projected anteriorly than in *P. sudrei*. *P. gaudryi* possesses a metaconule on upper molars, which is absent in *Propalaeotherium isselanum* Cuvier, 1824.

Comment

Apart from the two morphotypes of P2, the dental morphology does not show significant differences. These two morphotypes of P2 are therefore attributed to intra-specific variability.

Lectotype

Teilhard de Chardin (1921) designated the specimen MNHN-AL5210 as a lectotype. Unfortunately, this is a composite specimen whose two pieces were probably associated by Lemoine. The posterior part of the mandible does belong to *Propalaeotherium gaudryi,* but the anterior part (MNHN-AL6685) appears to be from a tapiroid (probably *Chasmotherium* [synonym of *Hyrachyus*]) (Savage *et al.* 1965). Specimen MNHN-AL5210 was therefore designated as a restricted lectotype by Savage *et al.* (1965).

Sexual dimorphism

There is a great disparity in mandible height of the horizontal ramus and diastema length. There is also a great variation in mandible width at the level of incisors. MNHN-CHO14787 has three well-developed incisors on each side, while those of MNHN-MA14902 are narrower and its alveolus indicates a very small I3. The same morphotypes as in *P. eulaliensis* Danilo, Remy, Vianey-Liaud, Marandat, Sudre & Lihoreau, 2013 (Danilo *et al.* 2013), *Pliolophus quesnoyensis* (Bronnert *et al.* 2018) and Lophiodontidae

FIG. 9. — Upper teeth in occlusal view and postcranial elements of *Propalaeotherium gaudryi* (Lemoine, 1878) from the Paris Basin: **A**, right P2 (MNHN-GR7400 [reversed]); **B**, left P2 (MNHN-MA14842); **C**, left P3 (MNHN-GR7576); **D**, left P4 (MNHN-GR7573); **E**, right DP3 (MNHN-GR7888 [reversed]); **F**, right M2 (MNHN-MA15571 [reversed]); **G**, left M3 (MNHN-MA14985); **H**, left maxillary with DP3-DP4 (MNHN-MTH53-L); **I**, left maxillary M2-M3 (MNHN-MA14788); **J**, left maxillary with P1-M3 (MNHN-MA14948); **K**, **M**, right astragalus (MNHN-GR10911) in anterior (**K**) and posterior (**M**) views; **L**, **N**, right astragalus (coll. Louis, MNHN) in anterior (**L**) and posterior (**N**) views; **O**-**P**, left calcaneus (coll. Louis, MNHN) in anterior (**O**) and medial (**P**) views; **Q**, **R**, left humerus (MNHN.F.MT18001) in posterior (**Q**) and anterior (**R**) views; **S**, **X**, left metatarsal II (MNHN.F.MT18000) in anterior (**S**) and posterior (**X**) views; **T**, **W**, left metatarsal III (MNHN.F.GR18003) in anterior (**T**) and posterior (**W**) views; **U**, **V**, left metatarsal IV (MNHN.F.GR18000) in anterior (**U**) and posterior (**V**) views; **Y**, **Z**, right metacarpal II (MNHN.F.MA18001) in anterior (**Y**) and posterior (**Z**) views; **A**-**H**, coated with magnesium. Scale bars: 5 mm.

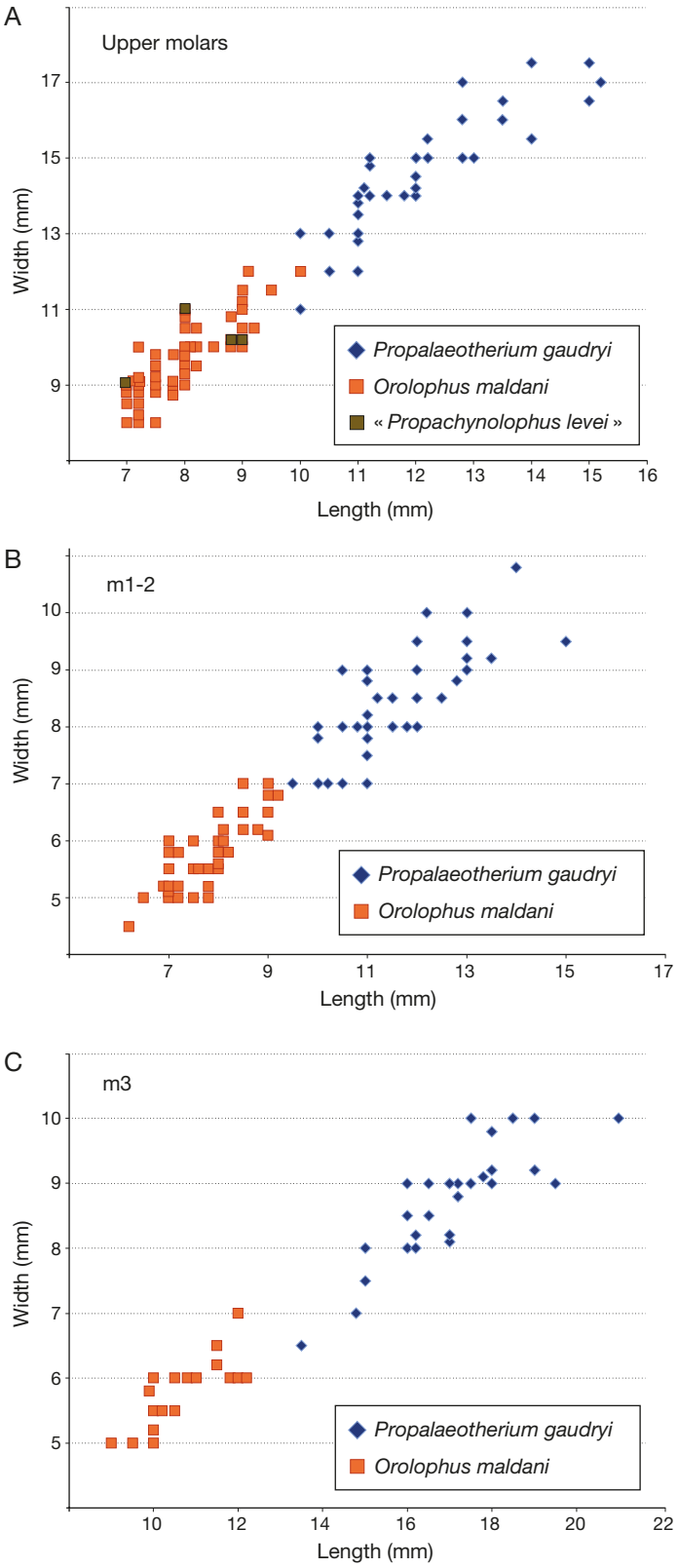

FIG. 10. —Scatter plots showing the distribution of teeth length and width of *Orolophus maldani* (Lemoine, 1878) and *Propalaeotherium gaudryi* (Lemoine, 1878): **A**, upper molars; **B**, m1-2; **C**, m3.

(Vautrin *et al.* 2019) are observable: variation in the height of the mandible and the angle of the vertical branch. Mandibles with a high horizontal ramus and a vertical ascending branch are assigned to males (Fig. 9L), mandibles with a low horizontal ramus and an inclined vertical branch are assigned to females (Fig. 9K, M).

Genus *Orolophus* Remy, 2017

Orolophus Remy, 2017: 14.

TYPE SPECIES. — *Pachynolophus maldani* Lemoine, 1878 by original designation.

DIAGNOSIS (Remy 2017). — Same as the type and only species.

Orolophus maldani (Lemoine, 1878) (Figs 11-13)

Pachynolophus maldani Lemoine, 1878: 24, pls I-V; 56, pls I-IV.

Pachynolophus paracuspidens Lemoine, 1878: 19.

Orotherium remense Lemoine, 1891: 286.

Propachynolophus maldani – Teilhard de Chardin 1921: 61, figs 33-34.

Propachynolophus levei Hooker, 1994: 57-59, fig. 24.

Pliolophus aff. *vulpiceps* – Hooker 1994: 54, fig. 16.

Orolophus maldani – Remy 2017: 14, figs 1-2.

LECTOTYPE (Savage *et al.* 1965). — MNHN-AL5199, right fragmentary mandible with p4 and m2-m3.

MATERIAL. — **Ageian**: symphysis (MNHN-AL5200); mandible dp3-m1 (R: MNHN-AL5201); mandible m1-m2 (R: MNHN-AL5203); mandible m2-m3 (R: MNHN-AL5194; L: MNHN-AL5204); dP4 (R: MNHN-AL6555; L: MNHN-AL6556); M1 (L: MNHN-AL6561); M2 (L: MNHN-AL6564); M1/2 (L: MNHN-AL5207, AL6550, AL6552, AL6562, AL6554); dp3 (R: MNHN-AL5206); dp4 (L: MNHN-AL5206); m1/2 (L: MNHN-AL6543); m3 (R: MNHN-AL6546; L: MNHN-AL5205), metatarsal II (R: MNHN.F.AL18001).
Condé-en-Brie: maxillary dP3-dP4 (L: MNHN-CB1530); maxillary P3-M3 (L: MNHN-CB16165 [cast]); dP3 (R: MNHN-CB4252, MNHN-CB4705; L: MNHN-CB1595, M.CB1C, M.CB306, CB4251, CB786, CB213, CB664, CB4915); dP4 (R: MNHN-CB1556, CB1558, CB1561, CB1564, CB1575, M.CB19, M.CB298, CB77; L: MNHN-CB4667); P2 (R: MNHN-CB1586; L: MNHN-CB1591); P3 (R: MNHN-CB1569, CB1181; L: MNHN-CB1583); P4 (R: MNHN-CB1563, M.CB72, CB5-CA; L: MNHN-CB1581, CB215); M1 (R: MNHN-CB4689, CB4689); M1/2 (R: MNHN-CB1559, CB1566, CB1567, CB1532, M.CB1B, M.CB299, M.CB114, CB4935, CB4736, CB1A; L: MNHN-CB1565, CB1573, CB1531, M.CB297, M.CB225); dp3 (R: MNHN-M.CB194, M.CB199, CB572, CB4730; L: MNHN-M.CB305, M.CB197, M.CB196, CB312); dp4 (R: MNHN-CB1576, CB1589, CB1593, M.CB301, CB221, CB4709; L: MNHN-CB223); p2 (R: MNHN-CB219; L: MNHN-CB1594, CB4702, CB669); p3 (R: MNHN-CB1580, CB1592, M.CB193; L: MNHN-CB1600, CB4700); p4 (R: MNHN-CB1599); m1 (R: MNHN-M.CB38, CB4688; L: MNHN-CB4701); m2 (R: MNHN-M.CB198, M.CB295, MNHN-CB4686, CB4757; L: MNHN-CB918); m1/2 (R: MNHN-CB1579, CB1584, CB1598, CB4703; L: MNHN-CB1578, CB1587, CB1590, M.CB296, CB4687); m3 (R: MNHN-M.CB195, CB8-CA; L: MNHN-CB1571, CB1585, CB4704, CB222); incisor (MNHN-M.CB303).
Cuis: dP4 (R: MNHN-CUI7-L; L: MNHN-CUI6-L); M1/2 (R: MNHN-2003-2 unnumbered; L: MNHN-CUI8-L, CUI10-L, MNHN-CUI11-L, MNHN-2003 unnumbered); dp4 (L: MNHN-CUI15550); p3 (R: MNHN-CUI15549); m1/2 (L: MNHN-2003-2 unnumbered); m3 (L: MNHN-2003-2-80), tibia (R: MNHN.F.CUI18000).
Gland: M1/2 (L: MNHN-GLD41-L [broken]); M3 (L: MNHN-GLD335-L).
Grauves: dP3 (R: MNHN-GR7825, GR242, GR175-L); dP4 (R: MNHN-GR10254, GR1-L); P2 (R: MNHN-GR7803); P4 (R: MNHN-GR7402); M1/2 (R: MNHN-GR7570, GR7568, GR7575, GR7379; L: MNHN-GR7378, GR10779, GR277-L, GR273-L, GR9-L, GR41-L, GR19-L, GR25-L, GR227); mandible p4-m3 (L: MNHN-GR10773); dp3 (R: MNHN-GR7808; L: MNHN-GR7807); dp4 (R: MNHN-GR7809, GR7830; L: MNHN-GR7889); lower premolar (MNHN-GR37-L); p2 (R: MNHN-GR6-L, GR51-L); p3 (R: MNHN-GR3-L); p4 (R: MNHN-GR5-L, GR274-L; L: MNHN-GR7829, GR7829); m1 (L: MNHN-GR178); m1/2 (R: MNHN-GR7383, GR10235, GR10229, GR49-L, GR44-L; L: MNHN-GR7382, GR16-L); m3 (R: MNHN-GR22-L; L: MNHN-GR7569, GR?8-L, GR63-L); astragalus (R: MNHN.F.GR18005); calcaneus (L: MNHN.F.GR18007); metatarsal III (L: MNHN.F.GR18008); distal phalanx (MNHN.F.GR18006).
Mancy: mandible p4-m1 (R: MNHN-MA2-L); mandible p4-m3 (R: MNHN-MA14792); dP4 (L: MNHN-MA24-L); M1/2 (R: MNHN-MA48-L, MA53-L; L: MNHN-MA44).
Mont Bernon: P4 (R: MNHN-BER1); dp4 (L: MNHN-B6-L), humerus (R: MNHN.F.MTB18001).
Monthelon: dP4 (R: MNHN-MTH13-L; L: MNHN-MTH7-L).
Oosterzele: M1/2 (R: IRSNB M 1867; L: IRSNB.M 1868); m1 (L: IRSNB.M 1863); m3 (R: IRSNB.M 1864, [broken], IRSNB.M 1865); M1 (R: IRSNB.M 1866).
Prémontré: maxillary with canine (R: MNHN-SLP-29-PE1378); maxillary dP2 (L: MNHN-SLP-29-PE1070); maxillary dP3-dP4 (L: MNHN-SLP-29-PE1863); maxillary P1 (R: MNHN-SLP-29-PE1559); maxillary P1-P2 (R: MNHN-SLP-29-PE1296); maxillary P2-P4 (R: MNHN-SLP-29-PE2388); maxillary P3 (L: MNHN-SLP-29-PR1953); maxillary M1-M2 (L: MNHN-SLP-29-PE1864, SLP-29-PE706, SLP-29-PE761 [composite?]); maxillary M1-M3 (R: MNHN-SLP-29-PE681); mandible dp2-m2 (L: MNHN-SLP-29-PE1467); mandible p3-p4 (R: MNHN-SLP-29-PE1362); mandible p3-m1 (R: MNHN-SLP-29-PE584); mandible p4-m3 (R: MNHN-SLP-29-PE1553, SLP-29-PE480); mandible m1 (R: MNHN-SLP-29-PE1069); mandible m3 (L: MNHN-SLP-29-PE1317); dP2 (R: MNHN-SLP-29-PE1436, SLP-29-PE631, SLP-29-PE1475; L: MNHN-SLP-29-PE950, SLP-29-PE717, SLP-29-PE44); dP3 (R: MNHN-SLP-29-PE803, SLP-29-PE742, SLP-29-PE1728, SLP-29-PE45, SLP-29-PR1973, SLP-29-PR1560, PRE448; L: MNHN-SLP-29-PE1243, SLP-29-PE1004, SLP-29-PE100, SLP-29-PE67, SLP-29-PR2049, PRE996); dP4 (R: MNHN-SLP-29-PE1703, SLP-29-PE1430, SLP-29-PE1275, SLP-29-PE807, SLP-29-PE150, SLP-29-PR1928, SLP-29-PR2054, SLP-29-PR3289, SLP-29-PR3077, SLP-29-PR1913, SLP-29-PE1998, PRE241, PRE1070; L: MNHN-SLP-29-PE1358, SLP-29-PE1201, SLP-29-PE1323, SLP-29-PR1988, SLP-29-PR3283, SLP-29-PR3000); P2 (R: MNHN-SLP-29-PE1421, SLP-29-PE599; L: MNHN-SLP-29-PE10); P3 (R: MNHN-SLP-29-PE644, SLP-29-PE1548, SLP-29-PE12, SLP-29-PE252, SLP-29-PE1914, SLP-29-PR1896; L: MNHN-SLP-29-PE731, SLP-29-PE590, SLP-29-PE254, SLP-29-PR1971); P4 (R: MNHN-SLP-29-PE678, SLP-29-PE622; L: MNHN-SLP-29-PE741, PRE246, PRE236, PRE995); M1 (R: MNHN-SLP-29-PE1383, SLP-29-PE896, SLP-29-PR1912, SLP-29-PR3287, SLP-29-PR3001, SLP-29-PR3107, PRE1065; L: MNHN-SLP-29-PE701, PRE1064); M2 (L: MNHN-SLP-29-PE508); M1/2 (R: MNHN-SLP-29-PE1695, SLP-29-PE1479, SLP-29-PE1527, SLP-29-PE987, SLP-29-PE707, SLP-29-PE151, SLP-29-PE1367, SLP-29-PE147, SLP-29-PE149, SLP-29-PE1699, SLP-29-PE479, SLP-29-PE448, SLP-29-PE982, SLP-29-PE865, PRE1069, PRE1067, PRE1068; L: MNHN-SLP-29-PE1544, SLP-29-PE394, SLP-29-PE1707, SLP-29-PE501, SLP-29-PE388, SLP-29-PE148, SLP-29-PE223, SLP-29-PE503, SLP-29-PR1925, SLP-29-PR1969, SLP-29-PR2009, SLP-29-PR3290, SLP-29-PR3288, SLP-29-PR3003, PRE238, PRE863, PRE1080); M3 (R: MNHN-SLP-29-PE1721, SLP-29-PE688,

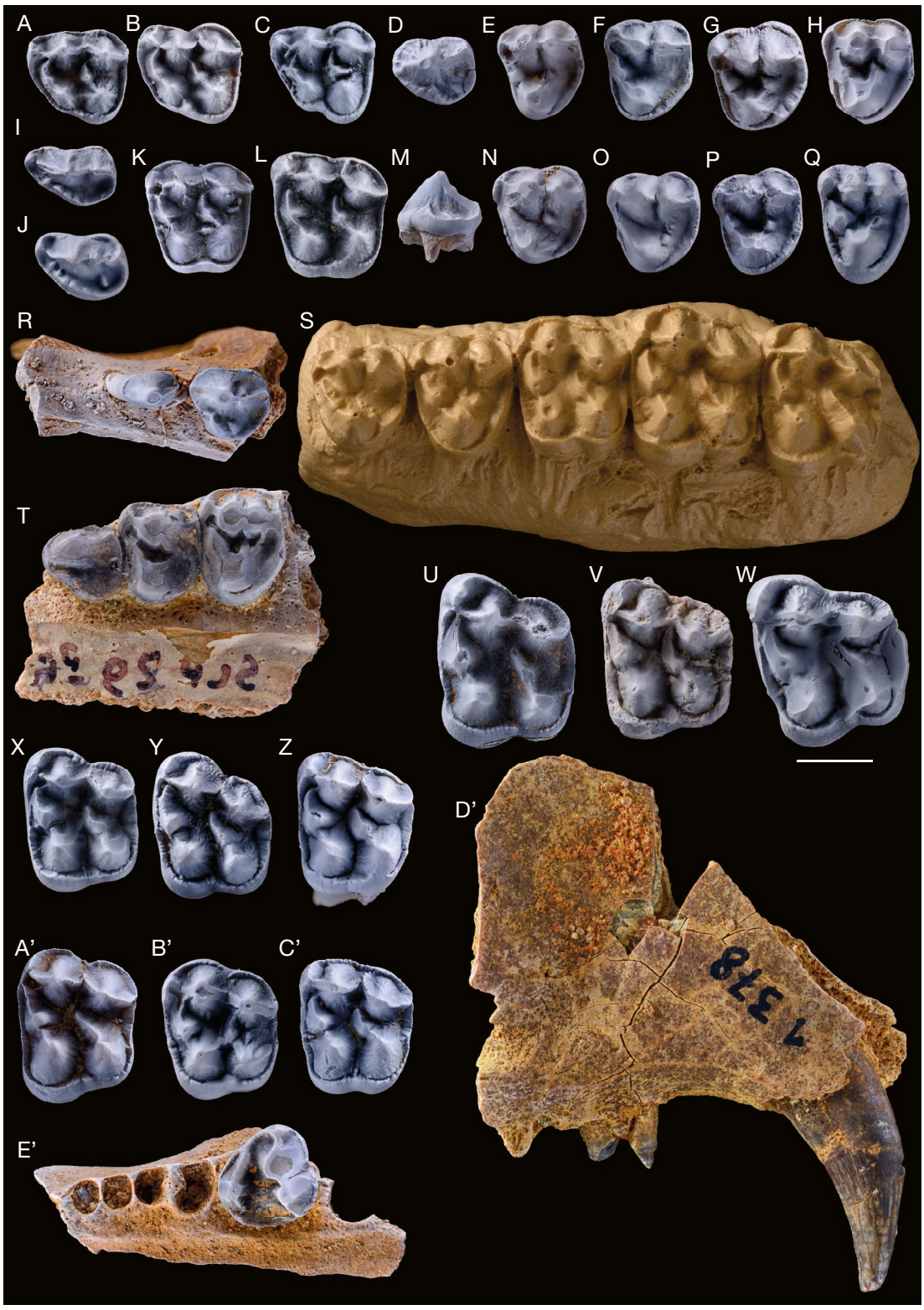

FIG. 11. — Upper teeth of *Orolophus maldani* (Lemoine, 1878) from the Paris Basin in occlusal (**A**-**L**, **N**-**D'**), lingual (**M**) and lateral (**E'**) views: **A**, left DP3 (MNHN-SLP-29-PE100); **B**, right DP3 (MNHN-SLP-29-PR1973 [reversed]); **C**, right DP3 (MNHN-GR7825 [reversed]); **D, M**, left P2 (MNHN-SLP-29-PE10); **E**, left P3 (MNHN-SLP-29-PE731); **F**, right P3 (MNHN-SLP-29-PE252 [reversed]); **G**, right P3 (MNHN-SLP-29-PE12 [reversed]); **H**, left P3 (MNHN-SLP-29-PE254); **I**, left DP2 (MNHN-SLP-29-PE950); **J**, left DP2 (MNHN-SLP-29-PE717); **K**, left dP4 (MNHN-MTH7); **L**: right DP4 (MNHN-SLP-29-PR1913 [reversed]); **N**, left P3 (MNHN-SLP-29-PE590); **O**, right P3 (MNHN-SLP-29-PR1896 [reversed]); **P**, right P3 (MNHN-SLP-29-PR1914 [reversed]); **Q**, left P4 (MNHN-SLP-29-PE741); **R**, right maxillary with P1-P2 (MNHN-SLP-29-PE1296 [reversed]); **S**, left maxillary with P3-M3 (holotype of "*Propachynolophus levei*", MNHN.CB16165 [cast]); **T**, right maxillary with P2-P4 (MNHN-SLP-29-PE2388 [reversed]); **U**, left M1/2 (MNHN-SLP-29-PE147); **V**, left M3 (MNHN-SLP-29-PE224); **W**, left M1/2 (MNHN-CB1531); **X**, left M1/2 (MNHN-SLP-29-PE148); **Y**, left M3 (MNHN-SLP-29-PR1968); **Z**, right M1/2 (MNHN-SLP-29-PE149 [reversed]); **A'**, right M1/2 (MNHN-SLP-29-PE987 [reversed]); **B'**, right M1 (MNHN-CB4689 [reversed]); **C'**, right M2 (MNHN-SLP-29-PE508 [reversed]); **D'**, left maxillary with P3 (MNHN-SLP-29-PE1953); **E'**, right upper canine (MNHN-SLP-29-PE1378); **A**-**R**, **T**-**D'**, coated with magnesium. Scale bar: 5 mm.

SLP-29-PE152, SLP-29-PE1009, SLP-29-PR1909, PRE235; L: MNHN-SLP-29-PE834, SLP-29-PE224, SLP-29-PE997, SLP-29-PE806, SLP-29-PR1903, SLP-29-PR1968, SLP-29-PR1891, PRE1066); dp3 (R: MNHN-SLP-29-PR1983, SLP-29-PE1355, SLP-29-PE1143, SLP-29-PE1057, SLP-29-PE1384, SLP-29-PE993, SLP-29-PE966, SLP-29-PE1012, SLP-29-PE878, SLP-29-PE303, SLP-29-PE1818, SLP-29-PE113, SLP-29-PE103, PRE997; L: MNHN-SLP-29-PR3022, SLP-29-PR1919, SLP-29-PR58, SLP-29-PE1562, SLP-29-PE868, SLP-29-PE263, PRE239, PRE244); dp4 (R: MNHN-SLP-29-PE1434, SLP-29-PE1024, SLP-29-PE1552, SLP-29-PE1438, SLP-29-PE488, SLP-29-PE185, SLP-29-PE653, SLP-29-PE1026, SLP-29-PE751, SLP-29-PE624, SLP-29-PE392, SLP-29-PE88, PRE247, PRE243; L: MNHN-SLP-29-PR2477, SLP-29-PR3026, SLP-29-PR2424, SLP-29-PR2044, SLP-29-PR2008, SLP-29-PE879, SLP-29-PE1713, SLP-29-PE1473, SLP-29-PE95, SLP-29-PE1048, SLP-29-PE1382, SLP-29-PE856, PRE242); p2 (L: MNHN-SLP-29-PE772, SLP-29-PE1499, SLP-29-PE1180, SLP-29-PE165); p3 (R: MNHN-SLP-29-PE180, SLP-29-PE1214, SLP-29-PE17, SLP-29-PE759; L: MNHN-SLP-29-PE1472, SLP-29-PE1474, SLP-29-PE1459) ; p4 (R: MNHN-SLP-29-PR1949, SLP-29-PE1325, SLP-29-PE977, SLP-29-PE745; L: MNHN-SLP-29-PE770, SLP-29-PE763, SLP-29-PE596, SLP-29-PE719); m1/2 (R: MNHN-SLP-29-PE667, SLP-29-PE1177, SLP-29-PE1848, SLP-29-PE1320, SLP-29-PE827, SLP-29-PE694, SLP-29-PE669, PRE240; L: MNHN-SLP-29-PR3106, SLP-29-PR2026, SLP-29-PE1375, SLP-29-PE951, SLP-29-PE1340, SLP-29-PE730, PRE245); m2 (R: MNHN-SLP-29-PE22; L: MNHN-SLP-29-PE1406, SLP-29-PE768, SLP-29-PE757); m3 (R: MNHN-SLP-29-PR3211, SLP-29-PE1306, SLP-29-PE682, SLP-29-PE48, PRE861; L: MNHN-SLP-29-PR1990, SLP-29-PR1954, SLP-29-PE1410, SLP-29-PE693); tibia (L: MNHN.F.PMT112); humerus (R: MNHN.F.PMT114; L: MNHN.F.PMT115); scapula (R: MNHN.F.PMT116); ulna (R: MNHN.F.PMT117, MNHN.F.PMT118); metatarsal II (L: MNHN.F.PMT119); calcaneus (R: MNHN.F.PMT123, MNHN.F.PMT124, MNHN.F.PMT125; L: MNHN.F.PMT126, MNHN.F.PMT127); astragalus (R: MNHN.F.PMT132, MNHN.F.PMT133, MNHN.F.PMT134, MNHN.F.PMT135; L: MNHN.F.PMT128, MNHN.F.PMT129, MNHN.F.PMT130, MNHN.F.PMT131); distal phalanx (MNHN.F.PMT137, MNHN.F.PMT138, MNHN.F.PMT139, MNHN.F.PMT140, MNHN.F.PMT141, MNHN.F.PMT142, MNHN.F.PMT143, MNHN.F.PMT144); navicular (R: MNHN.F.PMT145, MNHN.F.PMT146; L: MNHN.F.PMT147).

St Agnan: dP2 (R: MNHN-STA658; L: MNHN-STA633); dP4 (L: MNHN-STA24); P2 (R: MNHN-STA634, STA644, STA649; L: MNHN-STA648); P3 (L: MNHN-STA639, STA643, STA645); P4 (R: MNHN-STA635, STA656); P3-4 (R: MNHN-STA638); M1 (R:, MNHN-STA894); M1/2 (R: MNHN-STA869, STA637, STA652, STA653, STA654; L: MNHN-STA651, STA641, STA897); dp2 (L: MNHN-STA893); dp3 (R: MNHN-STA883; L: MNHN-STA881); dp4 (R: MNHN-STA627); p3 (L: MNHN-STA642); m1/2 (R: MNHN-STA624, STA628, STA629, STA630, STA632, STA876; L: MNHN-STA878, STA998, STA631, STA640, STA647, STA657); m3 (R: MNHN-STA1000-L; L: MNHN-STA626); incisor (MNHN-STA896).

Sézanne-Broyes: maxillary M1-M2 (L: MNHN-SEZ325); maxillary M1-M3 (L: MNHN-SZ7306); dP4 (R: MNHN-SEZ342, SEZ344; L: MNHN-SEZ337, SEZ343); P2 (L: MNHN-SEZ359); P3 (R: MNHN-SEZ347; L: MNHN-SEZ268); P4 (R: MNHN-SEZ355, SEZ357, SEZ358; L: MNHN-SEZ356); M1/2 (R: MNHN-SEZ332, SEZ333, SEZ338, SEZ339, SEZ341, SEZ360, SEZ7337; L: MNHN-SEZ331, SEZ340, SEZ345, SEZ7335); M3 (L: MNHN-SEZ7334); dp3 (L: MNHN-SEZ349); dp4 (R: MNHN-SEZ7340); p3 (R: MNHN-SEZ312; L: MNHN-SEZ7272); p4 (R: MNHN-SEZ313, SEZ351, SEZ353; L: MNHN-SEZ346, SEZ352); m1 (R: MNHN-SEZ314); m2 (R: MNHN-SEZ315); m1/2 (L: MNHN-SEZ326, SEZ7336); m3 (R: MNHN-SEZ316, SEZ329).

TYPE LOCALITY. — Environs d'Epernay, Cuisien (Ageian), MP10.

DISTRIBUTION. — Condé-en-Brie, St Agnan (Aisne, France), Sézanne-Broyes (Marne, France), MP8-9; Cuis, Grauves, Mancy, Mont Bernon, Monthelon (Marne, France), Prémontré (Aisne, France); Oosterzele (Belgique), MP10.

EMENDED DIAGNOSIS (modified from Remy 2017). — Small palaeotheriid Equoidea, with an estimated P2-M3 length of about 40 mm, a bunolophodont and brachyodont dentition, an occasional mesostyle and a parastyle not very protruding on upper molars, a protocone mesially shifted on P4, a distal expansion of the postero-lingual cingulum on P3-P4, narrow lower molars with thick and continuous labial cingulids, a cristid obliqua joining the middle of the protolophid and a hypoconulid linked to the hypolophid.

DIFFERENTIAL DIAGNOSIS (modified from Remy 2017). — Differs from species of *Pachynolophus* in having a wider P2 and an occasional mesostyle on upper molars. Further differs from more advanced Palaeotheriidae (*Lophiotherium*, "propalaeotheres", and Palaeotheriinae) in possessing an inconstant mesostyle on upper molars, a parastyle less protruding and a shallower protoloph groove on upper molars, a lingual cingulum on these teeth stronger than in most of them, a P4 triangular (instead of being subquadrangular), and a hypoconulid more developed en m1-m2. Smaller than *Propalaeotherium gaudryi*, larger than *Pliolophus* and *Cymbalophus*. Possesses a hypoconulid linked to hypolophid, whereas there is a hypoconulid-hypoconid junction in *Pliolophus*, *Cymbalophus* and *Hyracotherium*.

DESCRIPTION

Teeth

The maxillary has a short post-P1 diastema. The post-canine diastema can be long (Fig. 11D') or very short (MNHN-SLP-29-PE1559). The P1 is more or less elongated, and displays a single cusp in the middle of the tooth (Fig. 11R). The P2 is two-rooted, narrower anteriorly than posteriorly (Fig. 11M, R, T). The metacone is very small, closely appressed to the paracone and indistinguishable if the tooth shows wear. The cusps appear further apart and the metacone is larger on MNHN.STA-648 and MNHN-STA649. A bulge is present at the level of the protocone. The parastyle is absent. The parastyle of P3 is small but well formed (Fig. 11E-H, N-P, S). The paracone and metacone are closely appressed. The paraconule and the metaconule can be large (Fig. 11G), but the metaconule is often absent (Fig. 11F) or reduced (Fig. 11N). The sizes of the two conules do not vary together. The cingulum can be large and continuous or interrupted. The protoloph is interrupted before joining the preparacrista. MNHN-SLP-29-PR1953 is a P3 that has grown at 90° to the normal angle; its lingual side is found in anterior position (Fig. 11E'). The parastyle of P4 is smaller than the paracone (Fig. 11Q, S-T). The paraconule is almost as large as the paracone. Two lingual bulges are present at the level of the metaconule (Fig. 11R). The cingulum is continuous. The centrocrista of upper molars is slightly flexed (Fig. 11S, U-Z). The mesostyle is absent, but on some specimens a thin ridge is present (Fig. 11R, V, X-Y, C'). The paraconule is located in the center of the protoloph. The metaconule is a little less developed than the paraconule, and it is sometimes difficult to discern (Fig. 11A'). The protoloph is interrupted before joining the preparacrista. The metaloph is interrupted at the base of the metacone (Fig. 11U, X-Y) or

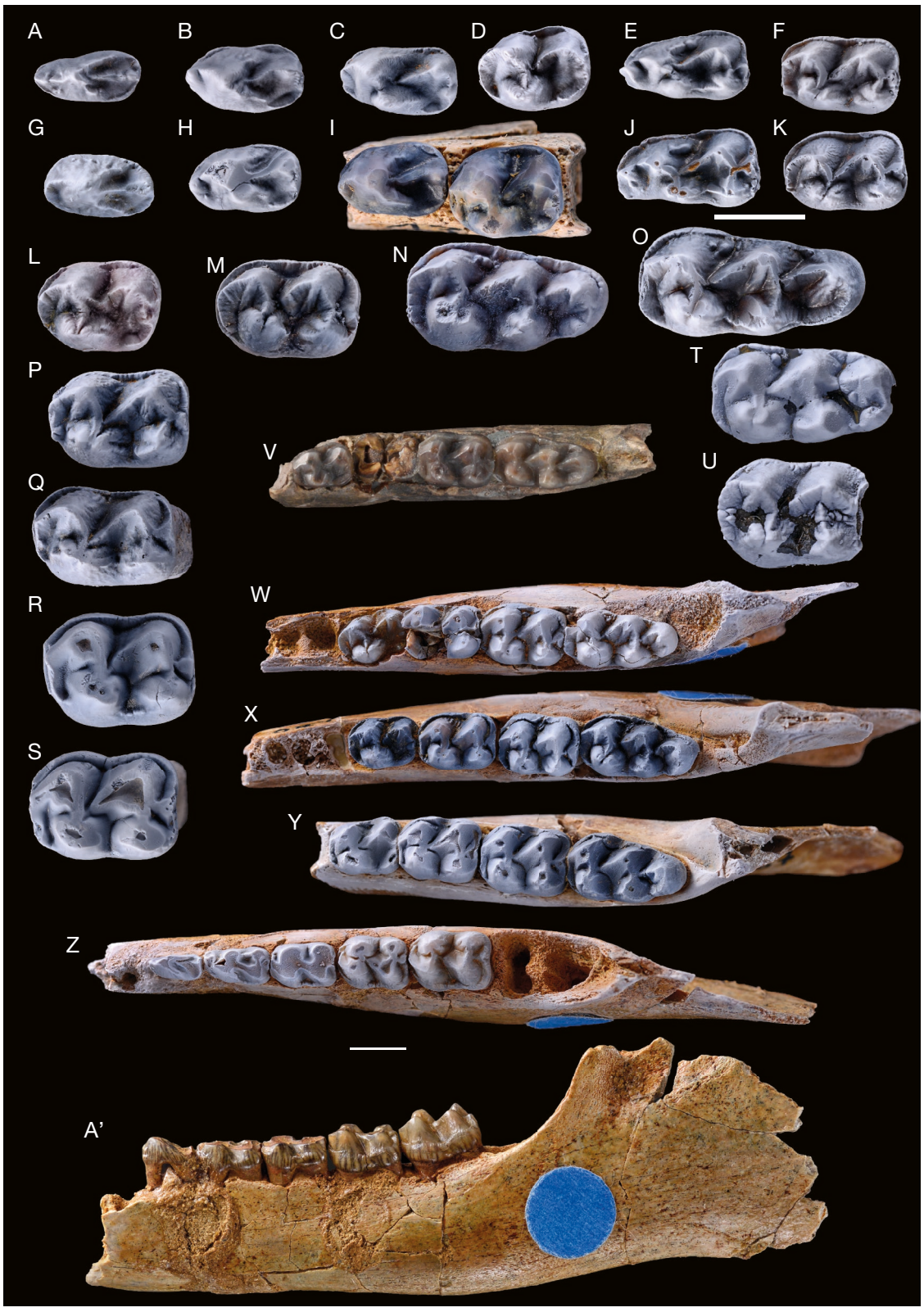

FIG. 12. — Lower teeth of *Orolophus maldani* (Lemoine, 1878) from the Paris Basin in occlusal (**A**-**Z**) and lateral (**A'**) views: **A**, right p2 (MNHN-SLP-29-PE1499); **B**, right p3 (MNHN-SLP-29-PE180); **C**, left p3 (MNHN-SLP-29-PE1472 [reversed]); **D**, right p4 (MNHN-SLP-29-PE1325); **E**, right dp3 (MNHN-SLP-29-PE1355); **F**, left dp4 (MNHN-SLP-29-PE856 [reversed]); **G**, left p2 (MNHN-SLP-29-PE165 [reversed]); **H**, right p3 (MNHN-SLP-29-PE1214); **I**, right mandible with p3-p4 (MNHN-SLP-29-PE1362); **J**, right dp3 (MNHN-SLP-29-PE303); **K**, right dp4 (MNHN-SLP-29-PE392); **L**, left p4 (MNHN-SLP-29-PE763 [reversed]); **M**, left m1/2 (MNHN-SLP-29-PE1340 [reversed]); **N**, right m3 (MNHN-PRE861); **O**, right m3 (MNHN-SLP-29-PE1306); **P**, right m1/2 (MNHN-CB4687); **Q**, right m1/2 (MNHN-CB1584); **R**, right m2 (MNHN-CB4686); **S**, right m2 (MNHN-CB198); **T**, left m3 (MNHN-CB1571 [reversed]); **U**, left m3 (MNHN-CB1585 [reversed]); **V**, right mandible with p4, m2-m3 (holotype, MNHN-AL5199); **W**, right mandible with p4-m3 (MNHN-SLP-29-PE1553); **X**, right mandible with p4-m3 (MNHN-SLP-29-PE480); **Y**, right mandible with p4-m3 (MNHN-MA14792); **Z**, **A'**, right mandible with dp2-m2 (MNHN-SLP-29-PE1467); **A**-**U**, **W**-**Z**, coated with magnesium. Scale bars: 5 mm.

connected by a metacone fold which joins the centrocrista in its center (Fig. 11V). This last morphology is found on a very reduced number of teeth. The parastyle is smaller than the other cusps. The cingulum is sometimes interrupted at the level of the hypocone.

There is no diastema between p1 and p2 (Fig. 12Z). The posterior border of the symphysis extends back to the level of p1. The p1 is two-rooted but on some specimens the roots are fused. The p2 protoconid is high and the metaconid is absent or small (Fig. 12A, G). The hypoconid is poorly developed, and a small paraconid is present. A ridge extends between the hypoconid and the protoconid. Two other crests extend posteriorly to the protoconid, joining the labial and the lingual border of the tooth respectively. The metaconid of p3 is smaller than the protoconid (Fig. 12B, C, H-I). It is very close to the latter and slightly posteriorly placed. The hypoconid is lower than the other cusps but well-developed. A small bulge (possibly an incipient entoconid) is sometimes present lingually to the hypoconid (Fig. 12C). The paralophid is very short. The cristid obliqua joins the lingual edge of the protoconid. A ridge extends posteriorly from the metaconid. The p4 entoconid is absent (Fig. 12D), but a small bulge is sometimes present on the cingulum (Fig. 12I). The protoconid and the metaconid are quite close and transversely aligned. The metaconid is either twinned or simple. The paralophid is short and joins the lingual edge of the tooth. The cristid obliqua runs from the hypoconid to a point situated at half height of the protolophid between the midpoint of protoconid and the metaconid. The paralophid of lower molars is variable, it can join the lingual edge of the tooth (Fig. 12Y) or be very short (Fig. 12Z). The cusps are aligned transversely. The metaconid is twinned. The cristid obliqua joins the midpoint of the protolophid at a half height. The protolophid is high, the hypolophid is lower. The cingulum is labially continuous. The hypoconulid is displaced lingually and it is attached medially to the hypolophid. The post-hypocristid is very small or absent. On some teeth, the hypoconulid is linked very close to the hypoconid by a postcristid (Fig. 12S). The cingulum of m3 is continuous labially (Fig. 12V, X, Y). The cristid obliqua joins the protolophid medially and at mid-height. The lophids are deeply notched. The paralophid is longer than on the other molars. The lobe of the hypoconulid is developed, it has the same size as the anterior part of the talonid. The postcristid links the hypoconulid to the center of the hypolophid. Two teeth of Condé-en-Brie (MNHN-CB1585, CB1571) show the hypoconulid linked to the hypoconid by a postcristid (Fig. 12T, U). The hypoconulid lobe forms a horseshoe in occlusal view.

Ontogeny

MNHN-SLP-29-PE1553 (Fig. 12W) shows that m3 is completely erupted while p4 only begins to erupt. On MNHN-SLP-29-PE1467 (Fig. 12Z), the m3 is absent but the alveoli seem to indicate that it was erupting while the dp2 to dp4 were still present.

Deciduous teeth

The DP2 is narrower anteriorly (Fig. 11I, J). The paracone is developed, the metacone is extremely reduced and closely appressed to the paracone. A crest is sometimes present at the lingual side of the metacone (Fig. 11J). The parastyle is small and projected anterolabially. Sometimes a small metacone is present posteriorly to the paracone (Fig. 11J). The parastyle of DP3 is projected anteriorly (Fig. 11A-C). The paraconule is less developed than the metaconule. The centrocrista is high and very slightly flexed. A mesostyle can be present (Fig. 11B). The metaloph is interrupted at the base of the metacone, sometimes oriented towards the paracone (Fig. 11B), sometimes ended by a metacone fold (Fig. 11C). The protoloph joins the preparacrista in its center or slightly posteriorly. The cingulum is developed. A small crest can be present between the protocone and the hypocone (Fig. 11C). The DP4 is molarized and very similar to molars (Fig. 11K, L). The centrocrista is slightly flexed labially. The conules are developed. The cingulum usually forms a ridge connecting the hypocone anteriorly. Sometimes, a mesostyle can be present (Fig. 11L).

The dp2 is narrow (Fig. 12Z). Two crests, one labial and one lingual, extend posteriorly from the protoconid. A small hypoconid appears to be present, a crest extends anteriorly from the hypoconid in the center of the tooth. The paraconid of dp3 is developed (Fig. 12E, J, Z). The cristid obliqua is oriented toward the center of the protolophid (Fig. 12Z). The metaconid is larger than the protoconid and the paralophid is developed. A postcristid links the hypolophid to the hypoconulid (Fig. 12J). The hypolophid can be absent and the hypoconulid can be linked to the hypoconid (MNHN. MCB-0196). Sometimes a crest extends posteriorly from the protoconid on its labial side. The lingual wall is developed between the metaconid and the entoconid. The dp4 is slightly narrower at the anterior part of the trigonid than at the posterior part of the talonid (Fig. 12F, K, Z). The metaconid is twinned. The cristid obliqua joins the metaconid on its labial side. The hypoconulid is salient and displaced lingually. The anterior, labial and posterior cingulums are continuous.

Postcranial elements

Humerus. The proximal part is missing. The distal trochlea is poorly marked (Fig. 13E-G). The epicondyles are poorly developed but the medial epicondyle is projected further than the lateral epicondyle. A distinct capitular keel is present (Fig. 13G). The supracondylar foramen is present in the radial fossa.

Ulna. The bone is elongated, arched anteriorly and compressed mediolaterally. A slight depression is present along the dorsolateral side of the bone (Fig. 13D). The olecranon process is extended posteriorly and relatively long. The trochlear notch is concave proximodistally. The medial and lateral coronoid processes bear oval facets for the humerus. A lateral radial facet is present below the lateral coronoid process. The medial radial facet, situated below the medial coronoid process is smaller than the lateral radial facet. A prominent ridge extends from

FIG. 13. — Postcranial elements of *Orolophus maldani* (Lemoine, 1878) from the Paris Basin: **A**, **B**, left tibia (MNHN.PMT-112) in anterior (**A**) and posterior (**B**) views; **C**, **D**, right ulna (MNHN.F.PMT117) in lateral (**C**) and anterior (**D**) views; **E**, **F**, right humerus (MNHN.F.PMT115) in posterior (**E**) and anterior (**F**) views; **G**, right humerus (MNHN.F.PMT114) in anterior view; **H**, right astragalus (MNHN.F.PMT133) in anterior view; **I**, left astragalus (MNHN.F.PMT136 [reversed]) in anterior view; **J**, right calcaneus (MNHN.F.PMT123) in anterior view; **K**, **L**, left calcaneus (MNHN.F.PMT126 [reversed]) in anterior (**K**) and medial (**L**) views; **M**, **N**, right astragalus (MNHN.F.GR18005) in anterior (**M**) and posterior (**N**) views; **O**, **P**, right astragalus (MNHN.F.PMT134) in anterior (**O**) and posterior (**P**) views; **Q**, **R**, left metatarsal II (MNHN.F.PMT119) in anterior (**Q**) and posterior (**R**) views; **S**-**U**, right navicular (MNHN.F.PMT146) in dorsal (**S**), ventral (**T**) and medial (**U**) views; **V**, **W**, distal phalanx (MNHN.F.PMT142) in dorsal (**V**) and ventral (**W**) views; **X**, **Y**, distal phalanx (MNHN.F.PMT140) in dorsal (**X**) and ventral (**Y**) views; **Z**, **A'**, distal phalanx (MNHN.F.PMT139) in dorsal (**Z**) and ventral (**A'**) views; **B'**, **C'**, distal phalanx (MNHN.F.PMT137) in dorsal (**B'**) and ventral (**C'**) views; **D'**, **E'**, distal phalanx (MNHN.F.PMT141) in dorsal (**D'**) and ventral (**E'**) views. Scale bars: 1 cm.

the lateral coronoid process and runs along the anterior border of the shaft. A second ridge extends along the shaft from the medial coronoid process.

Tibia. The proximal articular surface is triangular in dorsal view. The lateral condyle is slightly convexe and the medial condyle is more flat. The lateral intercondyloid eminence is slightly higher than the medial intercondyloid eminence. The diaphysis is slightly S-shaped in anterior view. The anterior tibial crest extends for about a third of the diaphysis. The distal end of the tibia has a medially extended medial malleolus and fovea on the mid-ventral surface (Fig. 13A, B).

Calcaneus. This bone is elongated and medio-laterally flattened (Fig. 13J-L). The distal part has a small, slightly concave astragalar facet. The sustentacular facet is rounded, slightly triangular. The proximal part of the ectal facet faces anteromedially below the tuber. The distal part of the ectal facet is distally facing. The cuboid facet is concave transversely and slightly convexe anteroposteriorly.

Astragalus. The trochlea is well marked, slightly oblique proximo-distally (Fig. 13H, I). The trochlea does not reach the navicular facet. The articular facets are well defined. In posterior view, a small facet of articulation with the calcaneus is present distolaterally. The navicular facet is saddle-shaped. The sustentacular facet is slightly concave. The astragalus MNHN.F.PMT134 (Fig. 13O, P) is much larger and has worn facets, however it seems to display the same morphology. It could be a large individual, or possibly a different species of larger size so far only represented by postcranial material, the locality of Prémontré not having yielded fossils of large size. This astragalus is much smaller than that of *Propalaeotherium gaudryi*, the only contemporary larger hippomorph species.

Navicular. The articular facet with the astragalus is concave (Fig. 13S). The articular facets with the mesocuneiform and the ectocuneiform are connected (Fig. 13T). Two small facets of articulation with the cuboid are present on the lateral face. A small facet of articulation with the entocuneiform is present posteriorly.

Metatarsals. The metatarsal II is curved medio-distally (Fig. 13Q, R). Proximally, a mediolateral compression is present. The proximal facet is slightly concave. Postero-medially on the proximal part, a small elliptical facet of articulation with the entocuneiform is present. The distal trochlea is asymmetrical. The metatarsal III is long and straight. The distal articulation is keeled and symmetric in shape.

Distal phalanges. Median ungual phalanges: They are bifid, constricted latero-medially in the center (Fig. 13V-Y, D', E'). The distal part bears two foramina in dorsal view, and a single foramen where the phalanx is constricted. In ventral view, the proximal part has two large foramina. The narrowest and longest phalanges might be attributed to fore limbs (Fig. 13V, W), and the widest and shortest to hind limbs (Fig. 13X, Y, D'-E'). On the hind limb phalanges, sometimes two foramina can be present on the distal part.

Lateral and medial ungual phalanges. They are bifid, constricted obliquely latero-medially. The distal part bears several foramina in dorsal view, and one in ventral view on the shortest side of the phalanx. In dorsal view, a foramen is present in the middle of the phalanx. The phalanx MNHN.F.PMT139 (Fig. 13Z, A') is slightly shorter and wider than MNHN.F.PMT137 (Fig. 13B'-C'). The former could belong to a hind limb, and the latter to a fore limb.

Comparisons

There is no noticeable difference between the mandibles and lower dentition of *Orolophus maldani* and *Pachynolophus eulaliensis*. On the other hand, the P2 displays closely appressed paracone and metacone, the metacone being sometimes indistinguishable due to wear, while these two cusps are more distant in *P. eulaliensis*. The postprotocrista is generally more developed on P3-4 of *P. eulaliensis*, although it varies in *O. maldani*. An entoconid is usually present on p4 of *P. eulaliensis*, but sometimes it is absent. This entoconid is generally absent in *O. maldani*, although a cingular bulge is observable on some specimens. The lophodonty is less marqued than in *Pachynolophus lavocati* Remy, 1972 and in *Pachynolophus livinierensis* Savage, Russell & Louis, 1965. The metaconule of upper molars is more developed than in *Pachynolophus duvali* Pomel, 1847 and in *P. livinierensis*. The conules of upper molars and premolars are more developed than those of *P. lavocati*. *Orolophus* is much smaller than *Pachynolophus cayluxi* Filhol, 1888. The labial cusps of upper premolars of *P. cayluxi* are oriented slightly more lingually than those of *Orolophus*. The metaconule of upper molars is more developed in *Orolophus* than in "*Hyracotherium*" *remyi* Checa-Soler, 1997. The lophodonty of *O. maldani* is more developped than in *Hallensia*. The centrocrista of the upper molars are more flexed than in *Pliolophus* and *Cymbalophus*. The hypoconulid of the lower molars is linked to the hypolophid, whereas it is linked to the hypoconid in *Cymbalophus* and in most specimens of *Pliolophus*. The teeth are smaller than in *Propalaeotherium gaudryi*.

Comments on "*Propachynolophus levei*"

P. levei has been described by Hooker (1994) on the basis of a maxilla with P3-M3 from Condé-en-Brie and three isolated teeth from Avenay and Sézannes-Broyes. The study of a large number of *O. maldani* specimens reveals that there is no difference between *O. maldani* and *P. levei*. The maxillary, holotype of the species, comes from the Levé collection, now lost, but two casts have been deposited at MNHN (MNHN.CB16165, Fig. 11S) and NHM (BMNH. M49399). This poorly known species was hardly comparable with *O. maldani*, which was poorly represented and described. The affinities of the two species have been discussed by Remy (2017), with the support of a phylogenetic analysis in which he coded several characters which differ between the two taxa. However, these differences appear

to fall in the range of intraspecific variability, observable with a larger sample: Character 8, lophodonty. *P. gaudryi* and *O. maldani* are coded with a higher degree of lophodonty than *P. levei* and *P. remyi*. But the observations do not indicate such a difference for *P. levei*, which present the same degree of lophodonty than *O. maldani*. Character 17, metaconule of P3. Absent in *P. levei* and weak in *O. maldani*. Observations on a large sample indicate that this trait varies from absent to present in *O. maldani*. Character 22, lingual cingulum of the P4. Continuous in *P. levei* and reduced to the level of protocone in *O. maldani*. This is a very variable character. Character 23, postero-lingual cingulum of P4. Distal expansion in *O. maldani*, absent in *P. levei*. This is also a very variable character. Character 26, position of the protocone on P4. Placed mesially in *O. maldani*, central in *P. levei*. This character can vary. Character 40, mesostyle. Absent in *P. levei*, sometimes present in *O. maldani*. This character from present to absent in *Orolophus*. Character 41, morphology of the mesostyle. Linked to the previous character. Character 44, morphology of the lingual cingulum of the upper molars. Continuous in *P. levei*, interrupted in *O. maldani*. This character varies, as on premolars. Character 54, relative area M3 / M2. M3 <M2 for *P. levei*, and small difference in *O. maldani*. This requires to be testing on a large sample. Only a small sample of *O. maldani* were available to Remy (2017), which did not allow him to observe all the intraspecific variations of this species. The characters that differentiate *O. maldani* from *P. levei* (known from a few specimens; Hooker 1994) in the phylogenetic analysis of Remy (2017), are mainly related to the cingula which are variable structures, but also to characters coded according to states that would require the knowledge of the intraspecific variability, thus requiring a wide sampling (for example, characters 40 and 54).

Therefore, our observation of a larger population of *Orolophus* has demonstrated that the type of *P. levei* is included within the variability of *O. maldani*, and it is thus considered as a junior synonym of *Orolophus maldani*.

Family *incertae sedis*

Genre *Hallensia* Franzen & Haubold, 1986

Hallensia Franzen & Haubold, 1986: 37.

TYPE SPECIES. — *Hallensia matthesi* Franzen & Haubold, 1986 by original designation.

INCLUDED SPECIES. — *Hallensia parisiensis*, Franzen, 1990; *Hallensia louisi*, Hooker, 1994.

EMENDED DIAGNOSIS. — Perissodactyl of medium size (basicranium length: 175 mm) with brachyodont and bunolophodont dentition. Dental formula 3.1.4.3/3.1.4.3. Nasal incisure extending at the posterior border of the I3 alveolus. Upper molars with or without mesostyle and without postprotocrista. Strong cingula on upper molars. M3 with strong hypocone. Upper and lower M3 larger than M2. Lower molars without paraconid. Hypoconulid of m3 relatively large.

COMMENT

Hallensia is a perissodactyl with a very characteristic morphology. This primitive morphology pushed Franzen & Haubold (1986) to classify it within the phenacodontid condylarths. The discovery of a complete skeleton of *H. matthesi* in Messel (Germany) indicates that it is a perissodactyl (Franzen 1990), mostly because of the saddle-shaped navicular facet of its astragalus, a synapomorphic feature of perissodactyls (Radinsky 1966).

Hallensia parisiensis Franzen, 1990
(Fig. 14)

Hallensia parisiensis Franzen, 1990: 193-195.

Propachynolophus gaudryi – Savage *et al.* 1965: 16, 19, 21 (*partim*), fig. 7.

Propachynolophus sp. – Louis *et al.* 1983: 12.

HOLOTYPE. — NMB.TS-631, fragmentary maxillary with P4-M1.

PARATYPE. — NMB.TS-367, fragmentary maxillary with DP2-DP3.

MATERIAL. — **Condé-en-Brie**: maxillary P3-M1 (R: MNHN-CB1529); DP3 (R: MNHN-CB1557; L: IRSNB M 2304 [Lepage collection in Hooker 1994]); P2 (R: MNHN-CB1562).
Saint-Agnan: P2 (L: MNHN-STA636); m1/2 (R: MNHN-STA625-L; L: MNHN-STA623-L).
Fossoy (MP 10): mandible p4-m3 (L: coll. Lhomme).

TYPE LOCALITY. — Monthelon (Marne, France), MP10.

DISTRIBUTION. — Condé-en-Brie (Marne, France), MP8-9; St Agnan, Monthelon (Marne, France), MP10.

EMENDED DIAGNOSIS. — Well-developed paraconule and metaconule of upper premolars and molars; reduced parastyles; large lower molars; cingulums large and continuous.

DIFFERENTIAL DIAGNOSIS. — Smaller species than *H. matthesi*. Conules more developed than in *Cymbalophus*, *Pliolophus*, *Hyracotherium* and *Orolophus*. Teeth more rounded in occlusal view.

DESCRIPTION

Teeth

The P2 is almost sub-circular in occlusal view (Fig. 14B). The parastyle is very small. The paracone and the metacone are close. The protocone is large and linked to the preparacrista by a well-developed protoloph. The cingulum forms a crest starting from the protocone and joining the metastyle. A small postprotocrista is present. The P3 is triangular in occlusal outine, and the cusps are rounded (Fig. 14A). The paracone and metacone are close. The protocone is large and the paraconule is a little smaller. The protoloph is interrupted before joining the preparacrista. The parastyle is very poorly developed. The P4 is triangular in occlusal view and is not molarized (Fig. 14A, F). The parastyle is absent (NMB.TS-631, Fig. 14F) or poorly developed (MNHN-CB1529, Fig. 14A). The paracone and the metacone are close and of the same size. The centrocrista is straight (Fig. 14A) or flexed labially with a faint rib mesostyle (Fig. 14F). The paraconule is almost as

developed as the main cusps. The protoloph joins the preparacrista. A small metaconule can be present, connected to the protocone by the postprotocrista, as well as to the anterior part of the metacone (Fig. 14F), or very reduced (Fig. 14A). An endoprotocrista is present posterior to the protocone. The cingulum is continuous all around the tooth. The parastyle of M1 is absent (Fig. 14F) or poorly developed (Fig. 14A). The paraconule and the metaconule are present but much worn on the upper teeth. The centrocrista is labially flexed. A crest is present at the position of the mesostyle, it forms an extension of the premetacrista. The cingulum is interrupted lingual to the hypocone and labial to the paracone.

The lower molars are wide, the lophs are well developed. The hypoconulid is linked to the hypoconid (MNHN-STA623, Fig. 14C) or hypolophid (MNHN-STA625; Fig. 14E). The metaconid is twinned. The cristid obliqua is oriented toward the center of the protolophid. The m3 has the same morphology as other molars, only the hypoconulid lobe is more developed (Fig. 14H). The hypoconulid is linked to the hypoconid by a postcristid.

Deciduous teeth

DP1/P1: The first premolar is not known but the alveoli indicate a biradiculate tooth and a post-canine diastema of unknown length (Fig. 14G). The metacone of DP2 is much more worn than the paracone (Fig. 14G). The parastyle is developed and projected anteriorly. A protoloph runs from the preparacrista but is interrupted before joining the protocone. The protocone is shifted posteriorly and it is connected to the paracone by a crest. A small metaconule is present. The DP3 is sub-molariform (Fig. 14G). The parastyle is present. The centrocrista is straight (Fig. 14D) or labially flexed (Fig. 14G). The paraconule and the metaconule are very small. The protoloph is developed and joins the preparacrista. The metaloph is developed and joins the anterior side of the metacone without interruption. The hypocone is slightly larger than the protocone. The cingulum s is well marked, but it tends to become thinner or absent below the hypocone and paracone in some specimens (Fig. 14G).

Comparisons

Hallensia parisiensis is larger than *Cymbalophus*, *Pliolophus*, *Hyracotherium*, *O. maldani* and *Hallensia louisi*, but smaller than *Hallensia matthesi*. The teeth have a typical inflated appearance, absent in other genera. The centrocrista of molars is slightly straighter than in *Orolophus* and *Hyracotherium*. A small-ridged mesostyle can be present, as in *Hyracotherium*, *Orolophus* and *P.gaudryi*. The postcristid of the lower molars presents the same morphology as in *Pliolophus* and *Cymbalophus*. The labial cingulids are more developed in *Hallensia*. The third lobe of m3 is longer in *Hallensia* than in *Cymbalophus*. The cristid obliqua of m3 is more labial in *C. cuniculus* and *Pliolophus* than in *H. parisiensis*.

Comment

The fossils of Condé-en-Brie, St Agnan and Sézanne are slightly smaller than the holotype from Monthelon. The centrocrista is straight and the lophs are less developed than in the holotype. These features are more primitive than those of the type specimen. As this species is poorly known, the creation of a new species solely on the basis of the incomplete material is not sufficient at this point. In addition, these differences could be due to intraspecific variation. This latter hypothesis is favoured and the fossils are therefore attributed to *H. parisiensis*.

Hallensia louisi Hooker, 1994
(Fig. 15)

Hallensia louisi Hooker, 1994: 49.

Propachynolophus sp. – Teilhard de Chardin 1921: 69, fig. 33C, pl. 3, fig. 30.

Hyracotherium [sic] – Teilhard de Chardin 1921: 52, fig. 26B. — Savage *et al.* 1965: 6-8, 10, 11, 13, figs 2d, f, i, j, 4f-h.

Holotype. — MNHN-MU218-L, left M1/2.

Paratypes. — MNHN-MU12371, right M3; MNHN-MU201-L, left M3; MNHN-MU221-L, left M3; MNHN-MU12303, right mandible with dp4-m2; MNHN-MU6283, right m1/2; MNHN-MU12391, right m1/2, broken.

Material. — **Avenay**: Fragment of dentary and symphysis (L: MNHN-AV-841-Ph), m3 (L: MNHN-AV65519), M1/2 (R: MNHN-AV4770).
Condé-en-Brie: DP4 (R: MNHN-CB1588; L: MNHN-CB1574); M1/2 (L: MNHN-CB216, MCB0132, CB217 [broken]); M3 (R: MNHN-CB1568; L: MNHN-CB1560); m2 (L: MNHN-CB668); m3 (R: MNHN-CB4-CA; L: MNHN-CB224).
Gland: DP4 (R: MNHN-GLD216-L); M1/2 (R: MNHN-GLD281-L).
Grauves: M3 (R: MNHN-GR7574).
Oosterzele: p4 (R: IRSNB.M 1862); m3 (L: IRSNB.M 1861) (Smith *et al.* 2004).

Type locality. — Mutigny (Marne, France), MP8+9.

Distribution. —Mutigny (Marne, France), Condé-en-Brie (Aisne, France), Avenay (Marne, France), Gland, Oosterzele (Belgium) (MP8+9); Grauves (Marne, France) (MP10).

Emended diagnosis. — Small species of *Hallensia*; small upper molar parastyle; m3 hypoconulid linked to the hypoconid; upper molar centrocrista more or less flexed, sometimes with a mesostyle; large cusps, with a "bloated" appearance.

Differential diagnosis. — Smaller than *H. parisiensis* and *H. matthesi*; more bunodont than *Cymbalophus*, *Pliolophus*, *Hyracotherium* and *Orolophus*; differs from *Orolophus* by a hypoconulid linked to the hypoconid. Mandibular symphysis shorter and larger than in *Cymbalophus* and *Pliolophus*.

Description

Teeth

The upper molars are bunodont or sub-lophodont, with (Fig. 15B) or without mesostyle (Fig. 15C, D). The parastyle is reduced, the cingulum is wider posteriorly. The metaloph is continuous or interrupted at the base of the metacone. The conules are developed and close to lingual cusps. The protocone is the largest cusp. The cingulum is crenellated, sometimes forming small cuspids.

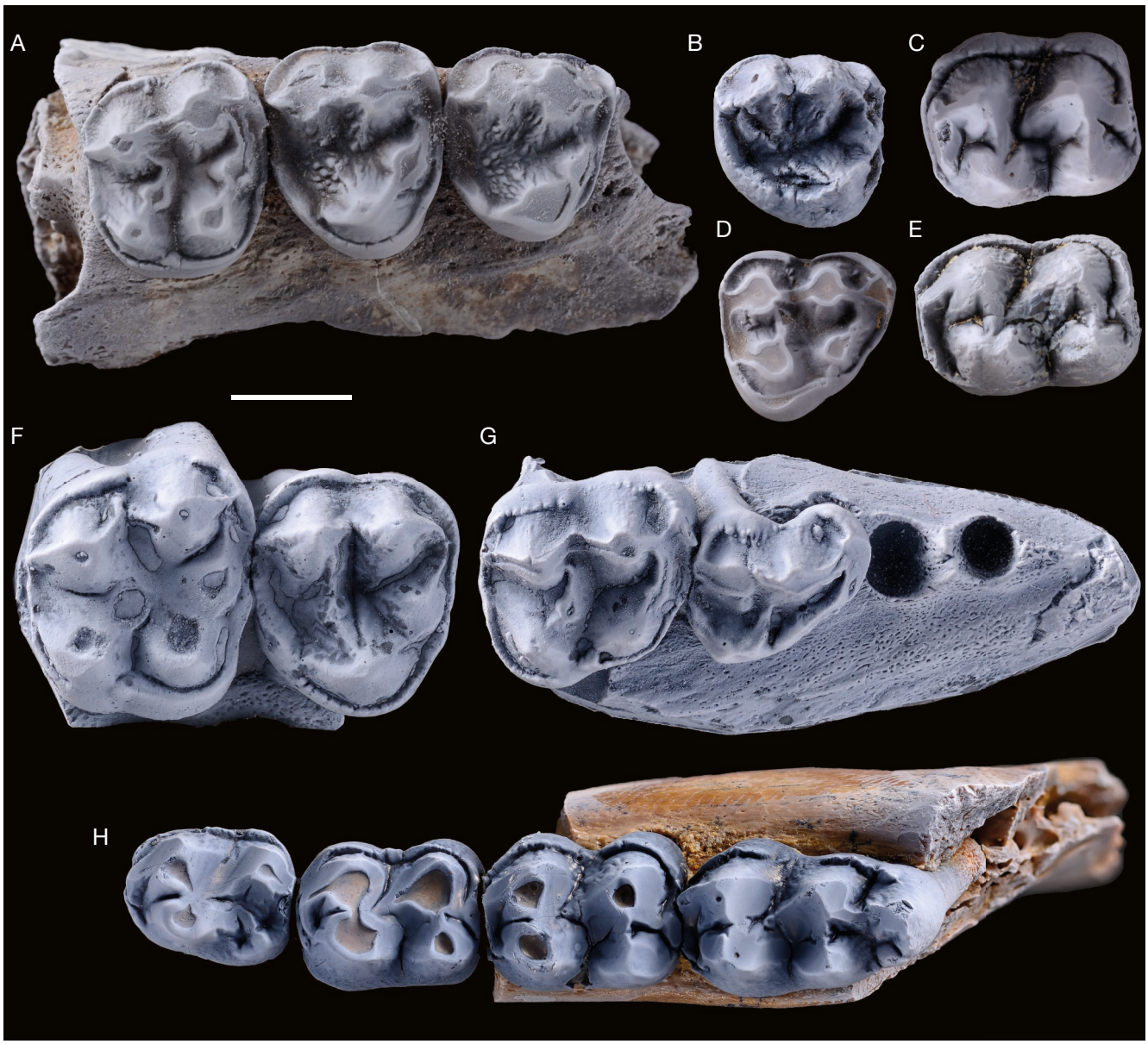

Fig. 14. — Teeth of *Hallensia parisiensis* Franzen, 1990 from the Paris Basin in occlusal view: **A**, right maxillary with P3-M1 (MNHN-CB1529); **B**, right P2 (MNHN-CB1562); **C**, left m1/2 (MNHN-STA623 [reversed]); **D**, right DP3 (MNHN-CB1557); **E**, right m1/2 (MNHN-STA625); **F**, right maxillary P4-M1 (cast of holotype, NMB-TS-631); **G**, right maxillary with DP2-DP3 (cast of paratype, NMB-TS-367); **H**, right mandible with p4-m3 (coll. Lhomme). Scale bar: 5 mm.

The mandibular symphysis is short and broad (Fig. 15I, K). It extends posterior to the limit p2-p3. A diastema is present anterior to the p2, up to the large alveoli which probably correspond to canine alveoli. The most anterior cheek tooth still present is presumed to be a p2. Its occlusal outline is elongated oval, and the two roots are widely separated. This corresponds to the morphology generally observed for a p2, the p1 usually has fused roots. The shape of the bone seems to indicate that resorbed alveoli, which could correspond to the alveoli of the p1, are present just ahead of the p2. The large alveoli situated anteriorly are deep and vertical, which is probably the alveoli of canines.

The m1-2 have a quite bunodont appearance, the cusps are very rounded (Fig. 15J). The paralophid is very short. The metaconid is twinned. The protolophid is notched. The hypolophid is either absent or very reduced. The hypoconulid is linked to the hypoconid by a postcristid when the hypolophid is absent; it is attached to the hypolophid when the latter is present. The cristid obliqua is poorly developed, it is oriented toward the base of the protolophid, in the middle. The labial cingulum is continuous. The labial sides of the protoconid and the hypoconid are very inclined (around 45°), whereas the lingual side of these cuspids is almost vertical. The m3 is wide and bunodont (Fig. 15E, F). The paralophid is quite elongated. The metaconid is twinned. The protolophid and the hypolophid are moderately developed. The cristid obliqua is oriented toward the protolophid almost in the center of the tooth, slightly labially. The labial cingulum is continuous.

The hypoconid is linked to the hypoconulid by a postcristid which is lingually flexed. A small cusp is sometimes present on the lingual side of the hypoconulid.

Deciduous teeth
The DP4 is molarized and narrower posteriorly (Fig. 15A). The centrocrista is straight. The paraconule and the metaconule are developed. The parastyle is small. The metaloph ends with a metacone fold.

The dp4 seems to be molarized, and a wide entoconid is present (Fig. 15J). The labial wall of the cuspids is very steep. A small hypolophid seems to be present. The lingual and labial cusps are obliquely aligned. The cristid obliqua is oriented low, toward the center of the protolophid.

Comparisons
The teeth are more bunodont than in other early Eocene perissodactyls. The species is smaller than *H. parisiensis* and *H. matthesi*. The junction of the lower molar hypoconulid is similar to that of *Pliolophus quesnoyensis* and *Pliolophus barnesi*. A small mesostyle is sometimes present, as in *Orolophus maldani* and *Hyracotherium*. The mandibular symphysis is shorter and more robust than in *Pliolophus*, *Cymbalophus* and *P. gaudryi*.

Comment
Hallensia was first identified as a phenacodontid condylarth (Franzen & Haubold 1986). The discovery of a complete skeleton in Messel (Germany) revealed that *Hallensia* displays a saddle-shaped navicular facet of the astragalus which led Franzen (1990) to place it within perissodactyls. Bajpai *et al.* (2006) considered *Hallensia* as close to the Indian cambaytheres, which they considered as a perissodactyl family. Indeed, the genus *Hallensia* has many similarities with the cambaytheres, recently described in India (Bajpai *et al.* 2006; Cooper *et al.* 2014; Rose *et al.* 2014). They notably have very bunodont teeth and a quasi-absence of lophs. The parastyles are very small or absent and the cingula are generally well developed. They mainly display the synapomorphy of the perissodactyls on the astragalus. *Cambaytherium*, however, has features found in phenacodonts but absent in perissodactyls and *Hallensia*, such as a developed deltopectoral crest and five metapodials per limb (Rose *et al.* 2014).

Hallensia also shows tooth wear that forms horizontal facets, as in *Cambaytherium*. This wear pattern is sometimes very pronounced (Fig. 15I). The bunodont morphology of the teeth, as well as this important wear pattern indicates a diet based on hard food. This is confirmed by the discovery of fine sand in the stomach contents of *H. matthesi*, as well as remnants of stems and few leaf remains (Franzen 1990). It probably had to feed on stems close to the ground, which explains the ingestion of clastic material such as sand.

The mandible attributed to *H. louisi* has very worn teeth. Hooker (1994) indicates that the anterior alveoli are those of p1. The shape of the bone, slightly "fenestrated" in front of the p2 seems however to indicate the presence of resorbed alveoli, which would correspond to the p1. In addition, the broad and deep shape of the alveoli is reminiscent to that of the canines of *Hallensia matthesi*, which are positioned quite vertically compared to European hippomorphs (*Cymbalophus cuniculus*, *Pliolophus quesnoyensis*).

The size of *Hallensia* increases through time. *Hallensia louisi* (MP8-9, 10) is the oldest species and is very small, and *H. parisiensis* (MP8-9, 10), which first appeared slightly later has an intermediate size between *H. matthesi* and *H. louisi*. The largest *Hallensia* species, *H. matthesi* (MP11-13), is similar in size to *Cambaytherium thewissi* and smaller than *Cambaytherium bidens*.

Hallensia aff. ***louisi***

Hallensia sp. – Smith & Hooker 1996: 120-121, fig. 1-2.

Material. — DP4 (R: IRSNB.M 1795); m1/2 (R: IRSNB.M 1796 [broken]).

Locality. — Hoegaarden (Belgium), MP8-9.

Description
Teeth
The upper molar cusps are rounded and inflated. The hypoconulid is linked to the hypoconid by a postcristid. The hypolophid is weak.

Deciduous teeth
The DP4 parastyle is poorly developed. The paraconule and the metaconule are developed. The centrocrista is slightly flexed labially. The metaloph joins the metacone. The cingulum runs on the anterior side of the hypocone. A small crest links the metaconule to the protocone.

Comment
These remains are very fragmentary (Smith & Hooker 1996). The junction of the hypoconulid with the hypoconid of the molar indicate that it does not belong to the genera *Cymbalophus* and *Orolophus*. They correspond in size and morphology to *Hallensia louisi*, presenting notably "blistered" cusps characteristic of *Hallensia*.

MORPHOLOGICAL EVOLUTION

Evolution of the morphology of cheek teeth
During the Eocene, several evolutionary trends can be identified, as well as an increase in size through time. Premolars tend to become molarized, but this is true mostly after the early Eocene, no hypocone being present in the early Eocene species here studied (Fig. 16). The P2 tends to become more triangular in occlusal view with a larger protocone. The postprotocrista and metaconules of P3-P4 are more developed in the youngest species (*Orolophus maldani*, *Propalaeotherium gaudryi*). Generally, the lophodont pattern of molars increases through time. The paraconule is always present but of variable size whereas the metaconule can be either present or absent. The centrocrista increases in height and becomes labially

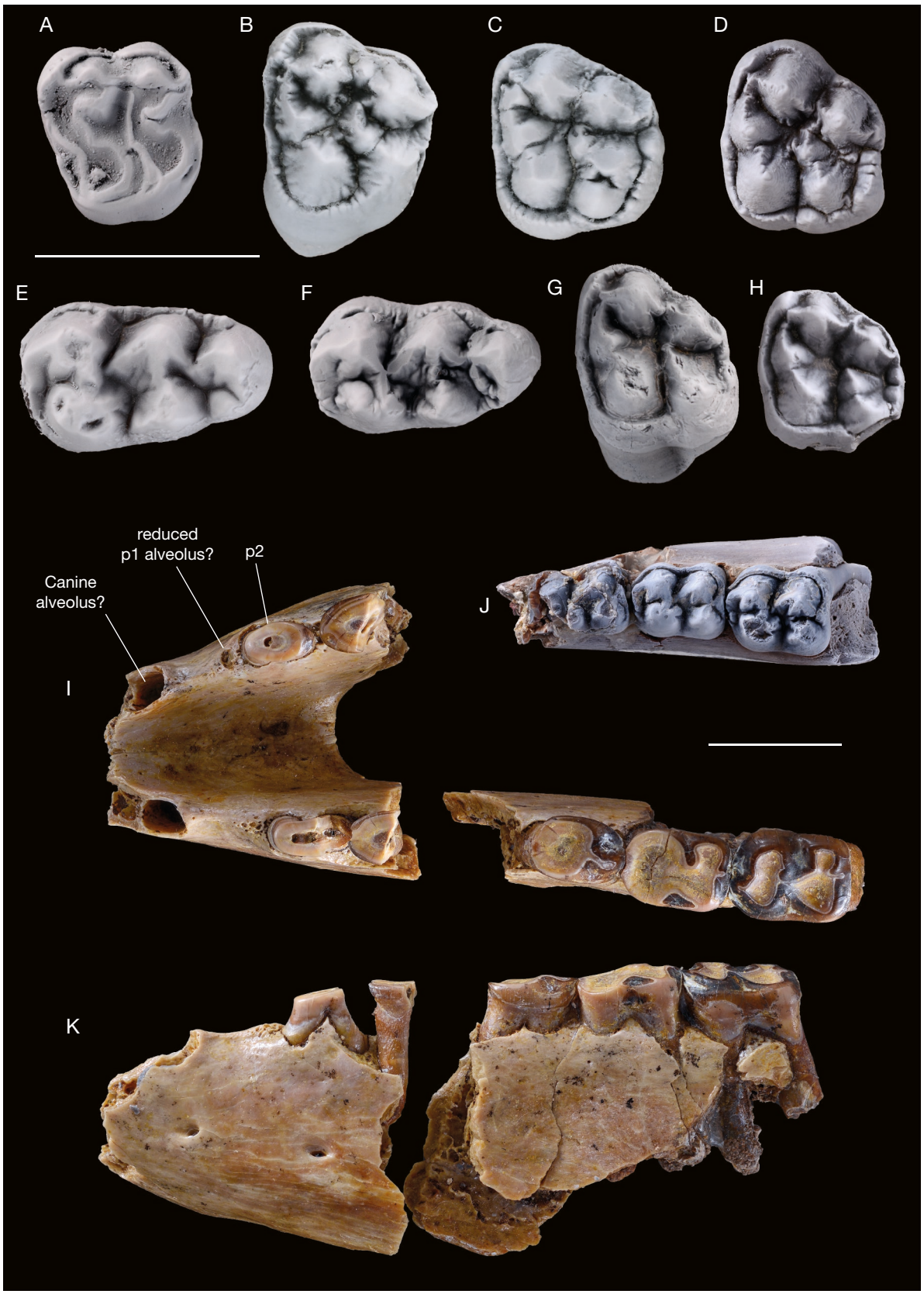

FIG. 15. — Teeth of *Hallensia louisi* Hooker, 1994 from the Paris Basin in occlusal (**A**-**J**) and lateral (**K**) views: **A**, left DP4 (MNHN-CB1574); **B**, left M1/2 (holotype, MNHN-MU218-L); **C**, left M3 (paratype, MNHN-MU221-L); **D**, left M3 (MNHN-CB1560); **E**, right m3 (MNHN-AV5672 [reversed]); **F**, left m3 (MNHN-CB224 [reversed]); **G**, right M3 (MNHN-GR7574 [reversed]); **H**, right M3 (MNHN-CB1568 [reversed]); **I, K**, mandible (AV-841-Ph, coll. Phélizon); **J**, mandible with dp4-m2 (paratype, MNHN-MU12303); **A**-**H**, **J**, coated with magnesium. Scale bars: 1 cm.

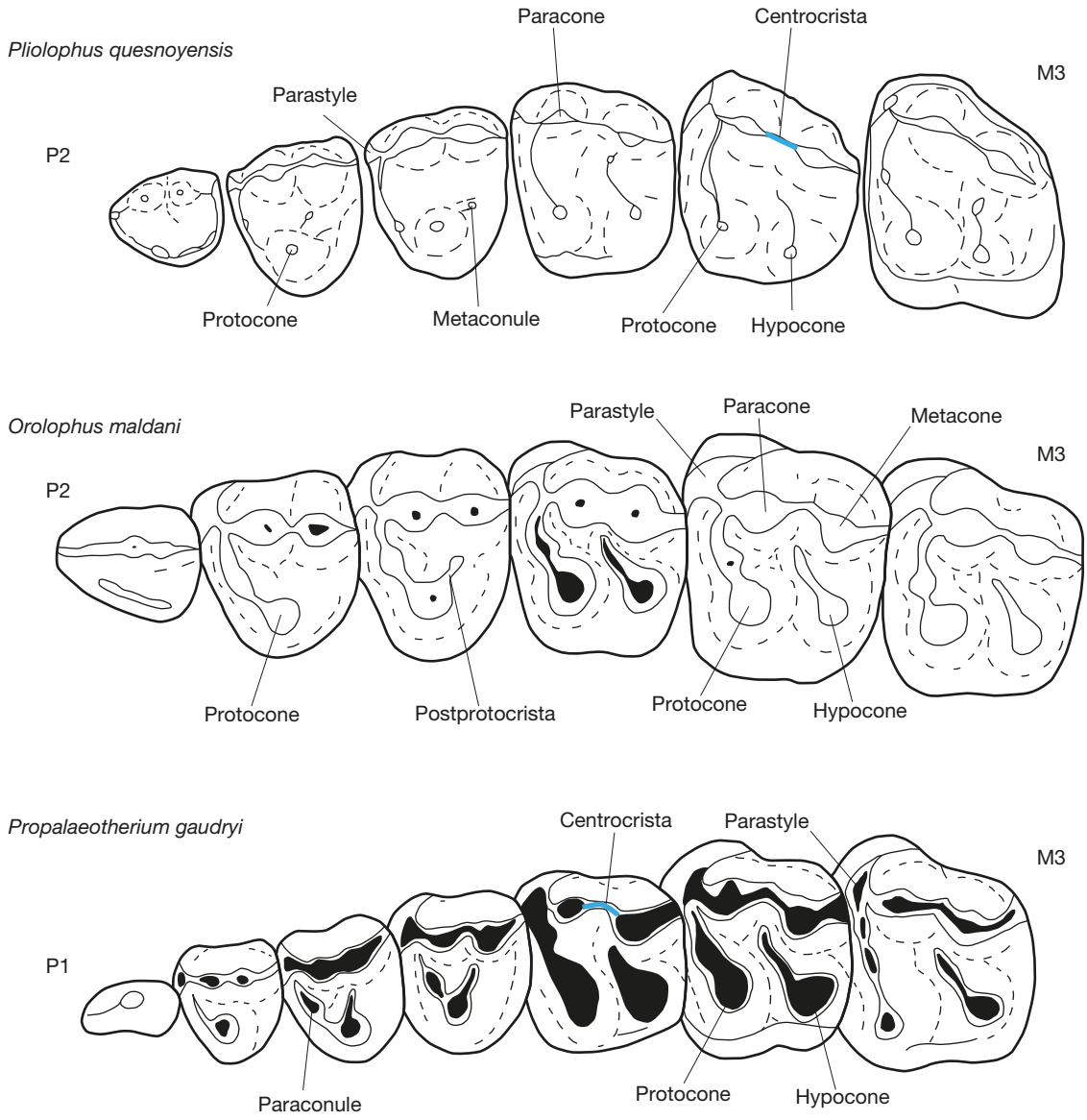

FIG. 16. — Occlusal outlines of upper teeth of *P. quesnoyensis* Bronnert, Gheerbrant, Godinot & Métais, 2018 (combined MNHN-QNY2-2900, QNY2-2869, QNY2-2867, QNY2-2858, QNY2-2852, QNY2-2815), *O. maldani* (Lemoine, 1878) (combined MNHN-SLP-29-PE10, CB16165) and *P. gaudryi* (Lemoine, 1878) (MNHN-MA14948), showing the evolutionary trends in the early Eocene hippomorphs in Europe. Scale bars: 5 mm.

flexed. The mesostyle tends to appear in the later genera with a flexed centrocrista (*Hyracotherium*, *Hallensia*, *Orolophus*).

Concerning the lower molars, the junction of the hypoconulid varies (Fig. 17). This cuspid can be connected to the hypoconid in the oldest species (*Pliolophus quesnoyensis*), but to the hypolophid in the most recent species (*Orolophus*, *Propalaeotherium*), some species displaying both morphologies (*Pliolophus barnesi*). This evolution appears first on the m1-2, and then on the m3. The cristid obliqua generally joins the protolophid at its center, but exhibits more lingual variations over time, especially in *Propalaeotherium gaudryi*. A twinned metaconid is generally observed in all the species of the early Eocene on lower molars. The twinned metaconid is absent on premolars in oldest species (*P. quesnoyensis*, *C. cuniculus*), but present on p4 in some specimens of *P.barnesi*, *Hyracotherium*, *O. maldani* and *P. gaudryi*. The entoconid on p4 is generally absent, but is sometimes present in *P. gaudryi*, and present as a small bulge in *Orolophus*.

We notice that *Hallensia* differs from the other perissodactyl genera by its bunodont morphology, which stays bunodont in *H. matthesi* from the Lutetian. The presence of clastic elements and sand in the digestive tube of *H. matthesi* (Franzen 1990) indicate that this pattern is probably related to a different feeding strategy than other perissodactyls, which consisted to ingest more clastic elements while eating close to the ground.

EVOLUTION OF THE MORPHOLOGY OF DECIDUOUS TEETH

The morphology of deciduous teeth during the lower Eocene, tends to acquire a dental pattern similar to that of molars. The DP2 has a small bulge on the cingulum, not well-developed lingual cusps in early Eocene species (*Pliolophus*

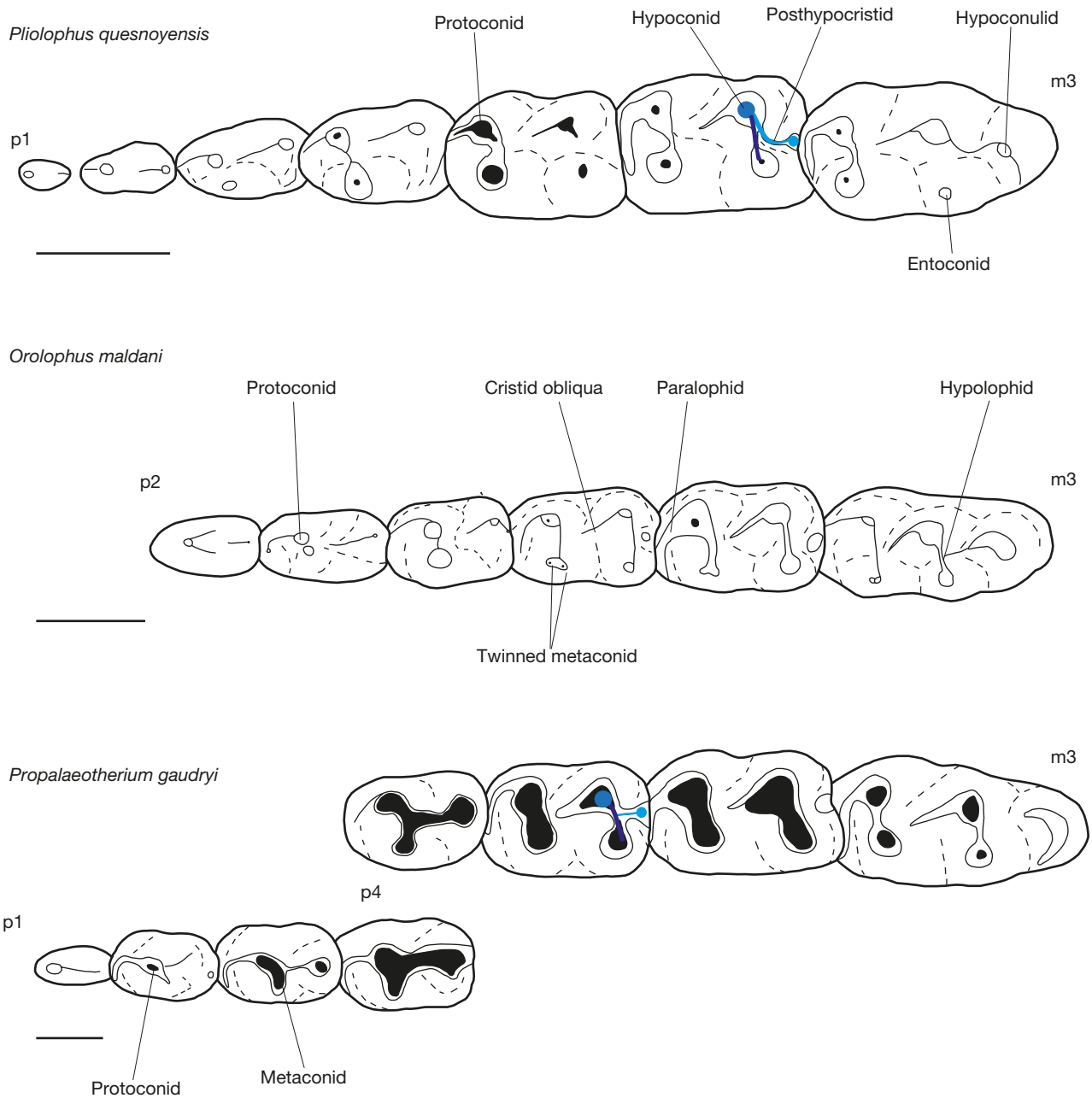

FIG. 17. — Occlusal outlines of lower teeth of *P. quesnoyensis* Bronnert, Gheerbrant, Godinot & Métais, 2018 (combined MNHN-QNY2-2637, 2633, 2560), *O. maldani* (Lemoine, 1878) (combined MNHN-SLP-29-PE165, SLP-29-PE759, SLP-29-PE480) and *P. gaudryi* (Lemoine, 1878) (combined MNHN-AL5212, MA14902), showing the evolutionary trends in the early Eocene hippomorphs in Europe. Scale bars: 5 mm.

quesnoyensis) (Fig. 18). In the more recent species (*Hallensia parisiensis*), a small hypocone is present and a cingulate bulge (incipient protocone?) is present. Only *Orolophus maldani* has a distinct morphology of the DP2 on which the lingual cusps are absent and the metacone reduced. The parastyle of DP3 tends to be less projected anteriorly in more recent genera (*Orolophus*, *Hallensia*, *Propalaeotherium*) (Fig. 18). The centrocrista becomes increasingly higher and flexed through time, and the protocone, very reduced in older genera (*Pliolophus*, *Cymbalophus*), becomes larger. The conules and the lophs also become larger. The DP4 are generally molarized and follow the same pattern as that of molars (Fig. 18). The accessory cusp present on the lingual cingulum in *Pliolophus*, is absent in *Orolophus*.

The crests of the dp2 become more developed through time. The morphology of the hypoconulid of dp3 and dp4 is the same as that of molars (Fig. 19). This cuspid is isolated or linked to the hypoconid in *Pliolophus quesnoyensis*, and connected to the center of the hypolophid in *Orolophus* and *Propalaeotherium*. The lophs become higher and more developed during the Eocene. The morphology of the deciduous teeth of European hippomorphs (*Pliolophus*) in the early Eocene is very similar to that observed in North American Wasatchian equids (Rose *et al.* 2018). The DP2

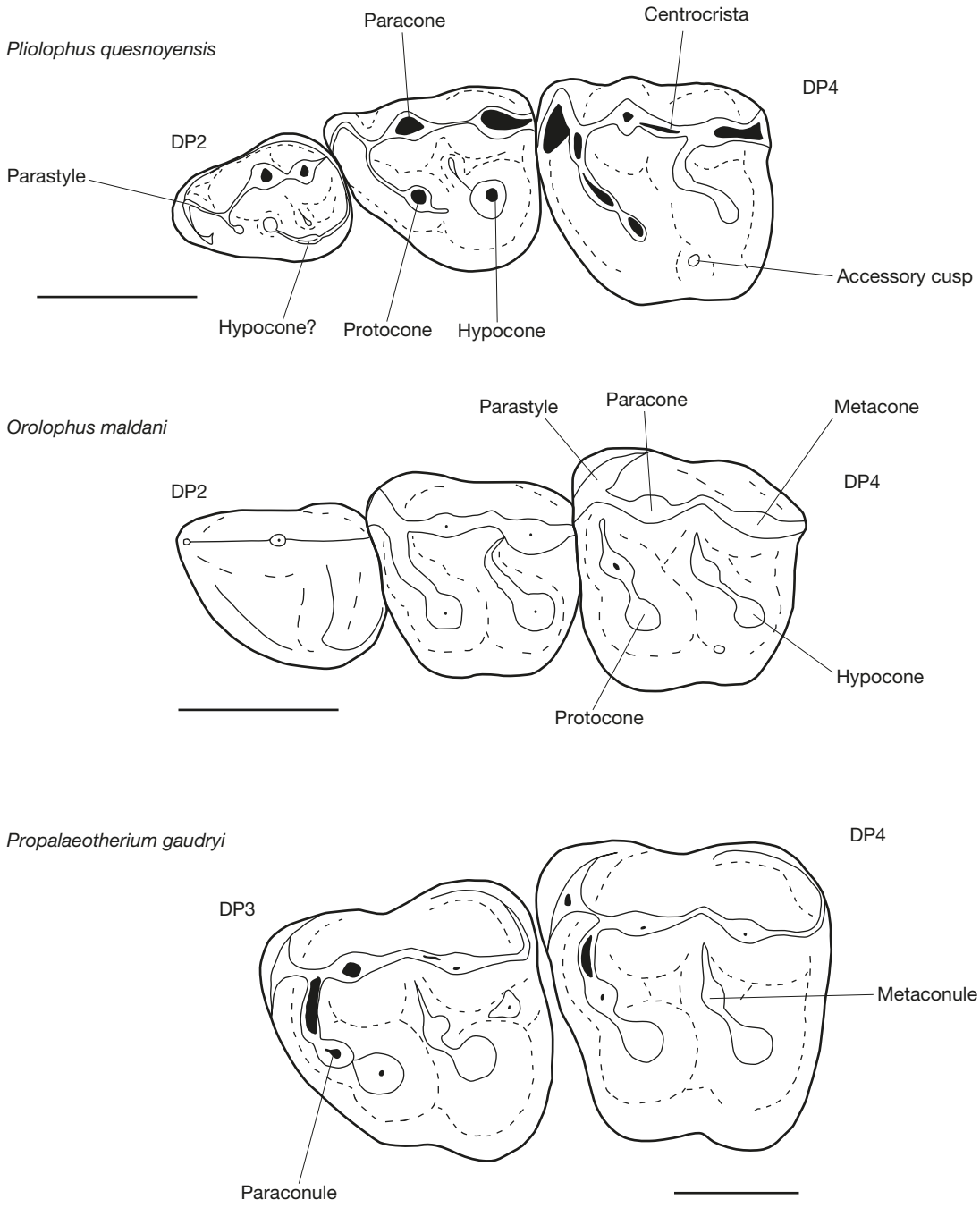

FIG. 18. — Occlusal outlines of upper milk teeth of *P. quesnoyensis* Bronnert, Gheerbrant, Godinot & Métais, 2018 (combined MNHN-QNY2-2840, 2883, 2903), *O. maldani* (Lemoine, 1878) (combined MNHN-SLP-29-PE1436 [reversed], SLP-29-PE100, SLP-29-PE1201) and *P. gaudryi* (MNHN-MTH53-L), showing the evolutionary trends in the early Eocene hippomorphs in Europe. Scale bars: 5 mm.

and DP3 have a large metacone which is separated from the paracone, the conules are developed and the lophs are well-marked. As in the American species, it is difficult to identify European species only by milk teeth. However, we can notice the more derived morphology of *Orolophus*, which possesses molarized DP2 with lingual cusps and well developed lophs, and DP3 which is very similar to DP4 with its developed protocone and its parastyle lower than in *Pliolophus* (Fig. 18). There is a clear trend toward the molarization of deciduous teeth early Eocene European hippomorphs, as in the American Wasatchian equids (Rose *et al.* 2018). Likewise, the intraspecific variation is of the same range than that observed in American equids. The hypolophid exhibits variable development on lower deciduous premolars, a feature found in early Eocene American equids (Rose *et al.* 2018).

Butler (1952a) identified three patterns of molarization of deciduous teeth in perissodactyls. In Ceratomorpha, the hypocone appears first, followed by the metacone, protocone and hypoconulid, and finally the metaconid and entoconid.

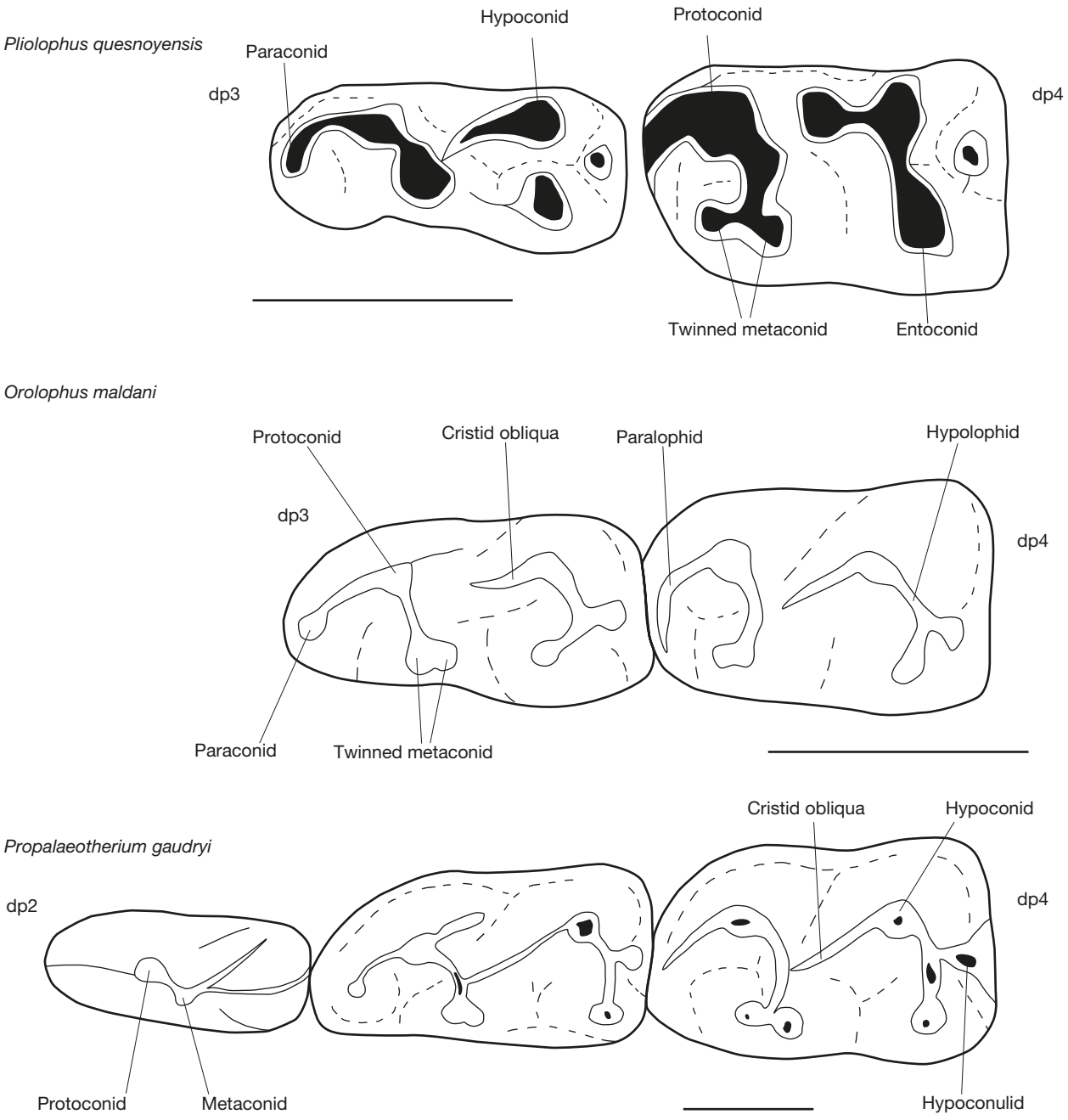

Fig. 19. — Occlusal outlines of lower milk teeth of *P. quesnoyensis* Bronnert, Gheerbrant, Godinot & Métais, 2018 (combined MNHN-QNY2-2778, 2762), *O. maldani* (Lemoine, 1878) (combined MNHN-SLP-29-PE1355, SLP-29-PE2477) and *P. gaudryi* (Lemoine, 1878) (MNHN-CHO14801), showing the evolutionary trends in the early Eocene hippomorphs in Europe. Scale bars: 5 mm.

In the equids and Brontotheriidae, the hypoconulid and metacone appear first, then the entoconid and hypocone and finally metaconid and protocone. European early hippomorphs display a pattern similar to that of equids and brontotherids. However, the Palaeotheriidae display a different pattern of molarization that is similar to that of Phenacodontidae, and in which the protocone becomes developed before the talonid, the metacone and the hypocone.

Butler (1952b) considered Palaeotheriidae as a distinct family that retains condylarth features of the decidual dentition, and which can't be derived from *Hyracotherium* (i.e. equids). However, he excluded *Pachynolophus* and *Propachynolophus* (i.e. *O. maldani* and *P. gaudryi*) from Palaeotheriidae because of their molarization pattern close to the one of *Hyracotherium*, and considered them as derived from *Hyracotherium* (i.e. equids).

According to our observations, the European hippomorphs fall into the second category, corresponding to equids and brontotheriids. It is probable that this molarization pattern was primarily present in Europe (or before hippomorphs arrived in Europe) and persisted in America after a dispersal of European hippomorphs to America.

TABLE 1. — Occurrences of European perissodactyls during the early Eocene in France and Northern Europe. Palette (Godinot *et al.* 1987), Fordonnes (Marandat 1997), Rians (Godinot 1981), Sainte-Eulalie (Danilo *et al.* 2013). Colours: **pink**, Southern France; **light-blue**, Paris Basin *s.l.*; **dark-blue**, Paris Basin *s.s.*

	MP7													MP8-9										MP10
	Palette	Fordonnes	Rians	Erquelinnes	Kyson	Le Quesnoy	Try	Meudon	Sinceny	Soissons	Pourcy	Abbey Wood	Harwich	Sainte-Eulalie	Herne Bay	Oosterzele	Mutigny	Avenay	Condé-en-Brie	Gland	Sézanne-Broyes	Saint-Agnan	Grauves s.l.	Prémontré
Cymbalophus cuniculus (Owen, 1842)	–	–	aff.	×	×	–	–	–	–	–	–	–	–	–	–	–	–	–	aff.	–	–	–	–	–
Cymbalophus hookeri Godinot, Crochet, Hartenberger, Lange-Badré, Russell, Sigé, 1987	×	×	–	–	–	–	–	–	–	–	–	–	–	–	–	–	–	–	–	–	–	–	–	–
Sifrhippus sandrae (Gingerich, 1989)	–	–	–	cf.	–	–	–	–	–	–	–	–	–	–	–	–	–	–	–	–	–	–	–	–
Pliolophus quesnoyensis Bronnert, Gheerbrant, Godinot & Métais, 2018	–	–	–	–	–	×	×	×	×	–	–	–	–	–	–	–	–	–	–	–	–	–	–	–
Pliolophus barnesi Hooker, 2010	–	–	–	–	–	–	–	–	–	×	×	×	–	–	–	–	–	–	–	–	–	–	–	–
Pliolophus vulpiceps Owen, 1858	–	–	–	–	–	–	–	–	–	–	–	–	×	–	–	–	–	–	–	–	–	–	–	–
Hyracotherium leporinum Owen, 1841	–	–	–	–	–	–	–	–	–	–	–	–	–	–	×	–	×	×	–	–	–	–	–	×
Hallensia louisi Hooker, 1994	–	–	–	–	–	–	–	–	–	–	–	–	–	–	–	×	×	×	×	×	–	–	×	–
Hallensia parisiensis Franzen, 1990	–	–	–	–	–	–	–	–	–	–	–	–	–	–	–	–	–	–	×	–	–	×	×	–
Pachynolophus eulaliensis Danilo, Remy, Vianey-Liaud, Marandat, Sudre & Lihoreau, 2013	–	–	–	–	–	–	–	–	–	–	–	–	–	×	–	–	–	–	–	–	–	–	–	–
Orolophus maldani (Lemoine, 1878)	–	–	–	–	–	–	–	–	–	–	–	–	–	–	–	–	–	–	×	×	×	×	×	×
Propalaeotherium gaudryi (Lemoine, 1878)	–	–	–	–	–	–	–	–	–	–	–	–	–	–	–	–	–	–	–	–	–	×	×	–

DIFFERENCES BETWEEN NORTHERN AND SOUTHERN EUROPE

There are distinct morphological trends observed between the hippomorph species of northern and southern Europe. The perissodactyls from the base of the Eocene in southern Europe display a more derived morphology compared to the northern species (well-marked lophodonty, hypoconulid reduced and linked to the hypolophid on m1-2, flexed centrocrista). Characters that are generally considered as more primitive (hypoconid-hypoconulid junction on lower molars, straight centrocrista on upper molars) are not present in Southern European species during the early Eocene (*Cymbalophus hookeri*, Godinot *et al.* 1987).

Species from southern Europe display a slightly smaller size than those from northern Europe at the beginning of the Eocene. This small size is observed in the localities of Palette (*Parvagula*, *Pseudoparamys*, *Cymbalophus*; Godinot *et al.* 1987) and Rians (*Cymbalophus*, *Diacodexis*, *Amphiperatherium*, *Proviverra*, *Phenacolemur*; Godinot 1981). Several mammalian genera have small representatives during or just after the PETM. These size changes are well documented in the Bighorn Basin (Wyoming, United States), where the phenacodontid condylarths *Copecion* and *Ectocion* become significantly smaller during the PETM interval, before returning a pre-PETM size after this climatic event (Gingerich 1989, 2003). *Hyracotherium*-like perissodactyls first appeared in North America in the Wa-0 with *Sifrhippus sandrae*, which is very small compared to the much larger *Arenahippus grangeri* (Wa-1-3) and *Arenahippus aemulor* (Wa-3). A warm climate could explain the small size of early Eocene species, especially in southern Europe. Following the Bergmann's law (Bergmann 1847; Ashton *et al.* 2000), the size of a species increases in a cool climate, and decreases in warmer climates. However, Gingerich (2003) suggests that this may not be the only factor to explain the small size observed in earliest Eocene mammals (Wa-0), and that the quality of food may have had an influence on size (Case 1979). Indeed, high atmospheric CO2 levels increase photosynthesis and inhibit the digestibility of plants by herbivores (Fajer *et al.* 1989; Kinney *et al.* 1997; Tuchman *et al.* 2002). This hypothesis remains to be tested in mammals. All the European hippomorph species of the earliest Eocene have a small size, especially the oldest (*C. hookeri*, *C. cuniculus*, *P. quesnoyensis*). Later in the early Eocene, the size of the species increases through time, *Propalaeotherium* being larger than genera known in the earliest Eocene (Figs 20-22).

INTRA-EUROPEAN DISPERSALS

Differences at the specific level are observed between northern and southern Europe perissodactyls at the beginning of the Eocene (MP7, Table 1). However, there is a homogenization of species between northern and southern Europe at MP8-9. These observations corroborate those made for other group such as mesonychids (Solé *et al.* 2017). Plaziat (1977) noticed a southward migration of continental molluscs suggesting a substantial cooling during the Thanetian followed by a return of these molluscan faunas to the North during the early Eocene warming. This climatic zonation between the North and South of Europe is consistent with the pollens, which indicate warming with tropical to subtropical vegetation in the South at the lower Ilerdian while this phenomenon occurs later (upper Sparnacian) in the Paris Basin (Gruas-Cavagnetto 1991). As no physical barrier (sea, mountain, etc.) were present between these two regions, the hypothesis of a climate barrier is currently favoured. A latitudinal gradient of the climate could indeed explain why certain groups

subservient to a less warm and wetter climate (pantodont, plesiadapids, arctocyonids...) did not colonize the South of Europe, which was probably warm and dry around MP7 (Marandat 1997; Marandat *et al.* 2012). The perissodactyls of the MP8-9 faunas from southern France such as Sainte-Eulalie (Danilo *et al.* 2013) and La Borie (pers. obs.) are very close morphologically or similar to those of Condé-en-Brie, Sézanne-Broyes and Saint-Agnan in the Paris Basin. This added to the generic turnover between the MP7 and MP8-9 sites (Table 1) indicates that at the end of the Sparnacian there was a faunal turnover and a homogenization of perissodactyl faunas between northern and southern Europe.

Inter-continental dispersals

The dispersal pathways of terrestrial vertebrates have long been debated. Godinot & Lapparent de Broin (2003), Hooker & Dashzeveg (2004) and Smith *et al.* (2006) have suggested that dispersals of modern mammalian orders at the Paleocene-Eocene boundary occurred between Asia and Europe, and then to North America. Beard & Dawson (1999) and Beard (2008) propose that the first Paleocene-Eocene dispersions occurred from Asia to North America before dispersal in Europe.

Godinot (1981) and Hooker (1980, 2015) suggested a dispersal from Europe to North America based on the artiodactyl *Diacodexis* and perissodactyls, respectively. This hypothesis has been questioned after the discovery of the primate *Cantius torresi* in North America, which appears more primitive than the European species *Cantius eppsi*, and therefore suggests a dispersal from America to Europe for primates, and probably for other groups of mammals (Gingerich 1986, 1989, 1991).

The identified symplesiomorphies (hypoconid-hypoconulid junction on lower molars, straight centrocrista on upper molars) in European hippomorphs suggest that the first dispersals could have occurred from Europe to North America for hippomorphs (Bronnert *et al.* 2018). The European and North American perissodactyls each display a strong endemism from the base of the Eocene. Froehlich (2002) suggested that *Hyracotherium leporinum* from the MP8-9 of England may be the most basal paleotheriid that diversified subsequently and exclusively in Europe, whereas equids would have originated and diversified in North America during the early Eocene. Unlike the basal paleotheriids, the P2 of *Hyracotherium leporinum* lacks the lingual cusps as in most basal equids in North America, suggesting that this taxon might be a North American equid not closely related to European paleotheriids. Bai (2017) reported paleotheriids from the middle Eocene of China suggesting at least intermittent exchanges between Europe and Asia during the early and/or middle-late Eocene. Hippomorphs have long been considered as absent in Asia during the early Eocene. The earliest occurrence of hippomorphs in Asia is documented by the basal equid *Erihippus tingae* Bai, Wang & Meng, 2018 from the earliest Eocene Lingcha Formation in Southern China (Bai *et al.* 2018). However, the validity of the genus should be questioned. *Erihippus* is not based

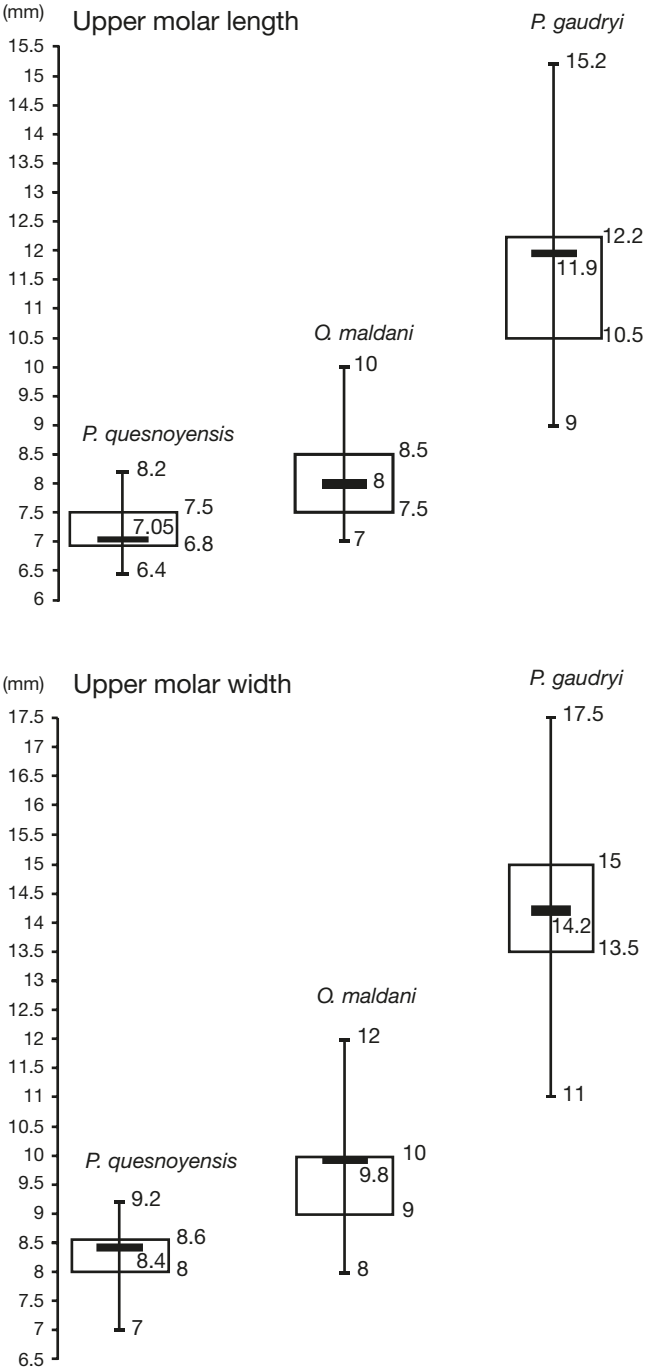

Fig. 20. — Boxplots showing the size distribution of upper molars of early hippomorphs. The rectangle represents the first and third quartiles (25% and 75% of data respectively), the bold line is the median (50% of data) and the vertical line extends to the minimum and maximum values. *Pliolophus quesnoyensis* Bronnert, Gheerbrant, Godinot & Métais, 2018: n = 26; *Orolophus maldani* (Lemoine, 1878): n = 111; *Propalaeotherium gaudryi* (Lemoine, 1878): n = 54.

on new material, but on the reinterpretation of dental material previously referred to *Orientolophus hengdonghensis* (Ting 1993). *Erihippus* is based on two specimens, a maxillary (DP4-M2) and a mandible (m1-m3) while the third specimen, a maxillary (DP4-M2), was left under the genus *Orientolophus*. The dental characters that supposedly serve to distinguish the two genera are not clearly discernable

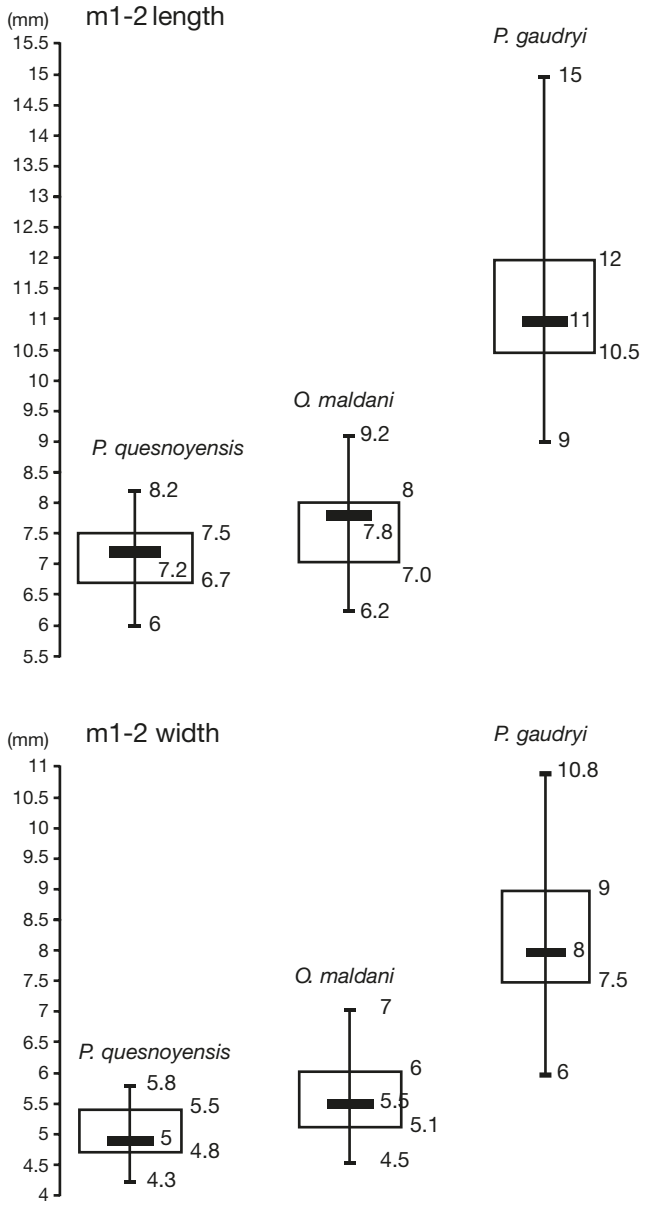

Fig. 21. — Boxplots showing the size distribution of m1-2 of early hippomorphs. The rectangle represents the first and third quartiles (25% and 75% of data respectively), the bold line is the median (50% of data) and the vertical line extends to the minimum and maximum values. *Pliolophus quesnoyensis* Bronnert, Gheerbrant, Godinot & Métais, 2018: n = 21; *Orolophus maldani* (Lemoine, 1878): n = 78; *Propalaeotherium gaudryi* (Lemoine, 1878): n = 59.

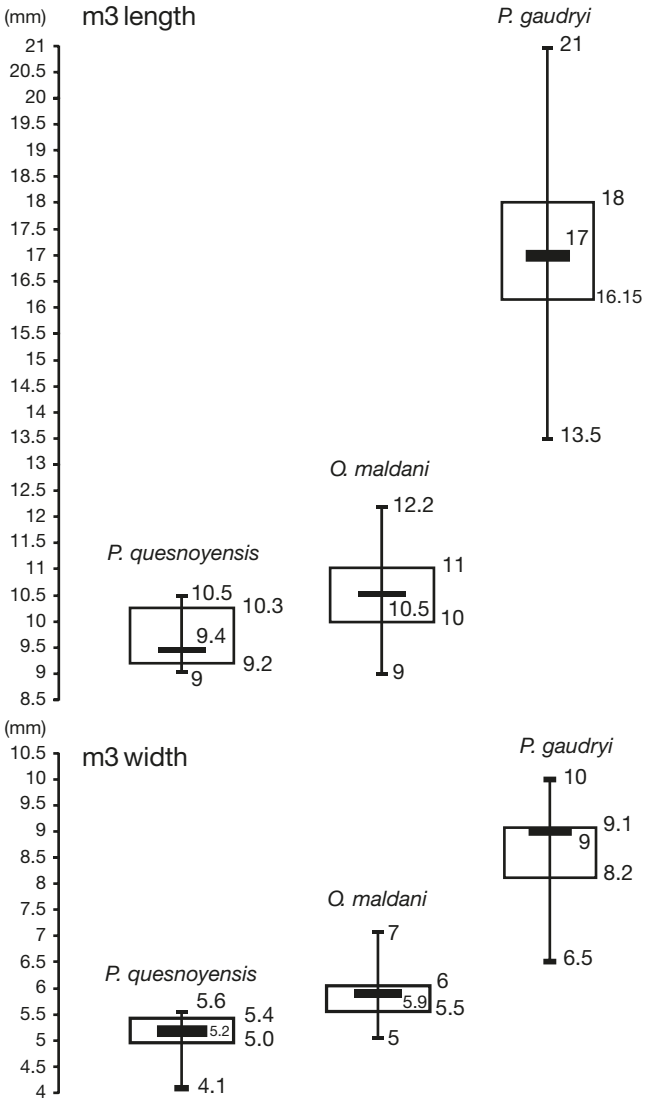

Fig. 22. — Boxplots showing the size distribution of m3 of early hippomorphs. The rectangle represents the first and third quartiles (25% and 75% of data respectively), the bold line is the median (50% of data) and the vertical line extends to the minimum and maximum values. *Pliolophus quesnoyensis* Bronnert, Gheerbrant, Godinot & Métais, 2018: n = 16; *Orolophus maldani* (Lemoine, 1878): n = 32; *Propalaeotherium gaudryi* (Lemoine, 1878): n = 28.

because of the wear of the teeth. For example, the relative size of the paraconules and metaconules on the DP4 and molars in *Erihippus* and *Orientolophus* is not obvious on the published material. Likewise the orientation of the metaloph at the base of the metacone might result from wear or intraspecific variation (Bronnert *et al.* 2018). Moreover, the relative position (separation) of the paracone and metacone on upper DP4 and molars is not significantively different. On the lower molars, the labial orientation of the cristid obliqua is rather a character that distinguishes tapiromorph (Wood, 1934). The differences seem too weak to create two species, moreover belonging to different suborders. These remains are poorly known, and display features of both hippomorphs (poorly developed lophodonty, small parastyle) and tapiromorphs (labial cristid obliqua, reduced conules). Consequently, *Erihippus* is currently an insufficiently defined genus, and if valid, its affinities with hippormorphs are not clearly demonstrated. Bai *et al.* (2018) suggest that hippomorphs may have originated in Europe on the basis of ancestral reconstruction of geographic distribution. This favour the hypothesis of Hooker (2015), which supposed a late Paleocene age for Le Quesnoy (Paris Basin). There is currently no basis to demonstrate a late Paleocene age for Le Quesnoy, an interval which is otherwise documented in that basin by the fossil locality of Rivecourt (Smith *et al.* 2014) where no perissodactyls have been reported. However, the early hippomorphs from the early Eocene of

Europe display a more primitive morphology than that of North American equids (Bronnert *et al.* 2018) suggesting that hippomorphs originated in the Old World, probably during the late Paleocene.

CONCLUSIONS

The study of early Eocene perissodactyls allows identification of nine hippomorph species in the Paris Basin during the Early Eocene (MP7 to MP10) (Table 1). The new material from various localities provide better documentation of otherwise poorly known species, such as *Hallensia louisi* and *Hallensia parisiensis*. The numerous fossils from MP10 localities allow us to refine the definition of *Propalaeotherium gaudryi* and *Orolophus maldani* as well as their variability, which have been little studied and figured. The fossils make possible observation of the morphological evolution of European hippomorphs during the early Eocene, especially the increase of the flexure of the upper molar centrocrista, the lingual cristid obliqua and the junction of the hypoconulid with the hypolophid on the lower molars. At the very beginning of the Eocene (MP7), there are differences between the faunas of Southern and Northern Europe. These faunas become homogenized in the sites related to the MP8-9, and a generic turnover takes place. The genera *Pliolophus* and *Cymbalophus* (MP7) are replaced by the genera *Hyracotherium*, *Orolophus* and *Hallensia* (MP8-10), with persistence of *Cymbalophus*, known from two sites related to the MP8-9. It appears that all perissodactyl groups appear very early in the early Eocene, as do other groups of mammals (e.g., artiodactyls, see Gingerich 2006), followed by rapid dispersal throughout the Northern Hemisphere from Asia. The fossil record of Asia is very scarce, it is possible that hippomorphs were present very early in the Eocene in Asia, even in the Paleocene. Dispersals between Europe and North America occurred very early during the early Eocene, resulting in groups of endemic hippomorphs on these two continents: equids in North America and palaeotheres in Europe.

Acknowledgements
We would thank all the contributors, professional and especially non institutional, who helped to build the fossil collections from the Paris Basin. We especially thank Gaël de Ploëg, Alain Phélizon, Jean-Louis Pellouin, François Duchaussois and Jean-François Lhomme for their contributions and discussions. We also thank the curators and staff for the access to the collection: G. Billet, C. Sagne and V. Pernègre (MNHN, Paris), P. Brewer and J. Hooker (NHM, London), L. Costeur (NMB, Basel), E. Robert (Université Lyon 1) and A. Folie and T. Smith (IRSNB, Brussels). We also thank the technical team of the CR2P (Y. Despres, C. Bouillet, R. Vacant) for the preparation and casts of the fossils. We are grateful to the MNHN photographers L. Cazes and P. Loubry who produced the photographs of this paper, and to V. Zeitoun (CR2P). Finally, we would thank Dr Bin Bai and Dr Luke T. Holbrook, who reviewed the manuscript, and thus allowed us to improve it.

REFERENCES

Ashton K. G., Tracy M. C. & De Queiroz A. 2000. — Is Bergmann's rule valid for mammals? *American Naturalist* 156 (4): 390-415. https://doi.org/10.1086/303400

Bai B. 2017. — Eocene Pachynolophinae (Perissodactyla, Palaeotheriidae) from China, and their palaeobiogeographical implications. *Palaeontology* 60 (6): 837-852. https://doi.org/10.5061/dryad.cv87j

Bai B., Wang Y. Q. & Meng J. 2018. — The divergence and dispersal of early perissodactyls as evidenced by early Eocene equids from Asia. *Communications Biology* 1 (1): 115. https://doi.org/10.1038/s42003-018-0116-5

Bajpai S., Kapur V., Thewissen J. G. M., Das D. P. & Tiwari B. N. 2006. — New Early Eocene Cambaythere (Perissodactyla, Mammalia) from the Vastan Lignite Mine (Gujarat, India) and an evaluation of cambaythere relationships. *Journal of the Palaeontological Society of India* 51: 101-110. http://repository.ias.ac.in/93951/

Beard K. C. 1998. — East of Eden: Asia as an important center of taxonomic origination in mammalian evolution. *Bulletin of the Carnegie Museum of Natural History* 34: 5-39. https://www.biodiversitylibrary.org/page/52329888

Beard K. C. 2008. — The oldest North American primate and mammalian biogeography during the Paleocene/Eocene Thermal Maximum. *Proceedings of the National Academy of Sciences* 105 (10): 3815-3818. https://doi.org/10.1073/pnas.0710180105

Beard K. C. & Dawson M. R. 1999. — Intercontinental dispersal of Holarctic land mammals near the Paleocene/Eocene boundary: paleogeographic, paleoclimatic and biostratigraphic implications. *Bulletin de la Société géologique de France* 170 (5): 697-706.

Bergmann C. 1847. — Über die Verhältnisse der Wärmeökonomie der Thiere zu ihrer Grösse. *Göttinger Studien* 3: 595-708. https://mdz-nbn-resolving.de/details:bsb10306637

Biochrom'97 1997. — Synthèse et tableaux de corrélations, *in* Aguilar J.-P., Legendre S. & Michaux J. (eds), Actes du Congrès BiocroM'97. *Mémoires et Travaux de l'École pratique des Hautes Études, Institut de Montpellier* 21: 769-805.

Bronnert C., Gheerbrant E., Godinot M. & Métais G. 2018. — A primitive perissodactyl (Mammalia) from the early Eocene of Le Quesnoy (Mp7, France). *Historical Biology* 30 (1-2): 237-250. https://doi.org/10.1080/08912963.2017.1341502

Bronnert C., Gheerbrant E., Godinot M. & Métais G. 2019. — First European 'Isectolophidae' (Mammalia, Perissodactyla): *Chowliia europea*, sp. nov., from the lower Eocene of Le Quesnoy, France. *Journal of Vertebrate Paleontology* 38 (4): 1-9. https://doi.org/10.1080/02724634.2018.1487448

Butler P. M. 1952a. — The milk-molars of Perissodactyla, with remarks on molar occlusion. *Proceeding of the Zoological Society of London* 121: 777-817. https://doi.org/10.1111/j.1096-3642.1952.tb00784.x

Butler P. M. 1952b. — Molarization of the premolars in the Perissodactyla. *Proceedings of the Zoological Society of London.* 121:819-843. https://doi.org/10.1111/j.1096-3642.1952.tb00785.x

Case T. J. 1979. — Optimal body size and an animal's diet. *Acta Biotheoretica* 28 (1):54-69. https://doi.org/10.1007/Bf00054680

Cooper L. N., Seiffert E. R., Clementz M., Madar S. I., Bajpai S., Hussain S. T. & Thewissen J. G. M. 2014. — Anthracobunids from the Middle Eocene of India and Pakistan are stem Perissodactyls. *PloS One* 9 (10): e109232. https://doi.org/10.1371/journal.pone.0109232

Cope E. D. 1872. — *On the Extinct Vertebrata of the Eocene of Wyoming: Observed by the Expedition of 1872, with Notes on the Geology*. US Government Printing Office, Washington, 104 p.

Cope E. D. 1884. — *The Vertebrata of the Tertiary Formation of the West*. US Government Printing Office, Washington. https://doi.org/10.3133/70038954

DANILO L., REMY J.-A., VIANEY-LIAUD M., MARANDAT B., SUDRE J. & LIHOREAU F. 2013. — A new Eocene locality in Southern France sheds light on the basal radiation of Palaeotheriidae (Mammalia, Perissodactyla, Equoidea). *Journal of Vertebrate Paleontology* 33 (1): 195-215. https://doi.org/10.1080/02724634.2012.711404

DEPÉRET C. 1901. — Révision des formes européennes de la famille des Hyracothéridés. *Bulletin de la Société géologique de France*, *4ème série*, 1: 199-225. https://www.biodiversitylibrary.org/page/30552662

FAJER E. D., BOWERS M. D. & BAZZAZ F. A. 1989. — The effects of enriched carbon dioxide atmospheres on plant-insect herbivore interactions. *Science* 243 (4895): 1198-1200. https://doi.org/10.1126/science.243.4895.1198

FORSTER-COOPER C. 1932a. — On some mammalian remains from the Lower Eocene of the London Clay. *Annals and Magazine of Natural History, London* 9 (53): 458-467. https://doi.org/10.1080/00222933208673518

FORSTER-COOPER C. 1932b. — The Genus *Hyracotherium*. A revision and description of new specimens found in England. *Philosophical Transactions of the Royal Society B: Biological Sciences* 221: 431-448. https://doi.org/10.1098/rstb.1932.0008

FRANZEN J. L. 1990. — *Hallensia* (Mammalia, Perissodactyla) aus Messel und dem Pariser Becken sowie Nachträge aus dem Geiseltal. *Bulletin de l'Institut royal des Sciences naturelles de Belgique, Sciences de la Terre* 60: 175-201. http://pascal-francis.inist.fr/vibad/index.php?action=getRecordDetail&idt=19633641

FRANZEN J. L. & HAUBOLD H. 1986. — The middle Eocene of European mammalian stratigraphy. Definition of the Geiseltalian. *Modern Geology* 10 (2-3): 159-170.

FROEHLICH D. J. 2002. — *Quo vadis Eohippus*? The systematics and taxonomy of the early Eocene equids (Perissodactyla). *Zoological Journal of the Linnean Society* 134 (2): 141-256. https://doi.org/10.1046/j.1096-3642.2002.00005.x

GINGERICH P. D. 1986. — Early Eocene *Cantius torresi* – oldest primate of modern aspect from North America. *Nature* 319: 319-321. https://doi.org/10.1038/319319a0

GINGERICH P. D. 1989. — New earliest Wasatchian mammalian fauna from the Eocene of Northwestern Wyoming: Composition and diversity in a rarely sampled high-floodplain assemblage. *University of Michigan Papers on Paleontology* 28: 1-97. https://hdl.handle.net/2027.42/48628

GINGERICH P. D. 1991. — Systematics and evolution of early Eocene Perissodactyla (Mammalia) in the Clarks Fork Basin, Wyoming. *Contributions from the Museum of Paleontology, the University of Michigan* 28 (8): 181-213. https://hdl.handle.net/2027.42/48544

GINGERICH P. D. 2003. — Mammalian responses to climate change at the Paleocene-Eocene boundary: Polecat Bench record in the northern Bighorn Basin, Wyoming. *Geological Society of America Special Papers* 369: 463-478. https://doi.org/10.1130/0-8137-2369-8.463

GINGERICH P. D. 2006. — Environment and evolution through the Paleocene-Eocene thermal maximum. *Trends in Ecology and Evolution* 21 (5): 246-253. https://doi.org/10.1016/j.tree.2006.03.006

GODINOT M. 1981. — Les mammifères de Rians (Éocène inférieur, Provence). *Palaeovertebrata* 10 (2): 43-126. http://pascal-francis.inist.fr/vibad/index.php?action=getRecordDetail&idt=PASCALGEODEBRGM8220097519

GODINOT M., CROCHET J. Y., HARTENBERGER J.-L., LANGE-BADRE B., RUSSELL D. E. & SIGE B. 1987. — Nouvelles données sur les mammifères de Palette (Éocène inférieur, Provence). *Münchner Geowissenschaftliche Abhandlungen* 10: 273-288.

GODINOT M. & LAPPARENT DE BROIN F. DE 2003. — Arguments for a mammalian and reptilian dispersal from Asia to Europe during the Paleocene-Eocene boundary interval. *Deinsea* 10: 255-275. https://natuurtijdschriften.nl/pub/538717

GRANGER W. 1908. — A revision of the American Eocene horses. *Bulletin of the American Museum of Natural History* 24: 221-264. http://hdl.handle.net/2246/1436

GRUAS-CAVAGNETTO C. 1991. — Pollens et dinophycées de l'Ilerdien moyen (Éocène inférieur) de Fordones (Corbières, France). *Cahiers de Micropaléontologie* 6: 51-66.

HOLBROOK L. T. 2015. — The identity and homology of the postprotocrista and its role in molarization of upper premolars of Perissodactyla (Mammalia). *Journal of Mammalian Evolution* 22 (2): 259-269. https://doi.org/10.1007/s10914-014-9276-3

HOOKER J. J. 1980. — The succession of *Hyracotherium* (Perissodactyla, Mammalia) in the English early Eocene. *Bulletin of the British Museum of Natural History (Geology)* 33: 101-114. https://www.biodiversitylibrary.org/page/36358364

HOOKER J. J. 1984. — A primitive ceratomorph (Perissodactyla, Mammalia) from the early Tertiary of Europe. *Zoological Journal of the Linnean Society* 82: 229-244. https://doi.org/10.1111/j.1096-3642.1984.tb00545.x

HOOKER J. J. 1989. — Character polarities in early Eocene perissodactyls and their significance for *Hyracotherium* and infraordinal relationships, *in* PROTHERO D. R. & SCHOCH R. M. (eds), *The Evolution of Perissodactyls*. Oxford University Press, New York: 79-101.

HOOKER J. J. 1994. — The beginning of the equoid radiation. *Zoological Journal of the Linnean Society* 112: 29-63. https://doi.org/10.1111/j.1096-3642.1994.tb00311.x

HOOKER J. J. 2010. — *The Mammal Fauna of the Blackheath Formation of Abbey Wood. Monographs of the Palaeontographical Society* 164 (634): 1-162. https://doi.org/10.1080/25761900.2022.12131814

HOOKER J. J. 2015. — A two-phase mammalian dispersal event across the Paleocene – Eocene transition. *Newsletters on Stratigraphy* 48: 201-220. https://doi.org/10.1127/nos/2015/0060

HOOKER J. J. & DASHZEVEG D. 2003. — Causes and Consequences of Globally Warm Climates in the Early Paleogene. *Special Papers of the Geological Society of America* 369: 479-500. https://doi.org/10.1130/Spe369

HOOKER J. J. & DASHZEVEG D. 2004. — The origin of chalicotheres (Perissodactyla, Mammalia). *Palaeontology* 47 (6): 1363-1386. https://doi.org/10.1111/j.0031-0239.2004.00421.x

HOOKER J. J., COOK E. & BENTON M. J. 2005. — British Tertiary fossil mammal GCR sites, *in* BENTON M. J., COOK E. & HOOKER J. J. (eds), *Mesozoic and Tertiary Fossil Mammals and Birds of Great Britain*. Geological Conservation Review Series, 32. Joint Nature Conservation Committee, Peterborough, 215 p.

KÜHNE W. G. 1969. — A multituberculate from the Eocene of the London Basin. *Proceedings of the Geological Society of London* 1658: 199-202.

KINNEY K. K., LINDROTH R. L., JUNG S. M. & NORDHEIM E. V. 1997. — Effects of Co2 and No3 availability on deciduous trees: Phytochemistry and insect performance. *Ecology* 78 (1): 215-230. https://doi.org/10.1890/0012-9658(1997)078[0215:Eocana]2.0.Co;2

KITTS D. B. 1956. — American *Hyracotherium* (Perissodactyla, Equidae). *Bulletin of the American Museum of Natural History* 110: 1-67. http://hdl.handle.net/2246/430

LEMOINE V. 1878. — Communication sur les ossements fossiles des terrains tertiaires inférieurs des environs de Reims, *in* Comptes rendus des séances du Congrès de l'Association française pour l'avancement des sciences. Société d'Histoire naturelle de Reims, Reims, 24 p.

LEMOINE V. 1891. — Étude d'ensemble sur les dents des mammifères fossiles des environs de Reims. *Bulletin de la Société géologique de France* 3 (19): 253-290. https://www.biodiversitylibrary.org/page/34506027

LYDEKKER R. 1886. — *Catalogue of the Fossil Mammalia in the British Museum (Natural History)*. Vol. 3. Order of the Trustees, 186 p. https://doi.org/10.5962/bhl.title.61849

MCFADDEN B. J. 1992. — *Fossil Horses: Systematics, Paleobiology, and Evolution of the Family Equidae*. Cambridge University Press, Cambridge, 369 p.

MARANDAT B. 1997. — La disparité des faunes mammaliennes du niveau Mp7 (Éocène inférieur) des domaines péri-mésogéens et nordiques. Investigation d'un provincialisme intra-européen. *Newsletters on Stratigraphy* 35 (2): 63-82. https://doi.org/10.1127/nos/35/1997/63

MARANDAT B., ADNET S., MARIVAUX L., MARTINEZ A., VIANEY-LIAUD M. & TABUCE R. 2012. — A new mammalian fauna from the earliest Eocene (Ilerdian) of the Corbières (Southern France): Palaeobiogeographical implications. *Swiss Journal of Geosciences* 105 (3): 417-434. https://doi.org/10.1007/s00015-012-0113-5

MCKENNA M. C. & BELL S. K. 1997. — *Classification of Mammals Above the Species Level*. Columbia University Press, New York, 631 p.

MISSIAEN P., QUESNEL F., DUPUIS C., STORME J. Y. & SMITH T. 2013. — The earliest Eocene mammal fauna of the Erquelinnes Sand Member near the French-Belgian border. *Geologica Belgica* 16: 262-273. http://hdl.handle.net/1854/Lu-4181357

NEL A., PLÖEG G. DE, DEJAX J., DUTHEIL D., FRANCESCHI D. DE, GHEERBRANT E., GODINOT M., HERVET S., MENIER J. J., AUGÉ M., BIGNOT G., CAVAGNETTO C., DUFFAUD S., GAUDANT J., HUA S., JOSSANG A., LAPPARENT DE BROIN F. DE, POZZI J.-P., PAICHELER J.-C., BEUCHET F. & RAGE J.-C. 1999. — Un gisement sparnacien exceptionnel à plantes, arthropodes et vertébrés (Éocène basal, Mp7): Le Quesnoy (Oise, France). *Comptes Rendus de l'Académie des Sciences de Paris* 329: 65-72. https://doi.org/10.1016/S1251-8050(99)80229-8

OWEN R. 1839. — Description of the Fossil mentioned in the preceding letter. *The Magazine of Natural History* 3: 446-448. https://www.biodiversitylibrary.org/page/2270419

OWEN R. 1841. — Description of the fossil remains of a Mammal (*Hyracotherium leporinum*) and of a bird (*Lithornis vulturinus*) from the London Clay. *Transactions of the Geological Society of London* 5: 203-206. https://doi.org/10.1144/transgslb.6.1.203

OWEN R. 1842. — Description of some molar teeth from the Eocene Sand at Kyson in Suffolk, indicative of a new species of *Hyracotherium* (*Hyr. cuniculus*). *The Annals and Magazine of Natural History; Zoology, Botany, and Geology* 48: 1-2. https://doi.org/10.1080/03745484109442721

OWEN R. 1846. — *A History of British Fossil Mammals, and Birds*. J. van Voorst, London, 560 p. https://doi.org/10.5962/bhl.title.13248

OWEN R. 1858. — Description of a small lophiodont mammal (*Pliolophus vulpiceps*, Owen), from the London Clay, near Harwich. *Proceedings of the Geological Society* 14: 54-71. https://doi.org/10.1144/Gsl.Jgs.1858.014.01-02.08

OWEN R. 1865. — On a new genus (*Miolophus*) of mammal from the London Clay. *Geological Magazine, London* (1) 2: 339-341. https://doi.org/10.1017/S0016756800470470

PLAZIAT J. C. 1977. — Les provinces biogéographiques continentales de l'Europe occidentale à la fin du Crétacé et au début du Tertiaire, *in* 5ème réunion annuelle des Sciences de la Terre. Société géologique de France: 380.

QUINET G. E. & VERLINDEN W. 1970. — Sur l'*Hyracotherium* d'Erquelinnes (Jeumont). *Bulletin de l'Institut royal de Sciences naturelles de Belgique* 46: 1-10. https://archive.org/details/bulletin-de-linstitut-royal-des-sciences-naturelles-de-belgique-46-034-001-010

RADINSKY L. B. 1966. — The adaptive radiation of the phenacodontid condylarths and the origin of the Perissodactyla. *Evolution* 20 (3): 408-417. https://doi.org/10.2307/2406639

REMY J. A. 2017. — Critical comments on the genus *Propachynolophus* Lemoine, 1891 (Mammalia, Perissodactyla, Equoidea). *Paleovertebrata* 41: 1-18. https://doi.org/10.18563/pv.41.1.e3

REMY J. A., KRASOVEC G. & MARANDAT B. 2016. — A new species of *Propalaeotherium* (Palaeotheriidae, Perissodactyla, Mammalia) from the Middle Eocene locality of Aumelas (Hérault, France). *Palaeovertebrata* 40: e1. https://doi.org/10.18563/pv.40.2.e1

ROSE K. D., HOLBROOK L. T., RANA R. S., KUMAR K., JONES K. E., AHRENS H. E., MISSIAEN P., SAHNI A. & SMITH T. 2014. — Early Eocene fossils suggest that the mammalian order Perissodactyla originated in India. *Nature Communications* 5: 1-9. https://doi.org/10.1038/ncomms6570

ROSE K. D., HOLBROOK L. T. & LUCKETT W. P. 2018. — Deciduous premolars of Eocene Equidae and their phylogenetic significance. *Historical Biology* 30 (1-2): 89-118. https://doi.org/10.1080/08912963.2017.1291637

RUSSELL D. E., GALOYER A., LOUIS P. & GINGERICH P. D. 1988. — Nouveaux vertébrés sparnaciens du conglomérat de Meudon à Meudon, France. *Compte-Rendus de l'Académie des Sciences de Paris*, *série II*, 307: 429-433. https://gallica.bnf.fr/ark:/12148/bpt6k6327064k/f443.item

SAVAGE D. E., RUSSELL D. E. & LOUIS P. 1965. — *European Eocene Equidae (Perissodactyla)*. University of California Press, Berkeley, 94 p. (University of California Publications in Geological Sciences; 56).

SIMPSON G. G. 1952. — Notes on British Hyracotheres. *Zoological Journal of the Linnean Society* 42: 195-206. https://doi.org/10.1111/j.1096-3642.1952.tb01858.x

SMITH R. & HOOKER J. J. 1996. — Sur la présence de dents de Mammifères (Creodonta, Perissodactyla) près de la limite Paléocène-Éocène à Hoegaarden, Belgique. *Palaeovertebrata* 25 (2-4): 115-124. http://pascal-francis.inist.fr/vibad/index.php?action=getRecordDetail&idt=2712878

SMITH R. & SMITH T. 2004. — Les Mammifères de l'Yprésien moyen du Bassin de Paris (Niveau-Repère Mp8-9) sont-ils présents à la limite Paléocène/Éocène de Dormaal (Niveau-Repère Mp7, Belgique) ? *Oryctos* 5: 75-82. https://www.naturalsciences.be/de/node/15683

SMITH T., DE WILDE B. & STEURBAUT E. 2004. — Primitive Equoid and Tapiroid mammals: Keys for interpreting the Ypresian-Lutetian transition in Belgium. *Bulletin de l'Institut royal des Sciences naturelles de Belgique, Sciences de la Terre* 74: 165-175.

SMITH T., ROSE K. D. & GINGERICH P. D. 2006. — Rapid Asia-Europe-North America geographic dispersal of earliest Eocene primate *Teilhardina* during the Paleocene-Eocene thermal maximum. *Proceedings of the National Academy of Sciences* 103 (30): 11223-11227. https://doi.org/10.1073/pnas.0511296103

SMITH T., QUESNEL F., DE PLÖEG G., DE FRANCESCHI D., MÉTAIS G., DE BAST E., SOLE F., FOLIE A., BOURA A., CLAUDE J., DUPUIS C., GAGNAISON C., IAKOVLEVA A., MARTIN J., MAUBERT F., PRIEUR J., ROCHE E., STORME J.-Y., THOMAS R., TONG H., YANS J. & BUFFETAUT E. 2014. — First Clarkforkian equivalent Land Mammal Age in the latest Paleocene basal Sparnacian facies of Europe: fauna, flora, paleoenvironment and (bio) stratigraphy. *PloS One* 9 (1): e86229. https://doi.org/10.1371/journal.pone.0093249

SOLÉ F., GODINOT M., LAURENT Y., GALOYER A. & SMITH, T. 2017. — The European Mesonychid Mammals: phylogeny, ecology, biogeography, and biochronology. *Journal of Mammalian Evolution* 1-41. https://doi.org/10.1007/s10914-016-9371-8

STEURBAUT E., MAGIONCALDA R., DUPUIS C., VAN SIMAEYS S., ROCHE E., ROCHE M. 2003. — Palynology, paleoenvironments, and organic carbon isotope evolution in lagoonal Paleocene-Eocene boundary settings in North Belgium, *in* WING S. L., GINGERICH P. D., SCHMITZ B. & THOMAS E. (eds), *Causes and consequences of globally warm climates in the early Paleogene*. Geological Society of America, Boulder: 291-317. https://doi.org/10.1130/0-8137-2369-8.291

TEILHARD DE CHARDIN P. 1921. — Les mammifères de l'Éocène inférieur français et leurs gisements. *Annales de Paléontologie, Paris* 10: 171-176. https://doi.org/10.5962/bhl.title.156400

TEILHARD DE CHARDIN P. 1927. — Les mammifères de l'Eocene inférieur de la Belgique. *Mémoires du Musée royal d'Histoire naturelle de Belgique* 36: 1-33.

TING S. 1993. — A preliminary report on an early Eocene mammalian fauna from Hengdong, Hunan Province, China. *Kaupia* 3: 201-207.

TUCHMAN N. C., WETZEL R. G., RIER S. T., WAHTERA K. A. & TEERI J. A. 2002. — Elevated atmospheric Co2 lowers leaf litter nutritional quality for stream ecosystem food webs. *Global Change Biology* 8 (2): 163-170. https://doi.org/10.1046/j.1365-2486.2002.00460.x

VAUTRIN Q., TABUCE R., LAURENT Y., VIDALENC D., & LIHOREAU F. 2019. — Intraspecific variation of *Eolophiodon laboriense*, a basal Lophiodontidae (Mammalia, Perissodactyla) from the early Eocene of Southern France. *Geobios* 53: 51-63. https://doi.org/10.1016/j.geobios.2019.02.005

WHITE E. I. 1931. — *The Vertebrate Faunas of the English Eocene*. Order of the Trustees, London, 123 p.

WOOD H. E. 1934. — Revision of the Hyrachyidae. *Bulletin of the American Museum of Natural History* 67 (5): 181-295. http://hdl.handle.net/2246/357

WOOD S. V. 1839. — Letter from S. V. Wood Esq., late curator to the Geological Society, announcing the discovery of Fossil Quadrumanous remains, near Woodbridge, Suffolk. *The Magazine of Natural History* 3: 444-445. https://www.biodiversitylibrary.org/page/2270417

WORTMAN J. L. 1896. — Species of Hyracotherium and allied perissodactyls from the Wahsatch and Wind River beds of North America. *Bulletin of the American Museum of Natural History* 8: 81-110. http://hdl.handle.net/2246/1576

Submitted on 22 January 2020;
accepted on 14 October 2022;
published on 8 June 2023.

APPENDIX 1. — Measurements (in mm) of the early Eocene perissodactyl fossils from the Paris Basin. Abbreviations: **L**, length; **W**, width. *, worn specimens with approximative measurements.

Pliolophus barnesi Hooker, 2010

Specimen	Anatomy	L	W
MNHN-PY-34-Cn	p3	6.4	3.6
MNHN-PY-45-L	p3	6	3.9
MNHN-PY-20-Ph	p4	6.1	4.2
MNHN-PY-43-L	m3	10.5	5.5
MNHN-PY-15715	P2	5.2	4.6
MNHN-PY-unnumbered	P4	6.2	7.6
MNHN-PY-46-L	M1	6	7.5
MNHN-PY-133-L	M1	6.2	7.8
MNHN-PY-146-LX	M1-2	7.2	8.8
MNHN-PY-39-L	M3	7.2	9
MNHN-PY-40-L	M3	8	9
MNHN-PY-41-L	M3	8	9.8

Hallensia louisi Hooker, 1994

Specimen	Anatomy	L	W
MNHN-MU6283	m2	7	6
MNHN-MU12303	m1	7	5.8
MNHN-MU12303	m2	8	6.5
MNHN-AV-841-Ph	m1	8	6
MNHN-AV-841-Ph	m2	9	6.8
MNHN-CB1588	DP4	6.1	6.9
MNHN-MU218-L	M1-2	8	10
MNHN-CB216	M1-2	7	9.5
MNHN-CB1574	M1-2	6.5	8.1
MNHN-CB1568	M3	7	7.5
MNHN-MU221-L	M3	8	9
MNHN-MU12371	M3	8	9.5
MNHN-CB1560	M3	7.5	9

Cymbalophus cuniculus (Owen, 1842)

Specimen	Anatomy	L	W
SLP-29-PR-1906	m3	9	5

Pliolophus quesnoyensis Bronnert, Gheerbrant, Godinot & Métais, 2018

Specimen	Anatomy	L	W
MNHN-ME-16322	m1-2	6	5
MNHN-SY-5-De	P3	6	6.8
MNHN-TRY23	M1-2	7.5	8.5
MNHN-TRY9	M1-2	6.8	8
MNHN-TRY11	M1-2	7	8.5
MNHN-TRY17-L	M1-2	7	8
MNHN-ME16325	M1-2	7.5	8.5
MNHN-SY-4-De	M2	7.5	9
MNHN, coll. Berton	M3	6.5	7.5
MNHN-TRY8	M3	7	8

Hallensia parisiensis Franzen, 1990

Specimen	Anatomy	L	W
MNHN-CB1529	M1	8.2	9
MNHN-STA623	m1-2	9.5	7.5
MNHN-STA625	m1-2	9.5	7
MNHN-CB1529	P3	8	8.5
MNHN-CB1529	P4	8	9.2
MNHN-CB1562	P2	7	7
MNHN-CB1557	dP3	8	7.8
MNHN-STA636	dP2	7.5	5.6
NMB.TS-631	P4	9	10.5
NMB.TS-631	M1	9.2	11.2
NMB.TS-367	dP2	7.9	6.8
NMB.TS-367	dP3	9	9

Hyracotherium leporinum Owen, 1841

Specimen	Anatomy	L	W
MNHN-MU12300	dp4	6.9	4.8
MNHN-MU5640	p3	6.1	3.8
MNHN-MU6574	p4	6.7	4.9
MNHN-MU12378	m3	9	6
MNHN-MU14684	DP3	6.3	5.8
MNHN-AV65512	P4	6	7.1
MNHN-AV65514	M1	6.3	7.2
MNHN-MU17167	M1-2	7.2	9
MNHN-MU192-L	M1-2	7.2	10
MNHN-MU220-L	M1-2	7	8.5
MNHN-MU222-L	M1-2	7	9
MNHN-AV1012-L	M1-2	7.5	9
MNHN-MU220-L	M1-2	7	8.5
MNHN-MU222-L	M1-2	7	9
MNHN-AV1012-L	M1-2	7.5	9

Appendix 1. — Continuation.

Orolophus maldani (Lemoine, 1878)

Specimen	Anatomy	L	W
MNHN-SLP-29-PR-1467	dp2	5	2.2
MNHN-SLP-29-PR-1467	dp3	6.1	3.5
MNHN-GR7808	dp3	6.3	3.2
MNHN-GR7807	dp3	6.5	4
MNHN-CB572	dp3	6.2	3.2
MNHN-CB312	dp3	5.8	3
MNHN-CB197	dp3	7.6	3.8
MNHN-CB196	dp3	6.9	3.6
MNHN-CB199	dp3	6.3	3.5
MNHN-SEZ349	dp3	7.8	4.1
MNHN-SLP-29-PR-1355	dp3	7	4
MNHN-GR180	dp3	10.9	6.2
MNHN-SLP-29-PR-113	dp3	7	3.9
MNHN-SLP-29-PR-1818	dp3	7	3.2
MNHN-SLP-29-PR-966	dp3	6.8	4
MNHN-SLP-29-PR-263	dp3	6.7	3.3
MNHN-SLP-29-PR-1143	dp3	7	4
MNHN-SLP-29-PR-1983	dp3	6.2	3.2
MNHN-SLP-29-PR-868	dp3	6.9	3.8
MNHN-SLP-29-PR-303	dp3	7.5	4.1
MNHN-SLP-29-PR-103	dp3	7	3.8
MNHN-SLP-29-PR-878	dp3	6.9	3.6
MNHN-SLP-29-PR-58	dp3	7	3.9
MNHN-SLP-29-PR-1057	dp3	6.5	3.5
MNHN-SLP-29-PR-1012	dp3	7	4
MNHN-SLP-29-PR-1919	dp3	7	3.5
MNHN-SLP-29-PR-1562	dp3	6.8	4
MNHN-PRE244	dp3	6.9	3.8
MNHN-SLP-29-PR-3022	dp3	7	4
MNHN-PRE997	dp3	6.8	3.8
MNHN-PRE247	dp4	6.1	4
MNHN-PRE242	dp4	7	4.6
MNHN-CB1576	dp4	6.7	4.8
MNHN-CB1587	dp4	8	5
MNHN-SLP-29-PR-1552	dp4	6.8	4.8
MNHN-SLP-29-PR-624	dp4	6.8	4.8
MNHN-SLP-29-PR-669	dp4	6.8	5.2
MNHN-SLP-29-PR-392	dp4	6.4	4.1
MNHN-SLP-29-PR-1382	dp4	6.5	4.2
MNHN-SLP-29-PR-1048	dp4	6.5	4.5
MNHN-SLP-29-PR-856	dp4	6.4	4.1
MNHN-SLP-29-PR-88	dp4	6.7	4.5
MNHN-SLP-29-PR-2477	dp4	7.1	5
MNHN-SLP-29-PR-1024	dp4	6.9	4.2
MNHN-SLP-29-PR-488	dp4	6.2	4.8
MNHN-SLP-29-PR-1026	dp4	6.9	4.8
MNHN-SLP-29-PR-3026	dp4	6	3.9
MNHN-SLP-29-PR-1467	dp4	6.1	4.1
MNHN-SLP-29-PR-165	p2	5.9	3.2
MNHN-SLP-29-PR-772	p2	6.4	4
MNHN-SLP-29-PR-1499	p2	5.6	2.9
MNHN-SLP-29-PR-1180	p2	5.3	3
MNHN-SLP-29-PR-180	p2	6.2	3.6
MNHN-CB219	p2	5.9	3
MNHN-CB1594	p2	5.5	3.3
MNHN-CB4702	p2	6	3.2
MNHN-CB669	p2	6.5	3.9
MNHN-SEZ312	p3	6.2	3.9
MNHN-CB1600	p3	7	4.2
MNHN-CB0193	p3	6.3	3.8
MNHN-CB1580	p3	6.8	4.1
MNHN-CB1592	p3	5.7	3.1
MNHN-CB4700	p3	6.9	4.8
MNHN-SLP-29-PR-1362	p3	6	4
MNHN-SLP-29-PR-1459	p3	6.2	4.1
MNHN-SLP-29-PR-1472	p3	6.2	3.9
MNHN-SLP-29-PR-759	p3	6.5	4.1
MNHN-SLP-29-PR-1474	p3	5.9	3.9

Specimen	Anatomy	L	W
MNHN-SLP-29-PR-17	p3	6	3.3
MNHN-SLP-29-PR-1214	p3	6	3.6
MNHN-CB1599	p4	7	5.1
MNHN-MA2-L	p4	6.1	4.9
MNHN-GR10773	p4	6.3	5
MNHN-SEZ351	p4	6.3	4.9
MNHN-SEZ353	p4	6.1	4.6
MNHN-SEZ346	p4	6.9	5
MNHN-SEZ313	p4	7	5
MNHN-SLP-29-PR-1362	p4	6.1	5
MNHN-SLP-29-PR-596	p4	7	5.1
MNHN-SLP-29-PR-1325	p4	6.3	4.5
MNHN-SLP-29-PR-763	p4	6.5	4.9
MNHN-SLP-29-PR-719	p4	6.3	4.6
MNHN-SLP-29-PR-745	p4	6.5	4.5
MNHN-SLP-29-PR-770	p4	7	5
MNHN-SLP-29-PR-1949	p4	6.3	4.9
MNHN-SLP-29-PE 480	m1	7	5.2
MNHN-SLP-29-PE 584	m1	7.5	5
MNHN-SLP-29-PE 1467	m1	6.5	5
MNHN-SEZ314	m1	8	6
MNHN-MA2-L	m1	7.5	5
MNHN-AL5204	m1	7	5
MNHN-AL5201	m1	7	5
MNHN-MA14792	m1	8	6
MNHN-AL5199	m2	10	5.2
MNHN-MA14792	m2	8	6
MNHN-GR10773	m2	7.5	6
MNHN-AL5204	m2	7	5
AT2-0010	m2	8.5	6.5
MNHN-SEZ315	m2	9	7
MNHN-SLP-29-PE 480	m2	7	5.5
MNHN-SLP-29-PE 1467	m2	7	5.8
MNHN-SLP-29-PE 1553	m2	8	5.5
MNHN-GR49-L	m1-2	8.5	7
MNHN-CB4688	m1-2	7.2	5.2
MNHN-CB4703	m1-2	8.8	6.2
MNHN-CB4686	m1-2	8.5	6.5
MNHN-M.CB0198	m1-2	8.5	6.2
MNHN-CB1584	m1-2	8	5.5
MNHN-CB1590	m1-2	9	6.1
MNHN-M.CB0038	m1-2	7.8	5.5
MNHN-CB4701	m1-2	8	5.5
MNHN-GR44-L	m1-2	8	6
MNHN-GR7383	m1-2	8	6.5
MNHN-MA14763	m1-2	8.5	6.2
MNHN-AL5199-2	m1-2	7	5.5
MNHN-CUI14760	m1-2	7.8	5.2
MNHN-B6-L	m1-2	7	6
MNHN-GR10229	m1-2	8	5.5
MNHN-MA14762	m1-2	8	5.5
MNHN-CUI14758	m1-2	7	5
MNHN-GR178	m1-2	6.2	4.5
MNHN-GR10235	m1-2	8	6
MNHN-CB1598	m1-2	8	5.5
MNHN-CB1579	m1-2	9	6.1
MNHN-CB1593	m1-2	7.2	5.2
MNHN-CB4757	m1-2	9	6.8
MNHN-CB4687	m1-2	7.8	5.5
MNHN-CB918	m1-2	9	6.5
MNHN-CB223	m1-2	7.5	5
MNHN-M.CB295	m1-2	8	6
MNHN-SEZ7336	m1-2	8	5.5
MNHN-SEZ352	m1-2	8.1	6.2
MNHN-SEZ326	m1-2	9.2	6.8
MNHN-STA624	m1-2	8.2	5.8
MNHN-STA657	m1-2	8	5.5
MNHN-STA628	m1-2	7.2	5

Appendix 1. — Continuation.

Orolophus maldani (Lemoine, 1878) – continuation.

Specimen	Anatomy	L	W
MNHN-STA629	m1-2	8	6
MNHN-STA630	m1-2	7.5	5.5
MNHN-SLP-29-PE 1320	m1-2	7	5
MNHN-SLP-29-PE 1375	m1-2	7	5
MNHN-SLP-29-PE 1848	m1-2	7	5.1
MNHN-SLP-29-PE 669	m1-2	6.9	5.2
MNHN-SLP-29-PR 2477	m1-2	7.2	5
MNHN-SLP-29-PE 730	m1-2	7.2	5.2
MNHN-SLP-29-PE 757	m1-2	7.2	5.2
MNHN-SLP-29-PR 3106	m1-2	7.8	5
MNHN-PRE245	m1-2	7.2	5.8
MNHN-SLP-29-PE 827	m1-2	7.6	5.5
MNHN-PRE243	m1-2	8	5.5
MNHN-SLP-29-PE 1340	m1-2	8	5.5
MNHN-SLP-29-PE 1406	m1-2	8	5.5
MNHN-SLP-29-PE 951	m1-2	8	5.5
MNHN-SLP-29-PE 1177	m1-2	8	5.5
MNHN-SLP-29-PE 694	m1-2	8	5.6
MNHN-SLP-29-PE 768	m1-2	8	5.8
MNHN-SLP-29-PE 1069	m1-2	8	6
MNHN-SLP-29-PE 22	m1-2	8.1	6
MNHN-GR10773	m3	10.5	5.5
MNHN-AT2-0010	m3	12	7
MNHN-AL6546	m3	11.8	6
MNHN-*Lyon 4041*	m3	11	6
MNHN-MA14792	m3	10.5	6
MNHN-GR22-L	m3	11	6
MNHN-GR63 L	m3	9.5	5
MNHN-CB4704	m3	11	6
MNHN-CB1571	m3	10	5.5
MNHN-SEZ316	m3	11.5	6.2
MNHN-SEZ329	m3	11.5	6.5
MNHN-STA626	m3	11	6
MNHN-SLP-29-PR 3211	m3	10.5	5.5
MNHN-SLP-29-PE 48	m3	10.8	6
MNHN-SLP-29-PE 693	m3	11	6
MNHN-SLP-29-PE 1317	m3	10.2	5.5
MNHN-SLP-29-PE 1410	m3	9.9	5.8
MNHN-SLP-29-PE 1306	m3	12.2	6
MNHN-SLP-29-PE 1906	m3	9	5
MNHN-SLP-29-PR 1990	m3	10	6
MNHN-SLP-29-PR 1954	m3	12	6
MNHN-PRE861	m3	11	6
MNHN-SLP-29-PE 1553	m3	10	5.2
MNHN-SLP-29-PE 480	m3	10	5.5
MNHN-SLP-29-PR-950	DP2	6	3.8
MNHN-SLP-29-PR-631	DP2	5.9	3.9
MNHN-SLP-29-PR-1436	DP2	6.1	4
MNHN-SLP-29-PR-1475	DP2	6.3	4.5
MNHN-SLP-29-PR-717	DP2	5.9	4
MNHN-SLP-29-PR-44	DP2	6	3.8
MNHN-SLP-29-PR-1070	DP2	6	4.1
MNHN-PRE448	DP3	6.6	5.9
MNHN-GR7825	DP3	7	6.8
MNHN-CB4915	DP3	6.8	6.5
MNHN-CB4705	DP3	7	6.7
MNHN-CB0001C	DP3	7.2	7.1
MNHN-CB1595	DP3	6.6	6.2
MNHN-CB1530	DP3	7.3	7
MNHN-GR242	DP3	7.2	6.7
MNHN-GR187	DP3	8	7.6
MNHN-GR175	DP3	6.9	6.5
MNHN-SLP-29-PR-2049	DP3	6.5	6
MNHN-SLP-29-PR-1243	DP3	6.9	6.9
MNHN-SLP-29-PR-1973	DP3	6.9	6.5
MNHN-SLP-29-PR-45	DP3	6.5	6
MNHN-SLP-29-PR-67	DP3	6	5.8
MNHN-SLP-29-PR-1728	DP3	6.8	6
MNHN-SLP-29-PR-1004	DP3	6.5	6.1
MNHN-SLP-29-PR-1560	DP3	6.3	6.1
MNHN-SLP-29-PR-742	DP3	7	6.5
MNHN-SLP-29-PR-100	DP3	6.2	6
MNHN-SLP-29-PR-803	DP3	6.5	6.1
MNHN-SLP-29-PR-1863	DP3	6.2	6
MNHN-GR242	DP3	7.2	6.7
MNHN-GR187	DP3	8	7.6
MNHN-GR175	DP3	6.9	6.5
MNHN-PRE996	DP3	6	6
MNHN-CB1530	DP4	7.2	8.1
MNHN-GR7889	DP4	6.4	4.2
MNHN-GR7809	DP4	6.1	4.1
MNHN-SLP-29-PR-1928	DP4	6.9	7.5
MNHN-SLP-29-PR-1201	DP4	7	7
MNHN-SLP-29-PR-1703	DP4	7.5	8.5
MNHN-SLP-29-PR-150	DP4	6.5	7.3
MNHN-SLP-29-PR-1998	DP4	6.2	6.6
MNHN-SLP-29-PR-1358	DP4	6.2	6.9
MNHN-SLP-29-PR-1275	DP4	6.2	6.9
MNHN-SLP-29-PR-807	DP4	6.5	7.9
MNHN-SLP-29-PR-1473	DP4	6.5	4.5
MNHN-SLP-29-PR-2044	DP4	6.8	3.8
MNHN-SLP-29-PR-185	DP4	6	4.1
MNHN-SLP-29-PR-879	DP4	6.1	4.2
MNHN-SLP-29-PR-3287	DP4	6	7
MNHN-SLP-29-PR-3289	DP4	6.3	7.2
MNHN-SLP-29-PR-3077	DP4	6.1	7
MNHN-PRE1064	DP4	6.5	7.5
MNHN-SLP-29-PR-1559	P1	5.5	2.4
MNHN-MA14948	P1	6.5	4.1
MNHN-SLP-29-PR-1296	P1	4.1	2.3
MNHN-SLP-29-PR-1296	P2	5.2	4.9
MNHN-SLP-29-PR-1421	P2	5	4.8
MNHN-SLP-29-PR-10	P2	5.2	4.5
MNHN-SLP-29-PR-2388	P2	5.5	5
MNHN-MA14948	P2	7.8	8.2
MNHN-SEZ359	P2	5.8	3.9
MNHN-CB1582	P2	5.5	5
MNHN-CB1591	P2	6.1	4.6
MNHN-CB1586	P2	5.7	4.1
MNHN-GR7803	P2	5	4.2
MNHN-GR7803	P2	5	4.2
MNHN-MA14948	P3	8.3	10.2
MNHN-SEZ347	P3	6.5	7.1
MNHN-SEZ268	P3	6.1	7.1
MNHN-CB1569	P3	6.1	6.5
MNHN-CB16165	P3	6.5	7.1
MNHN-SLP-29-PR-2388	P3	5.3	6.5
MNHN-SLP-29-PR-1953	P3	6.5	6.2
MNHN-SLP-29-PR-1914	P3	5.8	6.5
MNHN-SLP-29-PR-252	P3	5.5	6.2
MNHN-SLP-29-PR-12	P3	6.2	6.8
MNHN-SLP-29-PR-254	P3	5.9	6.6
MNHN-SLP-29-PR-1896	P3	5.9	6.2
MNHN-SLP-29-PR-731	P3	5.5	6.2
MNHN-SLP-29-PR-1971	P3	6.1	6.3
MNHN-SLP-29-PR-590	P3	6.1	6.2
MNHN-SLP-29-PR-678	P4	5.9	8
MNHN-SLP-29-PR-741	P4	6	7.5
MNHN-SLP-29-PR-622	P4	5.9	7.4
MNHN-SLP-29-PR-2388	P4	5.8	7.8
MNHN-SLP-29-PR-480	p4	6.4	4.5
MNHN-CB16165	P4	6.8	8.5
MNHN-GR7402	P4	6	7.8
MNHN-CB215	P4	6.8	9
MNHN-CB5-CA	P4	6.8	8.8
MNHN-SEZ356	P4	6.6	8.9

Appendix 1. — Continuation.

Orolophus maldani (Lemoine, 1878) – continuation.

Specimen	Anatomy	L	W
MNHN-SEZ357	P4	6.9	8.5
MNHN-MA14948	P4	9	12
MNHN-PRE246	P4	6.4	8
MNHN-SZ7306	M1	8	10
MNHN-CB16165	M1	7	9
MNHN-SEZ325	M1	8	9.8
MNHN-SEZ325	M2	9	11
MNHN-SLP-29-PE 1864	M2	8	10
MNHN-CB16165	M2	9	10.2
MNHN-SZ7306	M2	9	11
MNHN-SLP-29-PE 706	M2	7	8
MNHN-SLP-29-PE 681	M2	8	9.8
MNHN-SLP-29-PE 896	M1-2	7.2	8.2
MNHN-GR227	M1-2	7	8.8
MNHN-GR273-L	M1-2	7	9
MNHN-C8-L	M1-2	7.2	9.1
MNHN-AL6561	M1-2	7.5	9
MNHN-2003-2	M1-2	7.5	9
MNHN-GR7568	M1-2	8	9
MNHN-AL6563	M1-2	8	9.5
MNHN-GR25-L	M1-2	8	9.5
MNHN-GR10779	M1-2	8	10
MNHN-GR9-L	M1-2	8	10
MNHN-MAN 044	M1-2	8	10
MNHN-MA14730	M1-2	8	10
MNHN-GR10834	M1-2	8.5	10
MNHN-GR41-L	M1-2	8.5	10
MNHN-GR19-L	M1-2	8	10.8
MNHN-C11-l	M1-2	8	10.8
MNHN-AL6554	M1-2	8	11
MNHN-AL6564	M1-2	8.8	10
MNHN-AL6550	M1-2	9	10
MNHN-AL6552	M1-2	9	10
MNHN-MA53-L	M1-2	9	10.2
MNHN-GR7575	M1-2	9	11
MNHN-GR277-L	M1-2	9	11
MNHN-C10-L	M1-2	9	11
MNHN-AL6566	M1-2	9	11.5
MNHN-CB1531	M1-2	9.5	11.5
MNHN-CB1559	M1-2	8.5	10
MNHN-M.CB0225	M1-2	9	11.5
MNHN-M.CB297	M1-2	8.2	10.5
MNHN-CB1532	M1-2	9	10.5
MNHN-CB1565	M1-2	9	11
MNHN-CB4689	M1-2	7	9
MNHN-M.CB0114	M1-2	8	9.5
MNHN-CB1561	M1-2	7.2	8
MNHN-CB1566	M1-2	7.5	8
MNHN-SEZ7334	M1-2	7.2	10
MNHN-SEZ7337	M1-2	8	11
MNHN-SEZ331	M1-2	8.8	10.8
MNHN-SEZ332	M1-2	9	11
MNHN-SEZ333	M1-2	9	11.2
MNHN-SEZ339	M1-2	9	10

Specimen	Anatomy	L	W
MNHN-SEZ340	M1-2	9.2	10.5
MNHN-SEZ336	M1-2	7	9
MNHN-STA652	M1-2	8.5	10
MNHN-STA653	M1-2	7.5	9.8
MNHN-SLP-29-PR 3001	M1-2	7	8.5
MNHN-PRE1069	M1-2	7.5	8
MNHN-SLP-29-PE 508	M1-2	7.2	8.5
MNHN-SLP-29-PR 3288	M1-2	7	9
MNHN-SLP-29-PE 1367	M1-2	7.2	8.8
MNHN-SLP-29-PE 148	M1-2	7.1	9.1
MNHN-SLP-29-PE 1479	M1-2	7.2	9
MNHN-SLP-29-PE 151	M1-2	7.22	9.1
MNHN-PRE1080	M1-2	7.5	8.8
MNHN-SLP-29-PE 1695	M1-2	7.5	8.8
MNHN-SLP-29-PR 3290	M1-2	7.2	9.2
MNHN-SLP-29-PE 701X	M1-2	7.5	9
MNHN-SLP-29-PE 1699	M1-2	7.5	9
MNHN-SLP-29-PR 2009	M1-2	7.5	9
MNHN-SLP-29-PE 394	M1-2	7.8	8.8
MNHN-SLP-29-PE 982	M1-2	7.5	9.2
MNHN-SLP-29-PE 149	M1-2	7.8	9
MNHN-SLP-29-PE 448	M1-2	7.8	9.1
MNHN-SLP-29-PE 388	M1-2	7.8	9.1
MNHN-SLP-29-PE 501	M1-2	7.5	9.5
MNHN-SLP-29-PR 3283	M1-2	8	9
MNHN-SLP-29-PE 1707	M1-2	8	9
MNHN-SLP-29-PE 1721	M1-2	8	9
MNHN-SLP-29-PE 706-3	M1-2	8	9
MNHN-SLP-29-PE 152	M1-2	8	9.3
MNHN-SLP-29-PE 707	M1-2	8	9.5
MNHN-SLP-29-PR 1925	M1-2	8	9.5
MNHN-SLP-29-PR 3003	M1-2	7.8	9.8
MNHN-SLP-29-PE 987	M1-2	7.8	9.8
MNHN-SLP-29-PR 1968	M1-2	7.8	9.8
MNHN-SLP-29-PE 688	M1-2	8.2	9.5
MNHN-PRE1066	M1-2	8	10
MNHN-SLP-29-PE 1527	M1-2	8	10
MNHN-SLP-29-PE 997	M1-2	8	10
MNHN-SLP-29-PE 834	M1-2	8	10
MNHN-SLP-29-PE 761	M1-2	8	10
MNHN-SLP-29-PE 224	M1-2	8.1	10
MNHN-SLP-29-PR 1909	M1-2	8.1	10
MNHN-SLP-29-PE 1009	M1-2	8.2	10
MNHN-SLP-29-PE 223	M1-2	8	10.5
MNHN-SLP-29-PE 479	M1-2	8.5	10
MNHN-SLP-29-PR 1903	M1-2	8	10.8
MNHN-SLP-29-PR 1969	M1-2	9	10.2
MNHN-SLP-29-PE 147	M1-2	9.1	12
MNHN-SLP-29-PR 1891	M1-2	8	10
MNHN-SLP-29-PE 681	M3	8	9.5
MNHN-SZ7306	M3	10	12
MNHN-SLP-29-PE 1864	M3	8	10
MNHN-CB16165	M3	8.8	10.2

APPENDIX 1. — Continuation.

Propalaeotherium gaudryi (Lemoine, 1878)

Specimen	Anatomy	L	W
MNHN-CHO14801	dp2	8	4
MNHN-CHO14801	dp3	10	5.5
MNHN-MT5-L	dp3	10.2	6
MNHN-GR10784	dp3	9.7	4.7
MNHN-CHO14801	dp4	10	6.8
MNHN-MT5-L	dp4	10.2	7
MNHN-AL5212	p1	5.8	3.4
MNHN-GR7546	p1	6.1	4.1
MNHN-MA9-L	p1	7	3.5
MNHN-MA9-L	p2	8.5	5.9
MNHN-MA15501	p2	9	5.3
MNHN-AL5212	p2	9	5.5
MNHN-AL5212	p3	9.8	6.6
MNHN-GR4-L	p3	8.2	6
MNHN-MT2-L	p3	9	5.7
MNHN-MA14728	p3	8.4	6.2
MNHN-MA14977	p3	9.5	7
MNHN-MA14739	p3	9.2	5.5
MNHN-MA9-L	p3	10	7.6
MNHN-MA14907	p3	9.8	6.5
MNHN-AL5211	p3	8.8	5.8
MNHN-MA14907	p4	10	7.4
MNHN-MA14886	p4	9.2	6.4
MNHN-CHO14911	p4	10	7.5
MNHN-MA15502	p4	11.1	7.8
MNHN-CUI15510	p4	9	7
MNHN-GR7572	p4	10.3	7.2
MNHN-MA9-L	p4	10.2	8.8
MNHN-MA14902	p4	9	6.5
MNHN-AL5212	p4	11.2	7.5
MNHN-AL5211	p4	8.5	6.4
MNHN-MT2-L	p4	9.3	6.5
MNHN-MA10-L	p4	9.5	7.3
MNHN-MA25-L	p4	9.1	5.1
MNHN-CHO14911	m1	12	8.5
MNHN-MA10-L	m1	12	8.5
MNHN-MA14883	m1	13	9.2
MNHN-CHO14884	m1	12	8
MNHN-M55-L	m1	11	8.8
MNHN-CHO14953	m1	10.5	9
MNHN-MA14886	m1	10.8	8
MNHN-MA3-L	m1	11	7.5
MNHN-AL5210	m1	9.5	7
MNHN-MA14902	m1	10	7.8
MNHN-AL5211	m1	10	8
MNHN-MT2-L	m1	10	8
MNHN-MA14907	m1	11	9
MNHN-MA14886	m2	11.2	8.5
MNHN-AL5210	m2	10	7
MNHN-GR10788	m2	11	9
MNHN-CHO14953	m2	13	9
MNHN-MA14902	m2	12	8.5
MNHN-MA14791	m2	12	9
MNHN-MT2-L	m2	12	9
MNHN-AL5211	m2	12	9
MNHN-CHO14789	m2	12	9
MNHN-AL5217	m1-2	9	6.8
MNHN-MTH54-L	m1-2	9	7
MNHN-AL5217-A	m1-2	12	8
MNHN-AL5213	m1-2	10	7
MNHN-2003-2-20-	m1-2	10	7
MNHN-AL5217-J	m1-2	10	7
MTB 004	m1-2	10	7
MNHN-MA14999	m1-2	10.2	7
MNHN-AL5217-H	m1-2	10.5	7
MNHN-AL5217-I	m1-2	10.5	7
MNHN-GR272-L	m1-2	11	7
MNHN-GR30-L	m1-2	11	7
MNHN-AL5217-B	m1-2	11	7.5
MNHN-AL5217-F	m1-2	11	7.5
MNHN-MA14796	m1-2	11	7.5
MNHN-CHO14801-1	m1-2	10.5	8
MNHN-MA14803	m1-2	11	7.8
MNHN-GR57-L	m1-2	10.8	8
MNHN-AL5217-D	m1-2	11	8
MNHN-MA14986	m1-2	11	8.2
MNHN-AL5217-G	m1-2	11.5	8
MNHN-AT2-0011	m1-2	11.8	8
MNHN-CUI15511	m1-2	11.5	8.5
MNHN-MA18-L	m1-2	12	9
MNHN-GR27-L	m1-2	12.8	8.8
MNHN-MA17-L	m1-2	12	9.5
MNHN-AL5217-E	m1-2	13	9
MNHN-AL5217-C	m1-2	12.5	8.5
MNHN-CUI15505	m1-2	12	9
MNHN-AT2-009	m3	13.5	6.5
MNHN-AL5217	m3	17	8.2
MNHN-MTB027	m3	19	9.2
MNHN-CHO14789	m3	17.5	9
MNHN-MA14978	m3	18	9.2
MNHN-AL5213	m3	15	7.5
MNHN-AL5210	m3	16	8
MNHN-AL5211	m3	17.5	10
MNHN-GR10788	m3	17	9
MNHN-GR10776	m3	15	8
MNHN-MA14793	m3	21	10
MNHN-MA14790	m3	16.5	8.5
MNHN-MA14791	m3	16	8.5
MNHN-MA14902	m3	16.2	8
MNHN-CHO14911	m3	18.5	10
MNHN-MA14886	m3	17	9
MNHN-MA14907	m3	19	10
MNHN-MA10-L	m3	19.5	9
MNHN-MT2-L	m3	16.5	9
MNHN-MA70-L	m3	18	9
MNHN-MT27-L	m3	16.2	8.2
MNHN-GR56-L	m3	17.2	8.8
MNHN-GR47-L	m3	17.2	9
MNHN-GR270-L	m3	18	9.8
MNHN-GR17-L	m3	17.8	9.1
MNHN-GR52-L	m3	17	8.1
MNHN-B4-L	m3	14.8	7
MNHN-GR7888	DP3	9.3	9.2
MNHN-GR7409	P2	7.5	6
MNHN-MA14842	P2	7.4	6.2
MNHN-AL6540	P2	8.5	8
MNHN-AL6540	P3	8	10
MNHN-GR28-L	P3	8.2	9.9
MNHN-GR13	P3	8.3	10.1
MNHN-GR268	P4	9.2	12
MNHN-AL6540	P4	9	12
MNHN-GR7380	P3-4	8.2	9.7
MNHN-GR10850	P3-4	8.7	11.8
MNHN-GR7573	P3-4	8	10
MNHN-GR7576	P3-4	9.2	11.2
MNHN-MA14948	M1	10	13
MNHN-MTH48-L	M1	11.8	14
MNHN-MA14885	M1	12	14.5
MNHN-MTH48-L	M2	12.8	16
MNHN-MA14885	M2	12.8	17
MNHN-MA14795	M2	12.2	15
MNHN-MA14948	M2	12.2	15.5
MNHN-MA14907	M2	12.2	10
MNHN-CHO14911	M2	13	9.5
MNHN-MA14802	M2	12	15
MNHN-CHO14884	M2	13	10

Appendix 1. — Continuation.

Propalaeotherium gaudryi (Lemoine, 1878) – continuation.

Specimen	Anatomy	L	W
MNHN-MA2-10-L	M2	13	10
MNHN-MA14788	M2	11.2	15
MNHN-MA14883	M2	14	10.8
MNHN-MTH44-L	M1-2	13.5	9.2
MNHN-AL6565	M1-2	9	11
MNHN-AT2-0012	M1-2	9	11
MNHN-GR10787	M1-2	10	11
MNHN-AL6549	M1-2	10	11
MNHN-AL5215	M1-2	10	12
MNHN-GR271-L	M1-2	10.5	12
MNHN-GR10778	M1-2	15	9.5
MNHN-GR193-L	M1-2	10	13
MNHN- 2003-2-78	M1-2	11	12
MNHN-GR46-L	M1-2	10.5	13
MNHN-GR10847	M1-2	11	12.8
MNHN-AL5215	M1-2	11	13
MNHN-MA14989	M1-2	11	13.5
MNHN-GR61-L	M1-2	11	13.5
MNHN-MT14-L	M1-2	11	13.5
MNHN-GR60-L	M1-2	11	13.8
MNHN-GR10839	M1-2	11	14
MNHN-AL6533	M1-2	15	17.5
MNHN-AL5215-B	M1-2	14	17.5
MNHN-CHO15569	M1-2	12.8	15
MNHN-AL6536	M1-2	13	15
MNHN-MA14985	M1-2	13.5	16
MNHN-GR61-L	M1-2	12	15
MNHN-GR59-L	M1-2	12	15
MNHN-CHO15519	M1-2	11	14
MNHN-GR7408	M1-2	11.2	14
MNHN-GR42-L	M1-2	11.2	14
MNHN-C5-L	M1-2	11.1	14.2
MNHN-GR-2-62-L	M1-2	11.5	14
MNHN-MTH56-L	M1-2	11.5	14
MNHN-MA54-L	M1-2	11.8	14
MNHN-GR10786	M1-2	11.2	14.8
MNHN-AL6535	M1-2	12	14
MNHN-CUI15513	M1-2	12	14
MNHN-AL6534	M1-2	12	14.2
MNHN-MA14996	M1-2	12	14.5
MNHN-AL5215	M1-2	12	15
MNHN-AL5215	M1-2	12	15
MNHN-AL5215	M1-2	12	15
MNHN-MA14948	M3	14	15.5
MNHN-MA14788	M3	13	15
MNHN-MA14802	M3	13.5	16.5
MNHN-GR62-L	M3	12	15
MNHN-MTH48-L	M3	14	17.5
MNHN-MA14795	M3	15	16.5
MNHN-MA14885	M3	15.2	17

Appendix 1. — Continuation.

Orolophus maldani (Lemoine, 1878)

Specimen	Humerus MNHN.F. PMT114	Humerus MNHN.F. PMT115	Humerus MNHN.F. MTB18001	Tibia MNHN.F. CUI18000	Metatarsal II MNHN.F. AL18001	Metatarsal II MNHN.F. PMT119	Metatarsal III MNHN.F. GR18008
Max length	–	–	–	–	42.7	37.8	51.5
Proximal width (A-P)	–	–	–	–	4.8	5.7	8.5
Proximal width (L-M)	–	–	–	–	6.2	4.7	7.6
Distal width (A-P)	11.6	12.1	10.1	11.5	5.5	5.0	6.0
Distal width (L-M)	16.1	15.6	13.7	13.8	6.3	4.7	9.1
Midshaft width (A-P)	–	–	–	–	3.1	3.8	3.9
Midshaft width (L-M)	–	–	–	–	4.9	3.1	6.8

	Navicular		
Specimen	MNHN.F.PMT145	MNHN.F.PMT146	MNHN.F.PMT147
Height	5.1	5.5	6.6
Width (A-P)	6.4	7.1	7.4
Width (L-M)	8.2	9.1	9.6

	Astragalus					
Specimen	MNHN.F. GR18005	MNHN.F. PMT128	MNHN.F. PMT129	MNHN.F. PMT135	MNHN.F. PMT131	MNHN.F. PMT136
Max length	15.6	15.3	14.3	15.4	16.9	12.9*
Max width	13.3	12.4	12.3	12.6	14.6	13.7
Trochlea length	11.9	11.3	10.9	12.2	13.0	9.1*
Trochlea width	11.2	10.7	10.2	10.5	12.2	9.7
Distal width (A-P)	7.4	7.4	6.4	6.7	8.0	6.4
Distal width (L-M)	10.4	9.9	8.7	9.6	10.9	9.1

	Calcaneus			
Specimen	MNHN.F.GR18007	MNHN.F.PMT123	MNHN.F.PMT124	MNHN.F.PMT126
Max length	31.1	28.8	27.1	26.7
Max width	–	10.6	9.6	9.8
Proximal width (A-P)	8.3	7.5	6.8	7.2
Proximal width (L-M)	7.2	6.7	6.2	6.2
Distal width (A-P)	–	10.8	9.9	10.0
Distal width (L-M)	–	10.8	9.9	9.5

	Distal Phalanx							
Specimen	MNHN.F. PMT137	MNHN.F. PMT138	MNHN.F. PMT139	MNHN.F. PMT140	MNHN.F. PMT141	MNHN.F. PMT142	MNHN.F. PMT143	MNHN.F. PMT144
Max length	8.7	8.4	7.7	6.9	9.7	7.3	9.4	8.7
Proximal width (A-P)	3.1	3.2	2.7	2.7	3.7	2.6	3.0	2.8
Proximal width (L-M)	4.6	5.4	4.4	5.9	7.9	4.7	5.2	6.4

Appendix 1. — Continuation.

Propalaeotherium gaudryi (Lemoine, 1878)

	Humerus	Metacarpal II		Metacarpe V	Proximal phalanx
Specimen	MNHN.F.MT18001	MNHN.F.GR18004	MNHN.F.MA18001	MNHN.F.MA18002	MNHN.F.AL18000
Max length	–	62.2	51.8	41.9	13.0
Proximal width (A-P)	–	9.9*	9.4*	8.7	6.9
Proximal width (L-M)	–	7.8	8.3	6.7	9.5
Distal width (A-P)	18.8	10.3	10.6	7.6	4.5
Distal width (L-M)	25.8	12.6	11.0	8.6	7.9
Midshaft width (A-P)	–	6.0	6.0	4.6	3.9
Midshaft width (L-M)	–	8.7	8.6	6.8	7.8

	Metatarsal II	Metatarsal III				Metatarsal IV	
Specimen	MNHN.F. MT18000	MNHN.F. GR18002	MNHN.F. GR18003	MNHN.F. MTB18000	MNHN.F. MA18000	MNHN.F. GR18000	MNHN.F. GR18001
Max length	55.5	72.3	62.8	61.0	58.2	58.1	58.7
Proximal width (A-P)	11.6	12.3	11.0	11.6	–	8.8	–
Proximal width (L-M)	8.4	11.4	10.2	10.0	9.5	7.1	–
Distal width (A-P)	10.1	9.2	8.1	7.9	6.9	8.8	8.9
Distal width (L-M)	10.8	15.3	12.5	11.7	11.4	9.5	8.7
Midshaft width (A-P)	7.8	6.2	5.3	5.0	4.9	5.3	6.7
Midshaft width (L-M)	6.8	11.9	8.9	8.6	9.5	6.5	6.3

	Astragalus	
Specimen	MNHN.F.MA6105	MNHN.F.GR10911
Max length	27.7	25.0
Max width	24.5	23.5
Trochlea length	19.4	19.1
Trochlea width	20.7	19.5
Distal width (A-P)	12.5	12.2
Distal width (L-M)	18.5	17.3